RWTH AACHEN UNIVERSITY

CLAIX Projects 2020

High Performance Computing at RWTH Aachen University

Picture: EcurieAix & STCE

IT Center | RWTH AACHEN UNIVERSITY

CLAIX Projects 2020

High Performance Computing at RWTH Aachen University

Content

Imprint

IT Center
RWTH Aachen
University

Seffenter Weg 23
D-52074 Aachen

Phone:
+49 241 80 24680
Fax:
+49 241 80 22134

info@itc.rwth-aachen.de
www.itc.rwth-aachen.de

Editorial Design
HPC Offices,
IT Center

Aachen, July 2021

Picture: Alexander F. Müller

Preface

Dear reader,

In a challenging year in which much came to a standstill, the relevance of computer simulations has advanced even further. High performance computers such as the Cluster Aix-la-Chapelle (CLAIX) were also used to understand the pandemic. As an example, research on Metadynamics-based design of ligands targeting COVID-19 3CLPRO main protease with high potency and increased residence time can be mentioned. This project is still in progress and will be presented in one of the next reports. Nevertheless, we will show you a number of outstanding projects that were successfully completed in 2020 thanks to the CLAIX system.

CLAIX is not only used to conquer new challenges, but also contributes to the research of global issues that have always concerned humanity. For example, molecular dynamics (MD) simulations provide valuable contributions to elucidating the conformational transitions of monomeric and aggregated forms of amyloid-β (Aβ) peptide. Its aggregates are implicated as a causative substance in Alzheimer's disease, be it in solution or in the presence of other molecules (project by Institute of Biological Information Processing, Forschungszentrum Jülich and AICES Graduate School, RWTH Aachen University, see page 28).

Apart from medical topics, projects in the field of energy and climate research also contribute to addressing global problems and investigating them with the help of computer simulations.
With the help of CLAIX, the aim of the project "Atomistic modeling of energy materials" was to investigate the ability of different materials (electrolytes, catalysts, electrodes, waste forms) to catalyse organic compounds (e.g. CO2 reduction), incorporate charge carriers or radionuclides and to perform characterization of the organic ligands used in the liquid-liquid extraction. The long-term goal of simulation-based research in this project is to support the computer-aided development of new, advanced materials and technologies for energy storage and conversion (Institute of Energy and Climate Research, Forschungszentrum Jülich, see page 100).

The figure presented on the cover of this report is an example for the work of the Formula Student Team of RWTH Aachen University, who develop a completely new electric race car and adapt a previous car to be able to drive autonomously (Ecurie Aix-Formula Student Team RWTH-Aachen e.V, see page 94)

These are just a few highlights of the research topics that we supported and advanced with CLAIX last year. Details on these and many other exciting topics can be found in this CLAIX Report 2020.

We hope you enjoy reading it!

Yours sincerely,

Matthias Müller

PROF. DR. MATTHIAS MÜLLER

Advancing research together: RWTH becomes part of the National High Performance Computing Alliance

This year, together with TU Darmstadt, RWTH Aachen University is included in the National High Performance Computing Alliance. RWTH Aachen University and TU Darmstadt, together with the other six computing centers in the NHR alliance, create better conditions and the best possible support for high performance computing for scientists at German universities. The aim is to establish a central infrastructure and to advance high performance computing in a national alliance. Under the new funding concept, the federal and state governments will no longer only cover investment costs, but also operating and personnel costs. For this purpose, 62.5 million Euro will be available annually for the entire NHR alliance.

With TU Darmstadt as an experienced partner, RWTH Aachen University is advancing high performance computing with topics such as artificial intelligence, data science and simulation science. For years, both universities have successfully operated regional Tier-2 computers. Parts of both systems have been open to academic researchers from all over Germany for years. The expertise of both locations is now united in the “National High Performance Computer Center for Computational Engineering Sciences” (NHR4CES).

The goal is to combine HPC applications, algorithms and methods, and the efficient use of HPC hardware. This creates an infrastructure with which scientists can answer questions of central importance to the economy and society - whether in the field of engineering and materials sciences or engineering-oriented physics, chemistry or medicine.

To achieve these goals, scientists in NHR4CES collaborate in topic-specific so-called Simulation and Data Laboratories and Cross-Sectional Groups. As the link between users and the HPC infrastructure, they provide comprehensive support to all HPC users in Germany.

Under the leadership of Professor Matthias S. Müller (IT Center, RWTH Aachen University) and Professor Christian Bischof (University Computer Center, TU Darmstadt) both institutions have strongly promoted Computational Engineering Sciences (CES) in joint projects, graduate schools and study programs. They are pleased about the supported continuation of their good cooperation: “With NHR4CES, we are now developing an ecosystem for high performance computing that will advance simulation and data-based research, especially for the engineering-oriented, computer-aided research disciplines in Germany.”

The HPC system at RWTH Aachen University: CLAIX

The research projects in this report represent a selection of projects using the high-performance computing system CLAIX - Cluster Aix-la-Chapelle - at RWTH Aachen University in 2019. The system is operated by the IT Center and currently consists of three parts: the Tier-2 part from the procurement phases 2016 and 2018 and the Tier-3 part from the procurement phase 2018. In 2022, as part of NHR4CES@RWTH, new fast and large-capacity storage systems will go operational and will be available from CLAIX. An extension of compute capacity is expected to go operation towards the end of that year.

CLAIX-2016
The system consists of over 600 systems with 2x Intel Xeon Broadwell processors. Specialized node types with up to 144 cores at 1 Terabyte main memory or integrated GPGPUs or NVRAM complete the system for special tasks. All nodes as well as the parallel Lustre file system with a capacity of 3 petabytes are connected with an Intel Omni-Path network at 100-GigaBit/s speed. The overall system achieves a computing power of approx. 670 TeraFlop/s.

CLAIX-2016 started test operation in November 2016 and since December 2016 the system has been available without restriction for use by computing time projects.

CLAIX-2018
CLAIX-2018 consists of over 1000 computing nodes with 2x Intel Xeon Skylake processors, each with 24 cores and 192 GB RAM. In addition, there are 48 computing nodes of identical architecture, each equipped with two NVIDIA Volta V100 GPUs (incl. NVLink) as accelerators and available for special applications such as machine learning. A high-performance Lustre-based storage system offers a file system capacity of 10 petabytes and a bandwidth of 150 gigabytes/s (read and write). For interactive work with the system, CLAIX has eight additional dialog systems that are equipped with the same CPUs but have 384 GB more RAM. All nodes are connected to an Intel Omni-Path 100 Gigabit/s network.

The Tier-3 part consists of over 220 compute nodes with identical configuration (6 of those with GPUs) and are fully integrated into the overall cluster.

CLAIX-2018 started test operation in November 2018 and since January 2019 the system has been available without restriction for use by computing time projects.

Application for Compute Time
The allocation of compute time follows the recommendations of the Gauss Alliance for the establishment of nationally coordinated application and approval procedures. Depending on the amount of compute time request, independent national and international experts assess each proposal. According to regulations of the Deutsche Forschungsgemeinschaft (DFG), the Vergabegremium (VGG) of NHR4CES, JARA-HPC or RWTH determines detailed scientific and technical criteria for the assessment of proposals for computing time.

Technical Summary

	CLAIX-2016	CLAIX-2018
# compute notes for projects	609 standard nodes + special nodes	1080 standard nodes + 221 Tier-3 std. nodes
Processor type	Intel Xeon E5-2650v4 (Broadwell-EP)	Intel Xeon Platinum 8160 (Skylake)
# cores per node	24	48
Main memory per node [GB]	192	128
Capacity of Lustre HPC filesystem	3 PB	10 PB
Bandwidth of Lustre HPC filesystem	45 GB/s	150 GB/s
Theoretical peak performance	0.53 Pflops	3.55 Pflops
LINPACK performance	0.51 PFlops	2.04 Pflops on 2014 nodes

Humanities & Social Sciences

Picture: Pexels

Humanities/Social Sciences

Economics | DFG 112

In-depth analysis of neighborhood-based granular local search for capacitated vehicle routing

Project ID: rwth0335
CHRISTIAN BECKER,
Deutsche Post Chair - Optimization of Distribution Networks (DPO),
RWTH Aachen University

Project Report

Considering the growing market of e-commerce in the recent years, logistics companies such as DPDHL have an ever-increasing interest in constantly optimizing their distribution networks. For example, the last mile parcel delivery, as a part of their distribution network, can be optimized by modeling a vehicle routing problem (VRP). Given a set of customers, a depot and a set of vehicles, the VRP consists of finding the least cost vehicle routes such that each customer is visited exactly once, their demand is completely served, vehicles start and end their routes at the depot and the vehicles' limited capacity is not exceeded. The VRP is NP-hard, thus, realistically sized problem instances can best be solved by means of (meta-)heuristics. Local search (LS) belongs to the core components of most state-of-the-art metaheuristics for vehicle routing problems (VRPs). Given a starting solution to the VRP, LS iteratively transitions from one solution to a neighboring better one by modifying a small part of the solution using so-called neighborhood operators. These neighborhood operators exchange some present arcs in the underlying graph of the solution and replace them by new arcs. Granular LS reduces the search effort in each iteration by restricting the neighboring solutions to those that contain at least one new short arc.

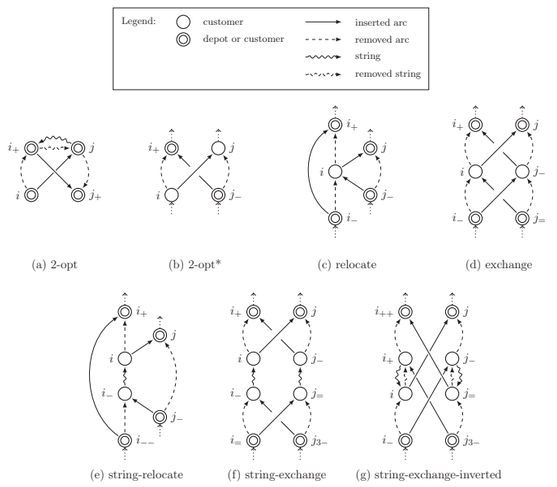

Figure 1: Neighborhood operators of granular local search

Over the last decades, many variants of (granular) LS using different neighborhood operators, exploration strategies, and speedup techniques have been developed. For instance, in each iteration of the LS, the so-called pivoting rule determines whether or not the search transitions to the first found improving neighboring solution (first improvement) or to the best among all neighboring solutions (best improvement). While algorithm variants using best improvement find better neighbors in each iteration, they also require a lot more neighbor evaluations than variants using first improvement. Another design decision is the selection of neighborhood operators to generate neighboring solutions. Figure 1 shows seven edge-exchange operators which are commonly used in the literature. While each additional operator gives access to new neighboring solutions, its evaluations take time and thus might slow down the algorithm. Design decisions like these can critically influence the performance of an LS in terms of both solution quality and computational effort. Despite the importance of LS in metaheuristics for VRPs, systematic investigations on the impact and importance of different design decisions in LS are nonexistent in the literature even for basic VRP variants, and clear recommendations on meaningful combinations of these decisions are not available.
To this end, we systematically studied the impact of design decisions in a granular LS for the capacitated VRP (CVRP). We formulated the most important and often used local search components and combined them in a full-factorial fashion, i.e., we pairwise combined design decisions to obtain 510 algorithmic variants in total. We compared the performance of these algorithmic variants of the granular LS on two CVRP benchmark sets. To obtain statistically sound results, we started each algorithm variant from 5000 randomized starting solutions. In this way, we made our conclusions and recommendations also reliable for metaheuristic frameworks that use different construction heuristics and for different metaheuristic frameworks in which LS is used as a component beside others. The immense number of computational tests could not be done with the limited resources of our chair. Therefore, we are very thankful that we could use the computer resources of the RWTH HPC department. To analyze the results of the extensive computational tests, we used the Wilcoxon signed-rank test. Comparing the algorithmic variants in a pairwise fashion, we were able to determine non-dominated algorithmic variants. We were further able to identify good combinations of decisions and give final design recommendations on granular LS. Several of these recommendations disagree with popular choices in the literature and are therefore valuable for both researchers and practitioners working on VRPs. For instance, we found out that the pivoting rule first improvement outperforms the rule best improvement for our granular LS in terms of both solution quality and runtime although most of the researchers in our field use best improvement.

Life Sciences

Life Sciences

Picture: Pexels

Life Sciences

Basic Biological and Medical Research | DFG 201

Towards Discovery of Molecular Determinants Underlying Organic Solvent Resistance of Enzymes: Large-Scale Molecular Dynamics Simulations of Bacillus subtilis

Project ID: jara0169
DAVARI MD,
ULRICH SCHWANEBERG,
HAIYANG CUI,
MARKUS VEDDER,
Institute of Biotechnology,
RWTH Aachen University

Project Report

Biocatalysis in organic solvents (OSs) has found various important applications, particularly in organic synthesis and for the production of pharmaceuticals, flavors, and fragrances. However, the use of enzymes in OSs often results in enzyme deactivation or a dramatic drop in catalytic activity. In JARA0169 project, we mainly focus on developing a comprehensive understanding of the interactions between enzymes and OSs based on numerous observables obtained from molecular dynamics simulation of Bacillus subtilis lipase A (BSLA). We have investigated the wild type enzymes and several beneficial/non-beneficial variants carrying single and multiple substitutions towards the organic cosolvent 2,2,2-trifluoroethanol (TFE, 12 % (v/v)), dimethyl sulfoxide (DMSO, 60 % (v/v)) 1,4-dioxane (DOX, 50 % (v/v))). After analyzing the distribution of numerous structural and dynamic observables, we uncovered that increased enzyme surface hydration of substituted sites as the predominant factor to drive the improved resistance in OS. Our findings prove that strengthening protein surface hydration via surface charge engineering is an effective and efficient rational strategy for tailoring enzyme stability in OSs.
In summary, this project provided not only a deep molecular understanding from enzyme stability in organic solvents, but also generated general design principles for rational protein engineering to improve enzyme stability in organic solvents.

Selected conference participations

- MEHDI D. DAVARI, "How to Engineer Enzymes for Catalysis in Non-Conventional Media: Insights from Combined Molecular Dynamics Simulation and Directed Evolution Study", International Conference on Biocatalysis in Non-conventional media (BNCM2020), Milan, Italy, May 7-9, 2020

Selected national and international cooperations

- KARL-ERICH JAEGER, Heinrich-Heine Universität Düsseldorf, Forschungszentrum Jülich GmbH, Jülich, Germany
- HOLGER GOHLKE, John von Neumann Institute for Computing (NIC), Jülich Supercomputing Centre (JSC), Germany
- LUO LIU, Beijing University of Chemical Technology (BUCT), China

Publications

- CUI H, ZHANG L, ELTOUKHY L, JIANG QJ, KORKUNÇ SK, SCHWANEBERG U, DAVARI MD.
  Enzyme hydration determines resistance in organic cosolvents. ACS Catalysis 2020, 10, 4847–14856.
- CUI H, STADTMÜLLER TH, JIANG Q, JAEGER KE, SCHWANEBERG UD, DAVARI M.
  How to engineer organic solvent resistant enzymes: insights from combined molecular dynamics and directed evolution study. ChemCatChem 2020, 12, 4073.
- CUI H, CAO H, CAI H, KARL-ERICH J, DAVARI MD, SCHWANEBERG U.
  Computer-assisted recombination (CompassR) teaches us how to recombine beneficial substitutions from directed evolution campaigns. Chemistry-A European Journal 2020, 26 (3), 643-649. (Cover Feature)

Basic Biological and Medical Research | DFG 201

The Mechanics of Brain Folding

Project ID: rwth0399

JENS ELGETI, Institute of Biological Information Processing (IBI-5), Forschungszentrum Jülich, Germany

LUCAS DA COSTA CAMPOS, Institute of Neuroscience and Medicine (INM-1), Forschungszentrum Jülich, Germany and Institute for Anatomy I, Heinrich-Heine-University Düsseldorf, Germany

SVENJA CASPERS, Institute of Neuroscience and Medicine (INM-1), Forschungszentrum Jülich, Germany, Institute for Anatomy I, Heinrich-Heine-University Düsseldorf, Germany, and JARA-BRAIN, Jülich Aachen Research Alliance, Germany.

Project Report

The overarching objective of this project is to better understand the mechanism by which mammalian brains obtain their folded landscape. This folding is highly stereotyped within each species, with misfolding in humans being associated with epilepsy, seizures, cerebral palsy, among many other issues. We perform finite element simulations, where the brain is modelled as a perfect nonlinear elastic divided into two regions: an outer growing region, modelling the brain cortex, and an inner non-growing region, modelling the brain white matter.

The current step of the project closely builds upon the results obtained last year, where we studied the influences of cortical thickness on folding of the mammalian brain. Those simulations were performed using the quasistatic approximation, an approach often used in the literature[1]. While prevalent, the validity of such an approach has not been thoroughly studied in the literature. Thus, in this stage of the work, we focused on both new results and methodological validation.

Our objectives were four folded:

1. Check that the simulations performed previously, in the quasistatic regime, were consistent by comparing them with dynamical simulations growing very slowly;
2. Study the interplay between fast growth and high cortical thickness in brain folding;
3. Study the effect of growth inhomogeneities in the folding landscape;
4. Study the interplay between the cortical thickness inhomogeneities (see previous report) and growth inhomogeneities.

To accomplish these objectives, the simulation software used previously was re-designed into a simulation library of growing materials, JuFold, which is planned to be released soon.

For the first objective, we simulated systems with constant cortical thickness growing at various rates. We observed that the folding wavenumber is consistent between dynamical systems growing very slowly and the simulations in the quasistatic regime. However, as growth speed is increased, the obtained wavenumbers would diverge, with these systems folding into a higher wavenumber right after buckling, followed by a period of relaxation. We also observed that these systems had a wider range in their frequency spectrum.

In the second objective, we expanded the phase space by also varying the cortical thickness of each system. We found that thick cortices lead to further overestimation in wavenumber, compounding with the effects of fast growth.

Once one considers the cumulative effects of growth rate and thickness on folding, it becomes necessary to revisit the results from the previous project, where cortical thickness was investigated as one of the drivers of folding. We resimulated a specific thickness profile using different growth rates and compared them to the results obtained from using the quasistatic approximation. While the rough folding profile was similar between the two methods -- folding concentrates at the thinnest point of the cortex, and decreases from there --, a few key differences were observed. Firstly, due to the effects found in the previous objectives, the folding of the thicker regions depends strongly on the growth rate, yielding a larger number of sulci and gyri pairs the faster the cortex grows. Secondly, we observed that the folding profile is more stable and reproducible than in the quasistatic simulation, which can jump between distinct energetical minima.

Differences in local growth rate have also been associated with complex folding landscapes. We investigate their effects by augmenting our system with an inhomogeneous growth profile in an otherwise homogeneous cortex. We observed the emergence of localised folding, similar to the previous project. However, this folding was less complex than that with inhomogeneous thickness, with folding concentrated in the regions of fast growth, while being mostly inhibited in other regions.

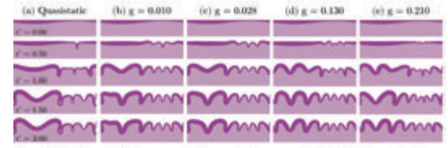

Figure 1: Cortices with inhomogenous thickness. (a) shows results obtained in the previous step of the project. (b-e) show cortices growing progressively faster, with growth rate indicated in the label. Comparing (a) to (b), it ist possible to see that the folding landscape is qualitatively similar, demonstrating the robustness of the approach taken in the previous project. Systems with faster growth rates (e.g, (e)) tend to fold into a larger number of gyri.

Finally, the two types of inhomogeneities were combined into a single system, in a complementary fashion. Namely, a higher growth rate, which is predicted to result in a large wavenumber, was applied to the thicker regions, where a low wavenumber is instead expected; vice-versa for the thinner regions. We found that the effects of the two inhomogeneity kinds were mutually exclusive, not additive. We observed that the systems either folded in the regions of thin cortices, or around the region of fast growth, but not in between, and most importantly, not in both regions at the same time.

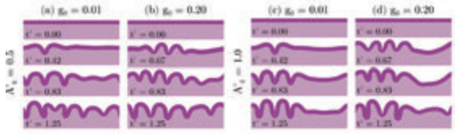

Figure 2: Cortices with inhomogenous growth. The quantity A'_g indicates the degree of growth inhomogeneity, with cortices growing faster on the left side than on the right side. These results indicate that the inhomogeneities in growth rate can also create localized patterns of the folding, but who are less complex than those created by inhomogenous thickness.

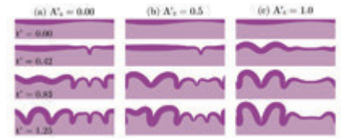

Figure 3: Cortices with both inhomogenous thickness growth, where the thicker regions of the cortex grow faster than the thinner regions, thus acting in a complementary fashion. We observe that the folding profile either follows those of systems with inhomogenous in thickness (a, b) or in growth (c), but the interplay does not create completely new folding patterns.

These configurations were understood using an linear stability theory derived from the Flopp-von Karman plate theory, which qualitatively agreed with our simulations results. Articles containing the results of this step in our project and describing JuFold in detail are under preparation to be published in peer-reviewed journals.

Publications

· DA COSTA CAMPOS ET AL. The role of thickness inhomogeneities in hierarchical cortical folding. Neuroimage. https://doi.org/10.1016/j.neuroimage.2021.117779

[1] Budday, Steinmann, and Kuhl, 'Secondary Instabilities Modulate Cortical Complexity in the Mammalian Brain'; Xu et al., 'Axons Pull on the Brain, But Tension Does Not Drive Cortical Folding'; Bayly et al., 'A Cortical Folding Model Incorporating Stress-Dependent Growth Explains Gyral Wavelengths and Stress Patterns in the Developing Brain'; Holland et al., 'Symmetry Breaking in Wrinkling Patterns'; Costa Campos et al., 'The Role of Thickness Inhomogeneities in Hierarchical Cortical Folding'.

Basic Biological and Medical Research | DFG 201

Molecular dynamics simulations of P2X receptors

Project ID: jara0180

JAN-PHILIPP MACHTENS
SASKIA CÖNEN
Institute of Biological Information Processing (IBI-1), Forschungszentrum Jülich, Germany, and Institute of Clinical Pharmacology, Uniklinik RWTH Aachen, Germany

RALF HAUSMANN
LINHAN CHENG
Institute of Clinical Pharmacology, Uniklinik RWTH Aachen, Germany

Project Report

P2X receptors are ligand-gated cation channels involved in a wide range of important physiological processes. The receptors are activated by the binding of ATP molecules to the large extracellular domain, which leads to ion-pore opening and consequent cation influx into the cell. The P2X subtypes named P2X1 to P2X7 assemble in homo- or heterotrimeric complexes and vary significantly in the kinetics of channel opening and closing. They are widespread across various cell types and are involved in nociception and muscle contraction, for example.

Mechanistic details of channel gating are still unknown but are required for rational drug development. X-ray crystal structures were resolved in the apo, open, and desensitized states and form the basis of our studies. It is currently known that ATP molecules associate with the agonist binding pocket in the apo resting state, followed by conformational changes of the transmembrane domains leading to the open ion-conductive state; however, under sustained presence of ATP most P2X isoforms adopt the non-conductive desensitized state.

Using extensive all-atom molecular dynamics (MD) simulations, based on high-resolution crystal structures, we first aimed to obtain a functional annotation of the resolved conformational states. We were able to show that ion access is blocked in the apo and desensitized states, in contrast to the open state, where the pore is continuously open and hydrated. Our results indicate that ions access the P2X receptor through three extracellular fenestrations, permeate through the pore perpendicular to the membrane and leave to the cytoplasmic side via three intracellular fenestrations (a). Whereas previous experimental studies on P2X receptors already hinted at the importance of the lipid environment, which could possibly modify functional properties of P2X receptors in different cell types, the molecular basis of this lipid modulation was still unknown. Our MD simulations now uncovered how lipids influence ion conduction by P2X receptors, with lipids of the lower lipid bilayer protruding deeply into the pore center (b); as a result, the pore is lined by lipid headgroups that assist in ion permeation.

We developed a new approach and software, termed g_elpot, to efficiently quantify electrostatics from all-atom biomolecular dynamics simulations (freely available at https://jugit.fz-juelich.de/computational-neurophysiology/g_elpot; [Kostritskii, Alleva, Cönen, Machtens, JCTC, in press]), which we used to quantify the electrostatic potential in the P2X ion pore. Our g_elpot revealed that charged lipid headgroups attract sodium ions which accumulate in the pore lumen, and may thereby modify the ion permeability and conductance of these unique channels (c).

To confirm these predictions, Computational Electrophysiology simulations were conducted to directly assess the effects of different lipid headgroups on ion conduction. Interestingly, by adding PIP2 molecules, the ion conductance is about two-fold higher compared to simulations in a POPC-only lipid bilayer, and even further increases were observed upon addition of POPS or POPG lipids to the membrane (d). In summary, our results suggest that the surrounding lipid membrane environment can markedly change the ion conductance of P2X receptors, and we are currently developing electrophysiological experiments to confirm these results experimentally in our laboratories.

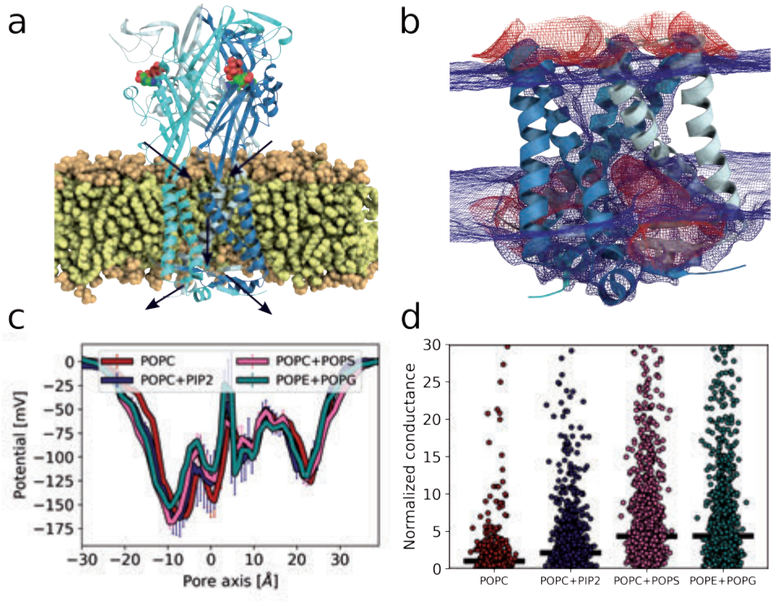

MD simulations of ion conduction by the human P2X3 receptor.

a) Permeation pathway. Cations enter the pore through three extracellular fenestrations, permeate and exit into the cytoplasma through three intracellular fenestrations.

b) Lipid headgroups protrude deeply into the pore centre. Averaged density meshes of water ions (blue, σ=0.002) and lipid headgroups (red, σ=0.005) illustrate how lipid headgroups of the lower lipid bilayer influence ion permeation by interacting with cations.

c) Electrostatic potential in the ion pore in different lipid environments calculated using g_elpot [Kostritskii, Alleva, Cönen, Machtens, JCTC, in press].

d) Ion conductance is largely changed by lipid environment. Median instantaneous conductances were calculated from Computational Electrophysiology simulations.

National and international cooperations

- FRITZ MARKWARDT, Julius-Bernstein-Institut für Physiologie, Martin-Luther-Universität Halle-Wittenberg, Halle

Publications

- ALLEVA C, KOVALEV K, ASTASHKIN R, BERNDT MI, BAEKEN C, BALANDIN T, GORDELIY V, FAHLKE C, MACHTENS JP.
(2020) Na^+-dependent gate dynamics and electrostatic attraction ensure substrate coupling in glutamate transporters. Science Advances 6(47):eaba9854

Life Sciences

Basic Biological and Medical Research | DFG 201

Molecular dynamics of the SLC26 family of ion channels and transporters

Project ID: jara0177

JAN-PHILIPP MACHTENS
Institute of Biological Information Processing (IBI-1), Forschungszentrum Jülich, Germany, and Institute of Clinical Pharmacology, Uniklinik RWTH Aachen, Germany

PIERSILVIO LONGO
Institute of Biological Information Processing (IBI-1), Forschungszentrum Jülich, Germany

Project Report

The Solute Carrier 26 (SLC26) family of membrane protein encompasses secondary active anion exchangers, channel-like transporters, and the motor protein prestin (SLC26A5). Malfunctioning of its members is associated with severe diseases such as diastrophic chondrodysplasia (SLC26A2), chloride diarrhea (SLC26A3), and deafness (SLC26A4/5).

Owing to their physiological importance, SLC26 transporters represent important, yet unexplored, drug targets for various diseases, including cystic fibrosis. Recently, the first high-resolution structure of a mammalian SLC26 transporter (murine Slc26a9) has been determined using cryo-electron microscopy. This transporter mediates uncoupled Cl^- transport across the membrane, and its human homologue (SLC26A9) is known to be an important disease modifier in cystic fibrosis. However, its transport mechanism is still unclear. For example, it is unknown whether SLC26A9 mediates channel-like conductive Cl^- transport or employs an alternating-access transport mechanism.

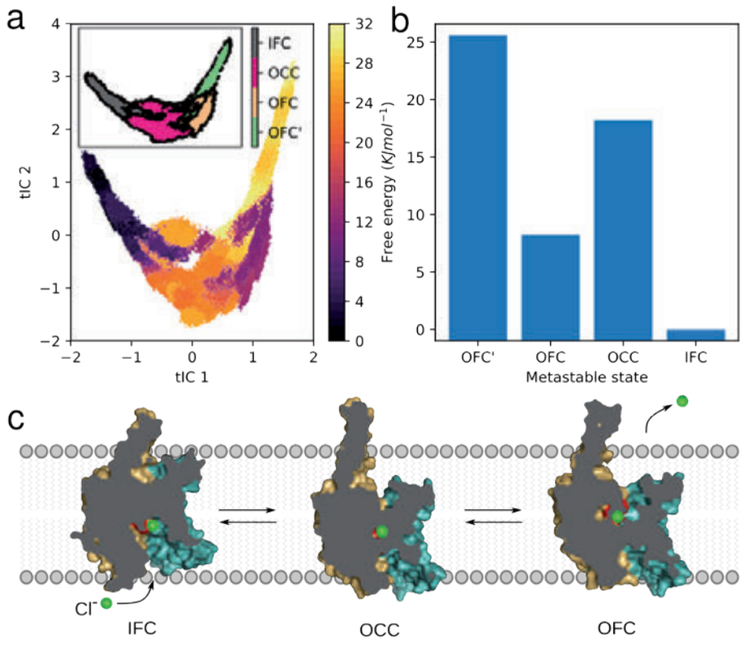

MD simulations illuminate Cl^- translocation by Slc26a9.

a) Free-energy landscape along the two slowest motions of the system calculated from the stationary distribution of a hidden Markov model (HMM) with 400 microstates and a lag time of 25 ns. The microstates were defined using k-means clustering after dimensionality reduction using time-structure independent components analysis (tICA). We identified four metastable states shown in the inset, including two outward-facing conformations (OFC and OFC').

b) Free energies of the four metastable states.

c) Representative snapshots of the metastable states suggest an elevator-like alternating-access transport mechanism. Starting from the inward-facing conformation (IFC) with the Cl^--binding site being exposed to the intracellular compartment, the so-called gate domain (cyan) undergoes a rigid-body motion relative to the static gate domain (brown) through an intermediate occluded state towards the outward-facing conformation (OFC).

So far, experimental structures of SLC26 transporters have been obtained only for the inward-facing conformation (i.e. with the putative Cl^--binding site being exposed to the intracellular site), leaving the transport mechanism elusive. We therefore employed extensive all-atom molecular dynamics (MD) simulations to obtain insights into the transport mechanisms of SLC26 transporters. Starting from the inward-facing conformation of Slc26a9, we developed a protocol based on the accelerated weight histogram method (AWH)—an enhanced sampling technique—to explore the conformational changes during substrate translocation towards the outward-facing conformation of the transporter. Subsequently, we initiated hundreds of unbiased MD simulations from the sampled conformations and analyzed them using state-of-the-art Markov state modeling techniques to investigate the thermodynamics and kinetics of Cl^- translocation, and to define functionally relevant metastable states, for experimental validation.

Our work illuminates the complete Cl^--translocation pathway, establishes an alternating-access elevator-like transport mechanism for this transporter, and defines an occluded intermediate state as well as two outward-facing conformations. This provides a foundation for further experiments and simulations to obtain a complete understanding of the transport cycle at atomic resolution.

National and international cooperations

This project is part of the DFG Research Unit FOR 5046 Integrated analysis of epithelial SLC26 anion transporters - from molecular structure to pathophysiology. This consortium, including the PI's project on molecular simulations of SLC26 transporters, was established in April 2020, and both have successfully evaluated for a four-years funding period by an international review board.

Collaborations:

- DOMINIK OLIVER, Institut für Physiologie, Uni Marburg
  ERIC GEERTSMA, Institute of Biochemistry, Goethe-University Frankfurt, Germany

Publications

- ALLEVA C, KOVALEV K, ASTASHKIN R, BERNDT MI, BAEKEN C, BALANDIN T, GORDELIY V, FAHLKE C, MACHTENS JP.
  (2020) Na^+-dependent gate dynamics and electrostatic attraction ensure substrate coupling in glutamate transporters. Science Advances 6(47):eaba9854

Life Sciences

Basic Biological and Medical Research | DFG 201

The effect of glycosaminoglycans on the aggregation of amyloid-β (Aβ) peptides

Project ID: rwth0400

BIRGIT STRODEL
Institute of Biological Information Processing, Structural Biochemistry (IBI-7), Forschungszentrum Jülich GmbH, Germany

SUMAN SAMANTRAY
AICES Graduate School, RWTH Aachen University, Germany

Project Report

Aggregates of the amyloid-β (Aβ) peptide are implicated as a causative substance in Alzheimer's disease. Molecular dynamics (MD) simulations provide valuable contributions to elucidating the conformational transitions of monomeric and aggregated forms of Aβ, be it in solution or in the presence of other molecules.

In the first phase of this project, we studied the behavior of monomeric Aβ peptide in solution by performing MD simulations. However, the results of an MD simulation can only be as good as the underlying force field. In general, a force field is used for modeling peptides or proteins and their environment, which is important for accurate modeling of the system of interest, and the length of the simulations, which determines whether or not equilibrium is reached. Through this study, we addressed key points by analyzing 30-μs MD simulations acquired for Aβ40 using seven different force fields.

We assessed the convergence of these simulations based on the convergence of various structural properties and of NMR and fluorescence spectroscopic observables. Moreover, we calculated Markov state models for each of the seven MD simulations, which provide an unprecedented view of the thermodynamics and kinetics of the Aβ peptide.

Our analysis allowed us to answers pertinent questions, like:
1) Which force fields are suitable for modeling Aβ?;
2) What does Aβ peptide really look like during the folding transitions of the disordered regions; and
3) How long does it take MD simulations of Aβ to attain equilibrium?

During the second phase of the project, we assessed the applicability of the various force fields to study the aggregation behaviour of the Aβ16–22 peptide, i.e., the sequence ^{16}KLVFFAE^{22} of Aβ, and mutations of it as test case. We investigated the performance in modeling the monomeric state, the aggregation into oligomers, and the stability of the aggregation end product, i.e., the fibrillar state. The main finding is that changing the force field parameters has a stronger effect on the simulated aggregation pathway than changing the peptide sequence. However, changing the force field should have no effect at all on the aggregation pathway, while changing the peptide should lead to largely different aggregation outcomes as known from experiments. Taken both force field benchmarks into account, we conclude that the overall best results are produced by the force field CHARMM36m and especially its modified version featuring enhanced protein–water interactions. We thus recommend to use CHARMM36m for performing peptide aggregation simulations, which we also did in the third phase of our study.

Here, we studied the effects of four different glycosaminoglycans (GAGs), three sulfated ones and a nonsulfated one, on the aggregation of Aβ16–22 . From experiments it has been suggested that GAGs, which are main components of the brain's extracellular space, favor amyloid fibril formation. Our simulation results revealed that the binding of Aβ16–22 to the GAGs is driven by electrostatic attraction between the negative GAG charges and the positively charged K16 of Aβ16–22. While these interactions have only minor effects on the GAG and Aβ16–22 conformations at the 1:1 ratio of Aβ16–22 and GAG, at the 2:2 stoichiometry the aggregation of Aβ16–22 is considerably changed. In solution, the aggregation of Aβ16–22 is strongly influenced by K16–E22 attraction, leading to antiparallel β-sheets. In the presence of GAGs, on the other hand, the interaction of K16 with the GAGs increases the importance of the hydrophobic interactions during Aβ16–22 aggregation, which in turn yields parallel alignments. A templating and ordering effect of the GAGs on the Aβ16–22 aggregates is observed. In summary, this study provides new insight at the atomic level on GAG–amyloid interactions, strengthening the view that sulfation of the GAGs plays a major role in this context.

Selected Conference Participations

- BIRGIT STRODEL, Molecular Modelling Workshop 2020, Plenary talk, Erlangen, Germany, February 2020
- BIRGIT STRODEL, 4th Ulm Meeting on "Biophysics of Amyloid Formation", Invited talk, Ulm University, Germany, February 2020
- BIRGIT STRODEL, ZOOMinar on "Molecular Bases of Proteinopathies", Invited talk, November 2020

Publications

- SAMANTRAY S, YIN F, KAV B, AND STRODEL B, Different force fields give rise to different amyloid aggregation pathways in molecular dynamics simulations, Journal of Chemical Information and Modeling, 2020; Vol.60, no.12:6462–6475.
- PAUL A, SAMANTRAY S, ANTEGHINI M, KHALED M, AND STRODEL B, Thermodynamics and kinetics of the amyloid-β peptide revealed by Markov state models based on MD data in agreement with experiment, Chemical Science, 2021; DOI: 10.1039/d0sc04657d

Picture: Pexels

Natural Sciences

Natural Sciences

Molecular Chemistry | DFG 301

Catalyst and Reaction Development Guided By Machine Learning

Project ID: rwth0509
FRANZISKA SCHOENEBECK
THERESA SPERGER
ABDURRAHMAN TÜRKSOY
WILLIAM REID
IGNACIO FUNES-ARDOIZ
SEBASTIAN WELLIG
JULIAN HÜFFEL
Institute of Organic Chemistry, RWTH Aachen University

CHRISTIAN TERBOVEN
JANNIS KLINKENBERG
NINA LÖSEKE
Chair for Computer Science 12 - High-Performance Computing, RWTH Aachen University

Project Report

Based on our development of a highly selective isomerization of terminal olefins catalyzed by a Ni(I) dimer (Figure 1), we were interested in finding similar catalysts.[1] As dinuclear Ni(I) catalysts are rare, but could have wide-spread applications in selective synthesis, their further development is of high interest.[2-5] In particular, the advance towards a chiral version of the Ni(I) dimer could offer numerous possibilities in enantioselective catalysis. However, finding ligands that can stabilize the dinuclear Ni(I)-Ni(I) core and hence display similar reactivity is challenging. Hence, we aim to employ machine learning, based on DFT-computed ligand descriptors, in order to find suitable ligands for this scaffold.

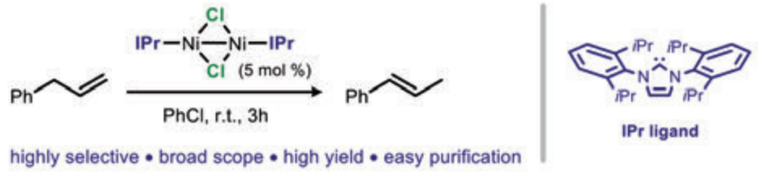

Figure 1 | Highly E-selective olefin isomerization by intramolecular radical relocation facilitated by Ni(I) dimer catalyst.[1]

The search for a compatible ligand represents a question of speciation as not only dimeric species can form, but also different types of monomers and different possible oxidation and ligation states. As the exact pathways and reactions to form these species and how they are intertwined is unknown, likely complex, and can therefore not be studied in a straightforward manner by experiments and calculations, machine learning can provide a more productive and efficient strategy towards the development of a novel reactive Ni(I) dimer catalyst.

To account for the question of speciation, the different species that can potentially form from the ligand and nickel metal need to be evaluated. Based on this, different core structures were selected and assessed for each ligand and subsequently used for the extraction of descriptors for the machine learning. From a library of ligands, different complexes, i.e. relevant species that can be formed either from the ligand itself or upon complexation with nickel, were assembled (Figure 2).

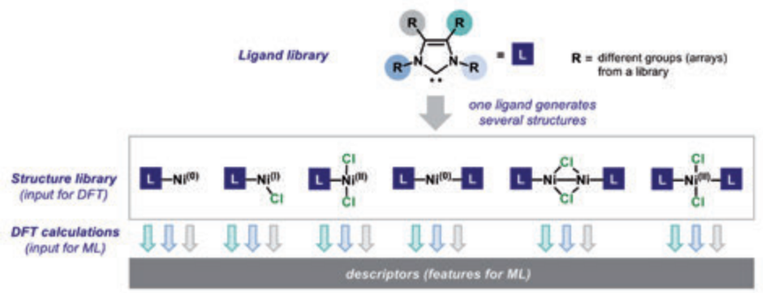

Figure 2 | Schematic outline for the generation of ligand descriptors as input features for machine learning using a library of ligands and DFT calculations.

All of the different species of a certain ligand were then optimized using DFT. In order to save computational time, for certain larger complexes, a molecular dynamics calculation was performed as a pre-optimization prior to the optimization at the DFT level.
As hand-picked descriptors can introduce unintended bias into the effectiveness of the machine learning algorithm, our aim was to compute as many descriptors as feasible. For this purpose, different properties and energies were calculated on the DFT level and then used as descriptors (either directly or after simple mathematical transformations). This includes not only different geometrical descriptors (bond lengths, angles, dihedral angles, bond orders), but also computed charges, NMR shifts, orbital energies and steric descriptors such as buried volume. This process was supported by a python-based framework in order to automatize certain steps and efficiently manage computational resources.
So far, roughly 290 Ligands were evaluated, i.e. their descriptors computed and compiled in a library (also supported by the aforementioned framework). The established library of descriptors was analyzed using Pearson correlation analysis, in order to locate any potentially redundant information. Using this purely computational feature set, we are currently exploring and evaluating different supervised and unsupervised machine learning methods. Ultimately we hope to use machine learning to gain new insights for the design of an improved ligand for selective catalysis.

References

[1] A. KAPAT, T. SPERGER, S. GUVEN, F. SCHOENEBECK, 'E-Olefins through intramolecular radical relocation', Science 2019, 363, 391-396.
[2] I. G. POWERS, C. UYEDA, 'Metal–Metal Bonds in Catalysis', ACS Catal. 2017, 7, 936-958.
[3] T. INATOMI, Y. KOGA, K. MATSUBARA, 'Dinuclear Nickel(I) and Palladium(I) Complexes for Highly Active Transformations of Organic Compounds', Molecules 2018, 23, 140.
[4] W. XU, M. LI, L. QIAO, J. XIE, 'Recent advances of dinuclear nickel- and palladium-complexes in homogeneous catalysis', Chem. Commun. 2020, 56, 8524-8536.
[5] C. FRICKE, T. SPERGER, M. MENDEL, F. SCHOENEBECK, 'Catalysis with Palladium(I) Dimers', Angew. Chem. Int. Ed. 2021, 60, 3355-3366.

Selected honors, prizes, and awards

- FRANKZISKA SCHOENEBECK, 2020 Novartis Lecturer at Yale University

Selected conference participations

- Invited Speaker Symposium on synthetic chemistry and catalysis at NTU Singapore, January 2020

Selected national and international cooperations

- Tomislav Rovis, Columbia University, New York, USA
- Erick M. Carreira, ETH Zürich, Zürich, Switzerland
- John Murphy, University of Strathclyde, Glasgow, UK

Natural Sciences

Molecular Chemistry | DFG 301

Computational evaluation and catalyst screening of the catalytic reduction of CO_2 to methanol via an indirect formate ester route with manganese complexes

Project ID: rwth0423
MARKUS HÖLSCHER
DAVID KUSS
Institute for Technical and Macromolecular Chemistry (ITMC), RWTH Aachen University

Project Report

The investigation of the catalytic mechanism for the manganese-pincer catalysed hydrogenation of formate esters let to a complete reaction network, which is summarized in figure 1. The hydride species 3 was identified as the most stable minimum and thus the turnover-determining-intermediate (TDI).

The Turnover-determining-transition state (TDTS) is the concerted transfer of a hydride from the manganese to the carbonyl carbon of the ester simultaneous to a transfer of the N-H proton to the carbonyl oxygen. The following decomposition of the formed hemiacetal can occur with a very low energy barrier and the hydrogenation of formaldehyde has a negligible barrier for the overall reaction. Therefore, the energy span of the reaction is determined to be 20.9 kcal/mol in the gas phase.

It must be noted, that the differences to alternative pathways, mainly the stepwise transfer of the hydride and proton are below 1 kcal/mol and therefore lie within the error region even with the most accurate Coupled Cluster methods. This makes an unrestricted confirmation of the mechanism difficult.

Future efforts will therefore try to refine the model by including solvation and match the theoretical results with experimental observations.

Nevertheless, first computations for a catalyst screening have been performed. Experimental hydricities were correlated with calculated ones and based on the obtained relationship the hydricity of 20 complexes were determined. The complexes were formally all in the d^6 electron configuration and featured different metal centers and ancillary ligands to probe the electronic effects.

They covered a wide range of the hydricity and subsequently the relative energies of the possible resting states, namely the activated complex 1, the alcoholate bounded complex 2, the hydride complex 3 and a formate adduct were calculated. The results in combination with the reaction mechanism suggest, that an intermediate hydricity between 50 to 60 kcal/mol is most favourable for the overall reaction of CO_2 hydrogenation to methanol.

A promising complex based on this knowledge is the Mn-MACHO complex with phenyl substituents and CO ancillary ligands.

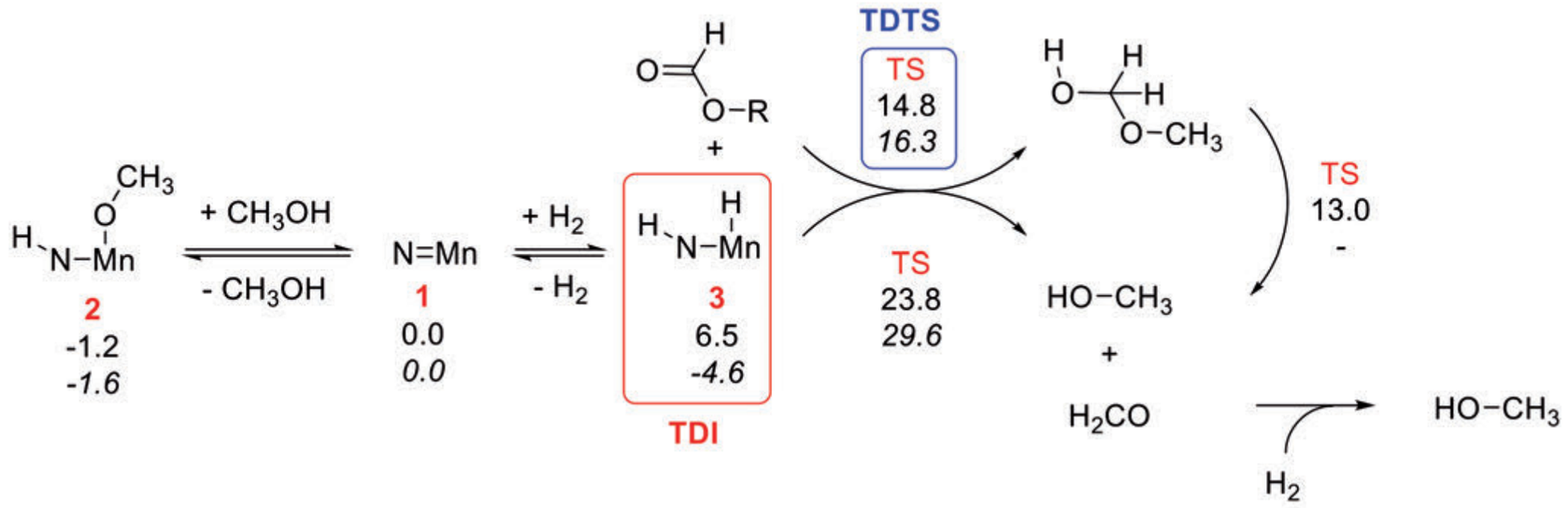

Figure 1: Summary of the calculated mechanism with all relevant structures. B97-D3BJ/def2-TZVP (top value) and B97-D3BJ/def2-TZVP//DLPNO-CCSD(T)/def2-TZVPP/RIJK (bottom value) ΔG in kcal/mol referenced to 1 in gas phase at 298 K and 1 atm.

Natural Sciences

Molecular Chemistry | DFG 301

Computational studies of reactivities in organic and organometallic transformations

Project ID: jara0091

FRANZISKA SCHOENEBECK
MAOPING PU
THERESA SPERGER,
ERDEM SENOL
CHRISTOPH FRICKE
CLAUDIA DIEHL
BHASKAR MONDAL
ABDURRAHMAN TURKSOY
SAMIR BOUAYAD-GERVAIS
WILLIAM REID
FILIP OPINCAL
IGNACIO FUNES-ARDOIZ
DANIEL HUPPERICH
SEBASTIAN WELLIG
JULIAN HÜFFEL
Institute of Organic Chemistry,
RWTH Aachen University

Project Report

The general aim of our research is the investigation of reactivity phenomena. By gaining a thorough understanding of reaction mechanisms, novel catalysts and transformations are designed. In particular, we intend to use the added benefits of the synergistic use of combining computational and experimental approaches. More specifically, we have explored competing radical pathways in the activation of aryl halides with Pd(0) to account for detrimental side reactions, as well as the reactivity of Pd nanoparticles as an alternative - and often unaccounted for - catalytically active species during cross-coupling reactions.
We have also extended our efforts to elucidate the mechanism of the Hiyama transmetalation, in particular with respect to observed solvent effects and also commenced an investigation on similar processes in corresponding nickel-based systems. Furthermore, we could address the divergent reactivity of diazonium salts and diazoethers in Stille and Suzuki cross-coupling showing that transmetalation at a Pd(II)-alkoxy complex is the likely cause for the pronounced difference in reactivity.[1] We have also explored the reactivity of diazonium salts under gold/light catalysis and photoredox catalysis.[2] Notably, the calculations could provide an explanation for a competing decomposition pathway and encouraged our search for a mechanistic alternative to overcome it. Lastly, we have also studied purely organic reactivity in the mechanism of the chemoselective ipso-halogenation of aryl germanes.[3] In the following some of these projects are highlighted.

In a previous reporting period, we explored the reactivity of diazonium salts and diazoethers in Stille and Suzuki cross-coupling reactions by exploring their oxidative addition to Pd(0). Our calculations showed similar barriers for both substrates which cannot account for the observed differences in reactivity. Meanwhile additional experimental findings identified Pd(II) alkoxy complexes as potential common reactive intermediates. Hence, we studied the transmetalation of both boronic acids and stannanes with Pd(II) alkoxy. Indeed, we found that transmetalation with boronic acids is greatly favored over transmetalation with an organostannane ($\Delta\Delta G^{\ddagger}$ = 17.6 kcal/mol). In the case of boronic acid, isomerization can occur at a stabilized pre-complex that is formed upon coordination of the boronic acid at Pd(II)-OMe, while for stannane no stable pre-complex was found. Moreover, we explored different ligands that are commonly employed in cross-coupling reactions of diazonium salts, i.e. pyridine and dibenzylideneacetone (dba). Due to the large conformational freedom additional evaluation and conformational searches were necessary. Pleasingly, we found that irrespective of the ligand employed and in line with experiments, transmetalation with boronic acid was favored.[1]

In continuation of our previous study on the reactivity of diazonium salts with a gold catalyst, we have additionally studied this process under photocatalytic conditions.[2] We have found that after excitation with light, the excited diazonium-gold complex can undergo intersystem crossing (ISC) to the triplet surface. At the triplet state the substrate is either activated under loss of N_2 or dissociates from gold. The latter process is favored in the case of electron-rich substrates and explains the observed decomposition. To avoid this unproductive pathway a photocatalyst was employed. This fundamentally changes the mechanism and our calculations suggest that photoredox catalysis takes place. In addition to computing the mechanistic pathway at the DFT level, the involved excited species were evaluated using time-dependent DFT (TD-DFT) calculations.

The selective halogenation of aryl germanes was studied by DFT calculations.[3] The ipso-bromination of aryl germane was found to be selective even in presence of other potentially reactive silyl moieties or boronic acids. A concerted S_EAr mechanism was found that is in line with this observed reactivity, displaying an activation barrier for C-$GeEt_3$ of 21.9 kcal/mol, which is 3.3 kcal/mol lower than the corresponding activation of C-$SiMe_3$. Additionally, the commonly proposed Wheland intermediate was not observed and instead a concerted ipso-substitution was found to be favored. This mechanism was evaluated for a range of electronically distinct substrates establishing the electrophilic nature of the involved transition state.

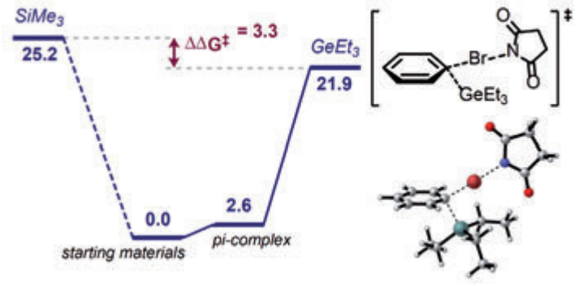

Figure 1 | Competing transition states for the selective halogenation of aryl germanes. Calculated at the CPCM (DMF) M06/6-311++G(d,p) (SDD)//ωB97XD/def2SVP level of theory.

References

[1] SANHUEZA IA, KLAUCK FJR, SENOL E, KEAVENEY ST, SPERGER T, SCHOENEBECK F. Base-Free Cross-Couplings of Aryl Diazonium Salts in Methanol: Pd^{II}-Alkoxy as Reactivity-Controlling Intermediate, Angew. Chem. Int. Ed. 2021, 60, 7007-7012.

[2] SHERBORNE GJ, GEVONDIAN AG, FUNES-ARDOIZ I, DAHIYA A, FRICKE C, SCHOENEBECK F. Modular and Selective Arylation of Aryl Germanes (C–GeEt3) over C–Bpin, C–SiR3 and Halogens Enabled by Light-Activated Gold Catalysis, Angew.Chem. Int.Ed. 2020,59, 15543-15548.

[3] FRICKE C, DECKERS K, SCHOENEBECK F. Orthogonal Stability and Reactivity of Aryl Germanes Enables Rapid and Selective (Multi)Halogenations, Angew. Chem. Int. Ed. 2020, 59, 18717-18722.

Selected honors, prizes and awards

- F. SCHOENEBECK, 2020 Novartis Lecturer at Yale University
- F. SCHOENEBECK, T. SCATTOLIN, EROS Best Reagent Award

Selected conference participations

- Invited Speaker Symposium on synthetic chemistry and catalysis at NTU Singapore, January 2020

Selected national and international cooperations

- PROF. TOMISLAV ROVIS, Columbia University, New York, USA
- PROF. ERICK M. CARREIRA, ETH Zürich, Zürich, Switzerland
- PROF. JOHN MURPHY, University of Strathclyde, Glasgow, UK

Publications

- KALVET I, DECKERS K, FUNES-ARDOIZ I, MAGNIN G, SPERGER T, KREMER M, SCHOENEBECK F. Selective ortho-Functionalization of Adamantylarenes Enabled by Dispersion and an Air-Stable Palladium(I) Dimer, Angew. Chem. Int. Ed. 2020, 59, 7721-7725.
- BOUAYAD-GERVAIS S, SCATTOLIN T, SCHOENEBECK F. N-Trifluoromethyl Hydrazines, Indoles and Their Derivatives, Angew. Chem. Int. Ed. 2020, 59, 11908-11912.
- SANHUEZA IA, KLAUCK FJR, SENOL E, KEAVENEY ST, SPERGER T, SCHOENEBECK F. Base-Free Cross-Couplings of Aryl Diazonium Salts in Methanol: Pd^{II}-Alkoxy as Reactivity-Controlling Intermediate, Angew. Chem. Int. Ed. 2021, 60, 7007-7012.

Natural Sciences

Chemical Solid State and Surface Research | DFG 302

Conversion-reaction mechanism in lithium-ion batteries from the first-principles point of view

Project ID: jara0179

KAIXUAN CHEN

Institute of Inorganic Chemistry, RWTH Aachen University

Project Report

In recent decades, the family of transition-metal carbodiimide[1-2], has attracted our intention. A lots of member in this family have been prepared due to the advancement of chemical routes, including MnNCN, CoNCN, NiNCN, FeNCN, $Cr_2(NCN)_3$ and so on. Based on the conversion reaction mechanism, the half batteries consisting of transition-metal carbodiimides turn out to provide a high cycling numbers without significantly reducing the available capacity. The intrinsic conversion mechanism may depend on the reversible cycling between the electrode materials and Li ions. As for now, the reaction mechanism for the family of transition-metal carbodiimide as active electrode materials in lithium ion batteries has not yet been investigated using first-principles simulations.

The objective of this proposal is to explore the intrinsic mechanism with regard to conversion mechanism. Most importantly, the study of transition-metal carbodiimides can be presented as a prototype to the investigation of conversion reaction, which can be generally applied to any other systems in the application of metal ion batteries.

To begin with, we studied the in-depth reason for the different structural preference in divalent carbodiimides. After then, by combining theoretical and experimental work (carried out by colleagues at the University of Montpellier), we revealed the reaction mechanism of divalent FeNCN and trivalent carbodiimides $Cr_2(NCN)_3$ as electrode materials in Li- and Na-ion batteries. Finally, we tried to explore the possible anionic redox mechanism in Li-rich tetravalent carbodiimides.

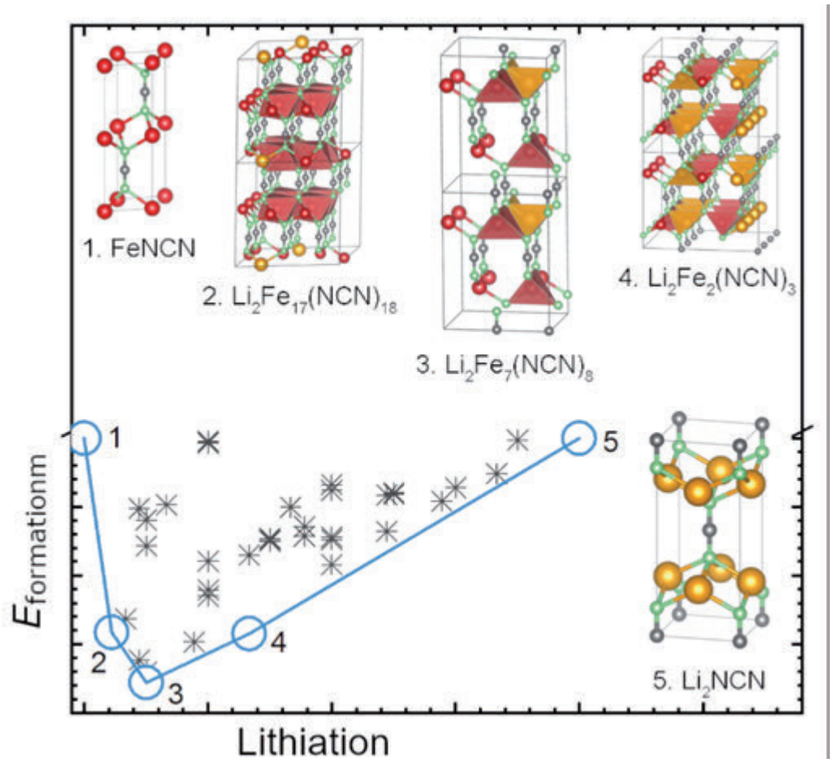

Take the theoretical study of FeNCN in battery application as an example, with a figure attached to illustrate the work. A computational DFT study on the conversion-reaction mechanism of FeNCN in Li- and Na-ion batteries yields calculated voltage profiles which agree nicely with experiments, and their characteristic lowering is well mirrored from chemical bonding and Mulliken charge analysis. In addition, a predicted ternary intermediate with composition $Li_2Fe_2(NCN)_3$ during lithiation is confirmed by operando XAS analysis. Results have been published at Angew. Chem. Int. Ed. 2020. 59, 3718-3723.

National and International cooperations

- LORENZO STIEVANO, University of Monterpellier, France
- MOULAY T. SOUGRATI, University of Monterpellier, France

Publications

- ARAYAMPARAMBIL JJ, CHEN K, IADECOLA A, MANN M, QIAO X, FRAISSE B, DRONSKOWSKI R, STIEVANO L, SOUGRATI MT. Energy. Technol. 2020, 8, 1901260.
- CHEN K, FEHSE M, LAURITA A, ARAYAMPARAMBIL JJ, SOUGRATI MT, STIEVANO L, DRONSKOWSKI R. Angew. Chem. Int. Ed. 2020, 59, 3718-3723.
- CORKETT AJ, CHEN K, DRONSKOWSKI R. EUR. J. INORG. Chem. 2020, 2020, 2596-2602.

Natural Sciences

Chemical Solid State and Surface Research | DFG 302

Quantum chemistry of functional chalcogenides for phase-change memories and other applications

Project ID: jara0033
RICHARD DRONSKOWSKI
JAN HEMPELMANN
RALF STOFFEL
Chair of Solid-State and Quantum Chemistry, RWTH Aachen University

Project Report

The project dealt with chalcogenide functional materials for storage-class memory. We utilized large-scale atomistic simulations based on density-functional theory (DFT) to model stabilities of solids and surfaces, investigate electronic properties, and perform chemical-bonding analysis. From the calculation of pristine surfaces, to surface oxidation, and ligand-covered terminations, this project has matured to include new concepts to understand the electronic properties of phase-change materials (PCMs) and to introduce new materials for future applications. Furthermore, this project keeps making important contributions to the collaborative research center CRC 917 “Nanoswitches”.

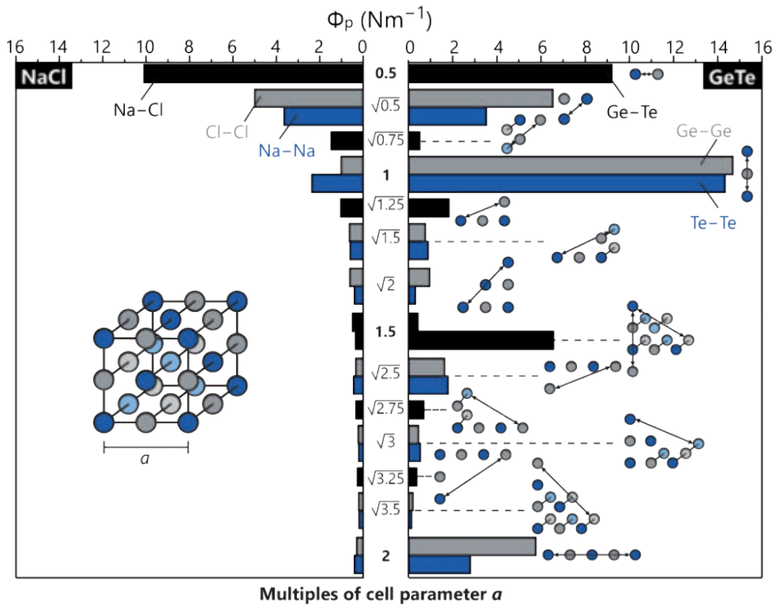

Figure 1 Projected force constants for rock salt type NaCl and GeTe. GeTe shows unusual long-range interactions along lattice parameter aligned vectors that do not appear between analogous atoms in NaCl.

Notwithstanding these ambitious goals, our project is necessarily based on fundamental research, some of which is reported here. DFT studies in the pseudo-binary chalcogenide system Sb_2Te_3–Sb_2Se_3 were carried out supported by experimental measures such as nuclear inelastic scattering and crystal structure investigations under pressure using synchrotron radiation. Within these structures, we also cleared the preferred incorporation of selenium and tellurium atoms, again in accordance with the experimentally observed data.

In an effort to advance mapping efforts and improve the chemical understanding of bonding in PCM-materials in general, we further developed the thermochemical descriptor of projected force constants to resolve unusual long-range interactions. The results of this research will be published in 2021.

In addition, we continued our study of pseudochalcogenide compounds containing the carbodiimide and the guanidinate anion such as to broaden the chemical perspective.

Publications

· HERRMANN MG, STOFFEL RP, SERGUEEV I, WILLE H, LEUPOLD O, AIT HADDOUCH M, SALA G, ABERNATHY DL, VOIGT J, HERMANN RP, DRONSKOWSKI R, FRIESE K. Lattice Dynamics of Sb_2Se_3 from Inelastic Neutron and X-Ray Scattering. Phys. Status Solidi B 2020, 257, 2000063.

· OGUTU G, KOZAR E, STOFFEL RP, HOUBEN A, DRONSKOWSKI R. Ammonothermal Synthesis, Crystal Structure, and Vibrational Properties of the Doubly Deprotonated Calcium Guanidinate, $CaC(NH)_3$, Z. Anorg. Allg. Chem. 2020, 646, 180–183.

· KÜPERS M, STOFFEL RP, BONG B, HERRMANN MG, LI Z, MELEDIN A, MAYER J, FRIESE K, DRONSKOWSKI R. Preferred selenium incorporation and unexpected interlayer bonding in the layered structure of $Sb_2Te_{3-x}Se_x$, Z. Naturforsch. B 2020, 75, 41–50.

Natural Sciences

Chemical Solid State and Surface Research | DFG 302

Ab-initio Molecular Dynamics Simulations of Apatite and Melilite Structures

Project ID: jara0392

STEFFEN NEITZEL-GRIESHAMMER
TIM SCHULTZE
Institute of Energy and Climate Research,
Helmholtz-Institute Münster:
Ionics in Energy Storage (IEK-12),
Forschungszentrum Jülich, Germany

MANFRED MARTIN
Institute of Physical Chemistry,
RWTH Aachen University

Project Report

Melilites of composition $La_{1+x}Sr_{1-x}Ga_3O_{7+x/2}$ and apatites of composition $La_{10-x}B_xSi_6O_{26\pm\delta}$ are promising as ion conductors for electrolytes in solid oxide fuel cells or oxide batteries. Melilites are composed of alternating layers of La/Sr cations and anionic GaO_4 tetrahedrons that are interconnected to form pentagonal rings. The variation of the La/Sr ratio leads to the introduction of oxygen defects into the structure, which enable 2D migration within the a/b-plane.

Lanthanum apatites crystallize in a hexagonal structure with cations forming a hexagonal tunnel. Oxygen interstitials are located in this tunnel and enable 1D migration in the c-direction.

In this project, the properties of oxygen ion transport in apatite and melilite structures were simulated by ab-initio molecular dynamics (AIMD) based on density functional theory (DFT). Simulations were conducted with the VASP code using the PBEsol xc-functional and the PAW method. An energy cutoff of 400 eV for plane waves was applied and the k-point sampling was limited to the Γ-point only.

Simulations in melilite structures were conducted for the compositions $La_{1.25}Sr_{0.75}Ga_3O_{7.125}$ and $La_{1.5}Sr_{0.5}Ga_3O_{7.25}$ in 2x2x2 supercells with a total of up to 196 atoms and two or four oxygen interstitials in the structure, respectively.
The simulated trajectories show that structural oxygen ions attached to Ga-ions vibrate mostly around their equilibrium position. The migration of oxygen interstitials between pentagonal rings proceeds by an interstitialcy mechanism, involving one interstitial ion and one oxygen ion at a regular position as previously found by DFT based nudged elastic band (NEB) calculations (Figure 1, left) and classical MD simulations. An example of the oxygen trajectory is given on the right hand side of Figure 1.

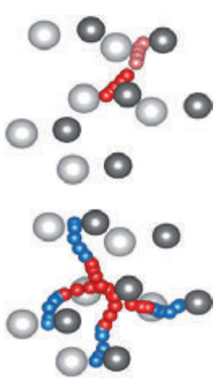

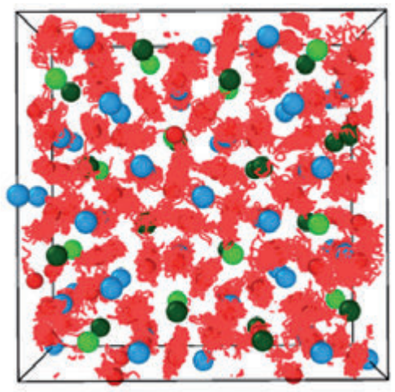

Figure 1: (Left) Migration paths for interstitialcy migration obtained from NEB calculation in melilites with migration across the O1 (top) and O3 (bottom) position.

Figure 2: (Right) MD trajectory for $La_{1.25}Sr_{0.75}Ga_3O_{7.125}$ at 1500 K. Oxygen ions are depicted in red

Nevertheless, even at a temperature as high as 2000 K only a limited number of jumps can be observed within the simulated time. Jumps only occur between positions in the a/b-plane and no transitions in c-direction were observed. Most of the jumps occur across the O1 positions. This path was already found to be favorable in DFT-NEB calculations. In addition, the interstitials locate preferably in La-rich environments. However, the number of transitions between sites is too small for a quantitative analysis of the site occupations or the jump probabilities.

Simulations in apatite materials were conducted for compositions $La_{9.33}Si_6O_{26}$, $La_8Sr_2Si_6O_{26}$, and $La_{10}Si_6O_{27}$ in 1x1x3 supercells with a total of up to 129 atoms. In the case of $La_{9.33}Si_6O_{26}$ and $La_8Sr_2Si_6O_{26}$ one additional oxygen interstitial was added, whereas three interstitials are present in $La_{10}Si_6O_{27}$ due to the composition.
Structural oxygen ions attached to the Si-ions vibrate mostly around their equilibrium position. Only oxygen ions located in the La-tunnel along the c-direction were found to be mobile. No jumps out of the tunnel, i.e. within a/b-plane, were observed. In the case of $La_{10}Si_6O_{27}$ interstitial ions were located either in the La-tunnel or at the edge of the tunnel to form a SiO_5-polyhedron.

As in the case of the melilites quantitative analysis of the migration behavior or the occupation of individual lattice sites is not possible due to the small number of jumps even at high temperatures.
For both materials determination of the diffusion coefficient was not possible due to the small number of migration steps and therefore insufficient statistics. Especially at temperatures below 2000 K the mobility of the ions is limited so far that transitions hardly occur. Nevertheless, results from static relaxations and NEB calculations were confirmed regarding the migration mechanism and the preference of specific cation environments.

Chemical Solid State and Surface Research | DFG 302

Ionic conductivity of NASICON materials from first principles

Project ID: rwth0445

STEFFEN NEITZEL-GRIESHAMMER
Institute of Energy and Climate Research,
Helmholtz-Institute Münster:
Ionics in Energy Storage (IEK-12),
Forschungszentrum Jülich, Germany

JUDITH SCHÜTT
Institute of Physical Chemistry,
RWTH Aachen University

Project Report

Na^+ superionic conductors are a class of fast sodium ion conductors that are promising as electrolytes in all solid state sodium ion batteries. The materials with the general composition $AMM'(PO_4)_3$ crystallize in a rhombohedral or monoclinic structure where corner-sharing PO_4 tetrahedra and MO_6 octahedra form a skeleton, which provides a network of three-dimensional pathways for the sodium ions. High ionic conductivities were reported for the composition $Na_{1+x+y}Zr_{2-x}Sc_xP_{3-y}Si_yO_{12}$ where Sc for Zr and Si for P are doped leading to the introduction of Na-ions on Na2 and Na3 sites in the lattice. The conductivity is maximized for x+y in the range of 2-2.5.

We investigated the NASICON structures with composition $Na_{1+x}Zr_2Si_xP_{3-x}O_{12}$ ($0 \le x \le 3$) by means of density functional theory to identify the origin of the conductivity maximum and the impact of the dopant ordering on the ionic conductivity.

Calculated cell parameters and volumes are in good agreement with experimental values for both the rhombohedral and monoclinic phase. The monoclinic phase is energetically more favorable for x = 2, as described in literature, whereas the energies for the other compositions are similar.

Different sodium ion sites were compared and the preferred arrangement of silicon and phosphorus ions studied. In accordance with literature, the Na1 site is energetically more favorable than the Na2 and Na3 site while the Na2 and Na3 sites are energetically equal. Furthermore, the calculations revealed that a homogenous distribution of Si^{4+} and P^{5+} ions within the cell is preferred. The Si^{4+} and P^{5+} ions have different charges as well as different ionic radii ($r_{Si^{4+}} = 0.26$ Å; $r_{P^{5+}} = 0.17$ Å). The clustering of highly charged phosphorous as well as large silicon ions causes unbalanced electrostatic repulsion and steric hindrance, which leads to distortion of the cell and seems to be energetically unfavorable.

To describe the influence of the cation occupation on the site energy of sodium ions, a pair interaction model was constructed to fit the energies obtained by DFT calculations. Individual energies for the monoclinic structure were calculated by:

$$E_{\mathrm{conf}} = \sum_{i=1}^{k} N_{\mathrm{Na}}^{i} \cdot E_{\mathrm{Na}}^{i} + \sum_{i=1}^{k} N_{\mathrm{Si}}^{i} \cdot E_{\mathrm{Si}}^{i} + N_{\mathrm{V_{Na1}}} \cdot E_{\mathrm{V_{Na1}}} + E_{\mathrm{s}}$$

The model includes the number of sodium-sodium pairs N^i_{Na} and the number of sodium-silicon pairs N^i_{Si} in the ith position. The corresponding interaction energies E^i_{Na} and E^i_{Si} were obtained by multiple linear regression. Sodium ions repulse each other with an interaction energy of 0.19 eV and 0.10 eV in 1st and 2nd nearest position, respectively. Between sodium ions and Si-dopants, a weak attractive interaction of -0.04 and -0.05 eV in 1st and 2nd nearest position is found.

The model shows that with increasing amount of silicon ions and decreasing amount of sodium ions in the first and second nearest neighbor position the energy decreases. Regarding the comparison of the Si^{4+} and P^{5+} ions, it seems that the stronger electrostatic repulsion of the P^{5+} ions has a more negative impact than the steric hindrance of the Si^{4+} ions.

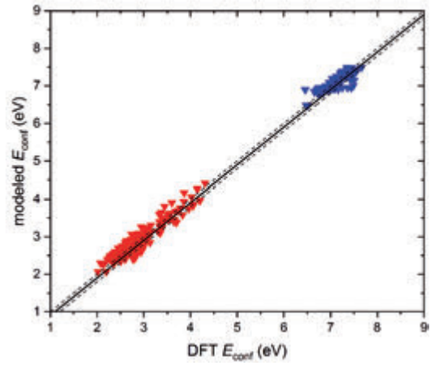

The configurational energies predicted by the model and the energies obtained from DFT calculations for different configurations with x = 1;2 are plotted in Figure 1. The dashed lines illustrate a deviation of 0.1 eV. The energies cannot be described exactly but the model is simple enough to implement in subsequent Monte Carlo simulations and still reflects the expected trend.

Figure 1: Modeled energies and energies obtained from DFT calculation of $Na_{1+x}Zr_2Si_xP_{3-x}O_{12}$ (x = 0.1 (red), 0.2 (blue)).

The distribution of Na-ions was simulated by Monte Carlo in a 10×10×10 supercell with $0 \le x \le 2.8$ in the temperature range of 300 K to 800 K. The simulations show that Na1 sites in the cell are always fully occupied whereas the occupation of Na2 and Na3 sites increase with x.

The migration of sodium ions was calculated using the climbing image nudged elastic band method (CI-NEB). Previous studies suggest a knock on migration of the Na^+ ions. The sodium ion migrates from the Na2 or Na3 site onto an occupied Na1 site whilst this ion moves to an unoccupied Na2 or Na3 site. Three different migration pathways were considered which are defined by their angles, as shown in Figure 2. The Na2/Na3 ion (orange/yellow) moves to the occupied Na1 site (pink) and pushes the Na1 ion onto a neighboring Na2/Na3 site.

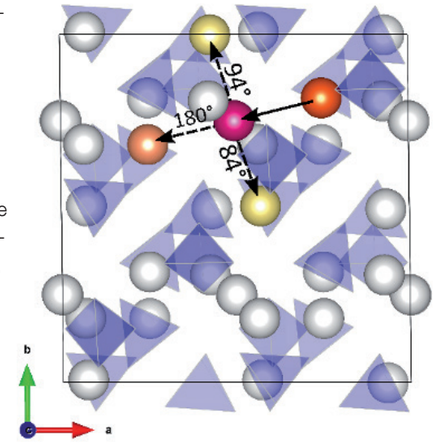

Figure 2: Different migration pathways regarding the migration angle. Na1 (pink), Na2 (orange), Na3 (yellow), SiO_4/PO_4 (blue). Na-ions not involved in the migration are white.

First results show that the migration energy decreases with increasing angle of migration pathway and increasing dopant fraction.

In future work, Monte Carlo simulations of the Na-ion transport will be performed to elucidate the impact of migration paths, composition, and ion dopant distribution on the ionic conductivity.

Natural Sciences

Chemical Solid State and Surface Research | DFG 302

Proton and Oxygen ion conductivity of doped $BaZrO_3$: A DFT and Kinetic Monte Carlo study

Project ID: jara0141
MANFRED MARTIN
FABIAN DRABER
Institute of Physical Chemistry,
RWTH Aachen University

Project Report

Main challenges of today's economy are related to energy problems: The usage of renewable energies, the energy storage in batteries, e.g. in electric cars, or the enhancement of solid oxide fuel cells require high-tech materials for high performance devices. Therefore, a major task for the scientific society is the investigation of these materials.

Here, acceptor-doped $BaZrO_3$ is a promising material and although this material has already been investigated, the understanding of the underlying processes is still limited. In the previous period we focused on different possible dopants like Gallium, Indium, Scandium or Gadolinium. Through a combination of density functional theory calculations and kinetic Monte Carlo simulations, we are looking for dopants that show an acceleration of protons through percolation pathways.

These pathways are formed by overlapping trapping zones, that are around dopant ions. The protons are accelerated along them under the condition of low migration energies in these pathways (see Fig. 1), while the oxygen vacancies are slowed down. Therefore, an extensive dopant screening was done accompanied by the calculation of migration energies of proton jumps around dopant ions to find promising dopant ions.

Thereby, it was possible to gain all information necessary to perform kinetic Monte Carlo simulations to extract the proton conductivity dependent on the dopant ion.

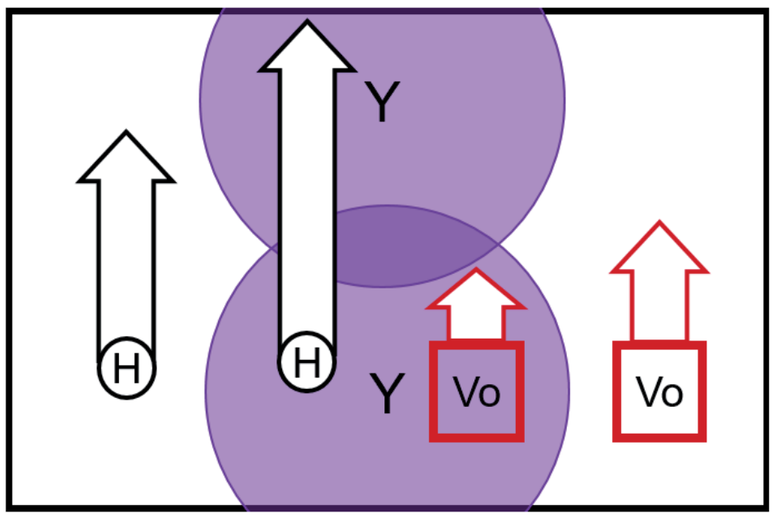

Figure 1

National and international cooperations

- SHU YAMAGUCHI, National Institute for Accreditation of Degrees and Quality Enhancement of Higher Education (NIAD-QE), Tokyo, Japan.
- STEFFEN GRIESHAMMER, Helmholtz-Institut Münster (IEK-12) and Forschungszentrum Jülich GmbH, Münster, Germany.

Publications

- DRABER FM, ADER C, ARNOLD JP, EISELE S, GRIESHAMMER S, YAMAGUCHI S, MARTIN M.
  Nanoscale percolation in doped $BaZrO_3$ for high proton mobility,
  Nature materials 2020, 19, 338–346.

Natural Sciences

Chemical Solid State and Surface Research | DFG 302

Ab-initio study of composition, structure and conductivity in interstitial oxygen conductors

Project ID: jara0156

MANFRED MARTIN
Institute of Physical Chemistry
RWTH Aachen University

STEFFEN NEITZEL-GRIESHAMMER
Institute of Energy and Climate Research,
Helmholtz-Institute Münster:
Ionics in Energy Storage (IEK-12),
Forschungszentrum Jülich, Germany

Project Report

Two types of oxygen interstitial conducting oxides, namely apatites of composition $La_{10-x}B_xSi_6O_{26\pm\delta}$ and melilites of composition $La_{1+x}Sr_{1-x}Ga_3O_{7+x/2}$, were investigated by means of densitiy functional theory. These materials are promising as ion conductors for electrolytes in solid oxide fuel cells or oxide batteries.

Melilites are composed of alternating layers of La/Sr cations and anionic GaO_4 tetrahedrons that are in-terconnected to form pentagonal rings. The increase of the La/Sr ratio leads to the introduction of oxygen interstitials that can migrate between adjacent rings by an interstitialcy mechanism. In our previous work, the migration barriers were calculated depending on the local environment, i.e. the occupation of La/Sr positions and the presence of other interstitials.

With the data, an energy model of ion migration was constructed and applied in kinetic Monte Carlo simulations of the ionic conductivity. The results show the increase of the ionic conductivity with the La-content due to an increase of mobile ions and a decrease of energetically unfavorable Sr-rich configurations.

Doping can further influence the ionic conductivity and thus we investigated the effect of Ga-site doping with several dopants X (X = B, Al, In, Si, Sc, Zn) on the site energies and migration barriers. Different configurations of the interstitial position and migration paths with respect to the dopant were considered (Figure 1).

The dopants can be classified in three groups regarding the effect on the site energies. (1) Al^{3+} and Si^{4+} stabilize the interstitial position, i.e. show an attractive interaction with the interstitial. This effect is moderate for Al^{3+} with -0.1 eV, and strong for Si with -0.2 to -1.0 eV. The strong interaction between Si and the oxygen ion interstitial is mainly attributed to the higher positive charge of Si compared to the other dopants. (2) B^{3+} and Sc^{3+} show a mixed behavior with interaction energies in the range of ±0.2 eV depending on the geometry. (3) For In and Zn the site energy of the interstitial is increased in the range of 0 – 0.3 eV and 0.1 – 0.6 eV, respectively. The destabilizing effect seems to be due to the larger radius of In (0.62 Å) and Zn (0.6 Å) compared to Ga (0.47 Å).

The effect of dopant ions on the migration barriers is more inconclusive and depends on the considered migration path and distance to the dopant. As a general trend, an overall decrease of the migration barriers is found for increasing dopant radius. Thus, B^{3+} (0.11 Å) shows the largest increase of the barrier between 0.1 and 0.6 eV compared to the pure Ga environment.

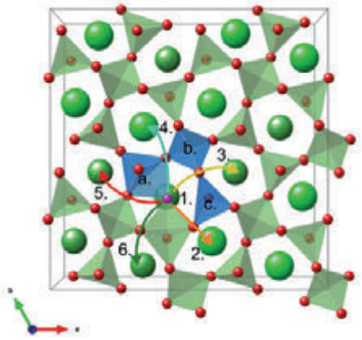

Figure 1: Calculated positions and migration paths of the oxygen interstitial with the dopant at the a), b) or c) position.

Lanthanum apatites crystallize in a hexagonal structure ($P6_3/m$). Cations form a hexagonal tunnel with oxygen ions where additional oxygen interstitials can be accommodated. Three important compositions were considered in our calculations, namely $La_{9.33}Si_6O_{26}$, $La_8B_2Si_6O_{26}$ (B = Mg, Ca, Sr, Ba) and $La_{10}Si_6O_{27}$. The calculations revealed fast migration along the c-direction in the tunnel and slow migration between tunnels in the a/b-plane. Thus, an optimization of the overall conductivity must focus on the transport in the a/b-plane.

Therefore, we investigated the migration in the a/b-plane in more detail. The a/b-migration in $La_8Sr_2Si_6O_{26}$ and $La_{10}Si_6O_{27}$ was analyzed to quantify the influence of cation and interstitial arrangement. The obtained migration barriers in the compositions are 0.53 eV and 1.13 eV, respectively. This is consistent with our findings that a/b-migration along a Sr-rich configuration is more favorable than along a La-rich configuration. Furthermore, the presence of two additional interstitials at SiO_5 polyhedrons in composition $La_{10}Si_6O_{27}$ seems to limit the structural relaxation during the migration.

In addition, we investigated the impact of different dopants on the Si-sites (X = Al, Ga, Ge, Fe, In, Mg) in $La_8Sr_2Si_6O_{26}$. The results for the Sr-rich configuration show that the dopant does not lower the migration barrier for the oxygen ion to exit or enter the La-tunnel but can lower the migration barrier for the migration between two SiO_4 tetrahedrons from 0.2 eV to 0.1. While the migration barrier for exiting and entering the La-tunnel is not significantly affected, the migration between SiO_4 polyhedrons is favored.

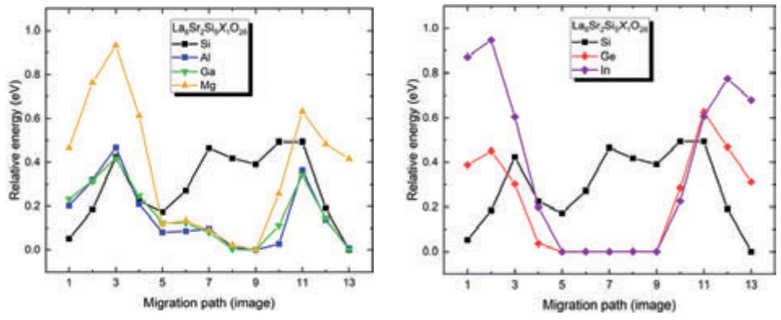

Figure 2: Energy profiles for the migration in the a/b-plane with different dopants

Publications

· SCHÜTT J, SCHULTZE T, GRIESHAMMER S.
Oxygen ion migration and conductivity in $LaSrGa_3O_7$ melilites from first principles,
Chem. Mater, 2020, 32, 4442-4450. (10.1021/acs.chemmater.9b04599)

Natural Sciences

Physical and Theoretical Chemistry | DFG 303

Development of reliable force fields for protein aggregation simulations

Project ID: rwth0499

BIRGIT STRODEL
FENG YIN
BATUHAN KAV
Institute of Biological Information Processing, Structural Biochemistry (IBI-7), Forschungszentrum Jülich, Germany

Project Report

Molecular dynamics (MD) simulations have helped tremendously in understanding the underlying physics and chemistry behind protein dynamics and aggregation. However, while the all-atom MD simulations of peptide aggregation reported till date have provided crucial information, most of these published studies suffer from a fundamental challenge involving force fields that either over-stabilise or underestimate protein-protein interactions: in essence such force fields lack the capability to distinguish between amyloidogenic and non-amyloidogenic peptides, which renders the aggregation process into a rather unspecific event when visualized from an in silico point of view. To gain a better understanding of the underlying reasons for the failure of the various force fields, we performed two benchmark studies using the aggregation of the fibril-forming Aβ(16-22) peptide (sequence KLVFFAE) and two mutants of it with different aggregation propensities as a test case. This showed that Charmm36m is currently the best, but still not perfect force field for modelling peptide aggregation. We therefore intend to reparameterise Charmm36m to make it better suitablefor modelling peptide aggregation. To this end, we performed a pair interaction energy decomposition analysis (PIEDA) for dimers of Aβ(16-22) based on CHARMM36m and GROMOS54a7 (one of the worst force fields for modelling peptide aggregation) potentials, as well at the MP2/6-31G*(PCM) quantum mechanics (QM) level of theory. From the obtained results, the total interaction energy between residue pairs calculated with the CHARMM36m force field is closer to the QM values compared with the GROMOS54a7 force field. The PIEDA additionally revealed H-bonding energies to be overestimated relative to QM data, while the dipole-dipole C=O - C=O is underestimated. For charged residue pairs the interaction energy difference between force field and QM values is substantial. For this reason, efforts to correctly model the aggregation kinetics will necessitate a reparameterisation of the non-bonded terms. For this to happen it will be useful to identify all the 200 possible amino acid pair combinations that are most affected.

One shortcoming of the classical treatment of particles as employed by MD simulation is the fact that electronic polarization is usually treated as static. Electronic polarization, however, specifies a response of all electronic degrees of freedom to an external electromagnetic field, which can only be accurately treated at QM levels of theory. The static treatment adopted in classical MD fails to capture dynamic changes in atomic charges in response to the local environment. Polarizable forcefields (PFF) aim to solve this shortcoming by explicitly incorporating electronic polarizability. This is commonly achieved via the fluctuating charge methods (CHARMM-FQ model), the Drude oscillators (CHARMM-Drude model), and the multipole expansions method (AMOEBA force field). However, a comprehensive study of their performance and suitability in protein aggregation in general and the Abeta peptide in particular is still missing.

In this project we aim to fill this void by assessing the performace of the CHARMM-Drude force field within the context of Aβ(16-22) aggregation. Since this particular polarizable force field is based on the CHARMM36 force field, we believe there is a lot of shared features between CHARMM-Drude and CHARMM36m, which will allow us understand the immediate effects of electronic polarizability. We believe that a benchmark study on these forcefields will be instructive for the collective efforts of developing better force fields for protein aggregation.

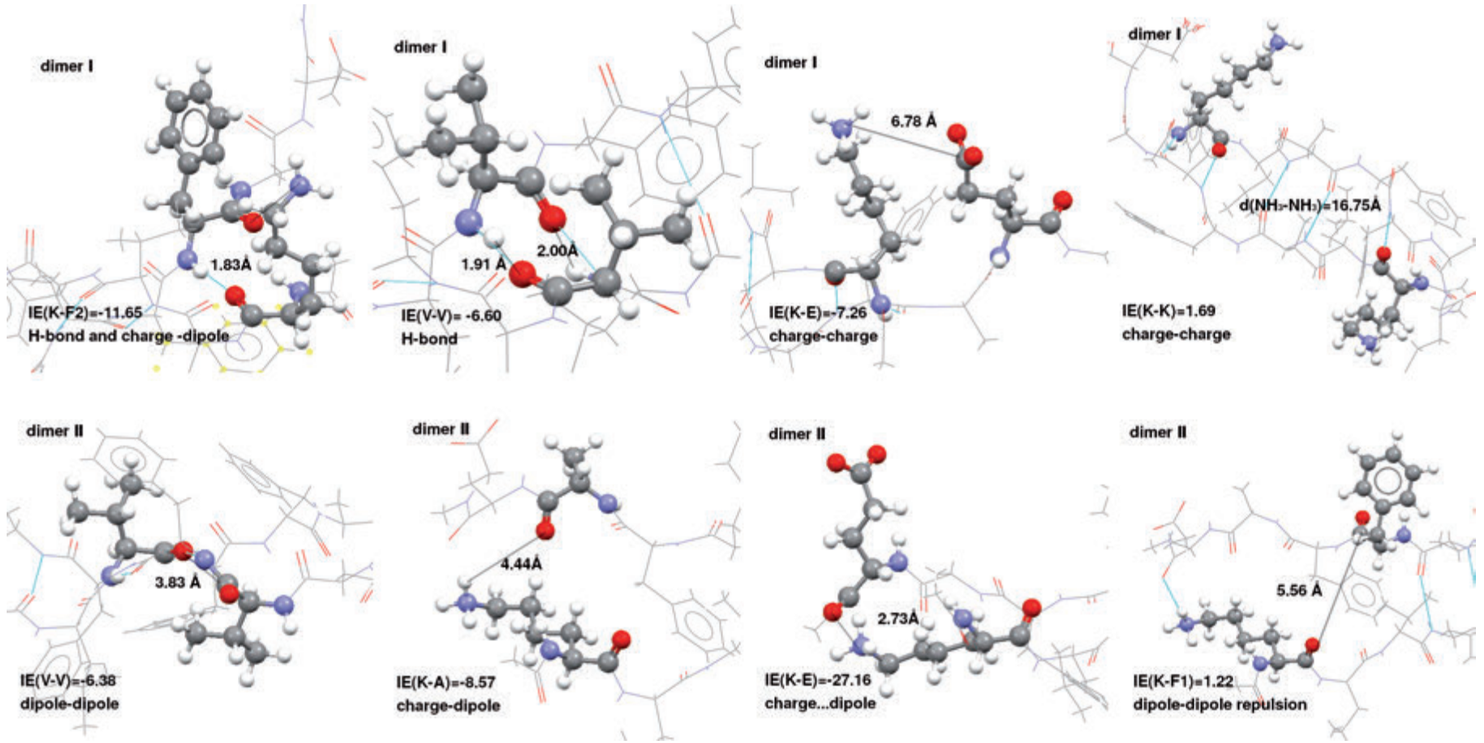

Figure 1: PIEDA for various amino-acid combinations as present in two of the Aβ(16-22) dimer structures

Condensed Matter Physics | DFG 307

Ab initio investigation of the structure-dynamics-bonding relation in phase-change materials

Project ID: jara0198 & jara0207

RICCARDO MAZZARELLO
IDER RONNEBERGER
YAZHI XU
MATHIAS SCHUMACHER
VALENTIN EVANG
PETER SCHMITZ
Institute for Theoretical Solid State Physics, RWTH Aachen University

MATTHIAS WUTTIG
I. Institute of Physics (IA), RWTH Aachen University

Project Report

Subproject 1: We have carried out a first-principles study of the structural, electronic and ferroelectric properties of the crystalline phase of selected binary PCM tellurides (GeTe and SnTe) and selenides (GeSe and SnSe) as a function of film thickness up to 18 bilayers [1]. Aside from their phase-change properties, quasi 2D group IV Chalcogenides (IV = Ge, Sn; chalcogen = S, Se, Te) are attracting significant interest due to their remarkable electronic properties, which include in-plane ferroelectric polarization. In our work, we have shown that, while in selenides a few bilayers are sufficient to recover the bulk crystalline behavior, the Te-based compounds deviate strongly from the bulk, irrespective of the slab thickness (see Figure 1) [1].

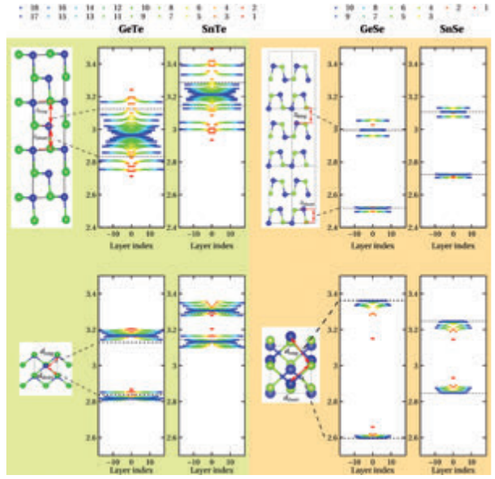

Figure 1: Out-of-plane (top) and in-plane (bottom) structural features (i.e. interlayer distance z and nearest neighbour bond distances d) in slab models of monochalcogenides as a function of the layer index. The data points are color-coded according to the thickness of the films: from red (thinnest) to blue (thickest). The two (short and long) bulk values are shown in dashed lines. Figure adapted from Ref. [1].

We have explained these results in terms of depolarizing fields in Te-based slabs and the different nature of the chemical bond in selenides and tellurides. More specifically, GeSe and SnSe films exhibit covalent bonding, whereas GeTe and SnTe slabs inherit the metavalent bonding of the bulk phase. Since the latter bonding mechanism stems from a delicate balance between electron localization and delocalization, it is particularly sensitive to confinement in one dimension, as occurs in thin-film models. The elucidation of the nature of bonding in few-layers structures offers a powerful framework to tune material properties for applications in information technology. Furthermore, it provides insight on the ultimate thickness limit for applications of PCMs in memory and neuro-inspired devices. Our work has been recently published in Advanced Materials [1].

Subproject 2: Tailoring the degree of disorder in PCMs plays an important role in memory and neuromorphic computing devices. Disorder-driven insulator-metal transitions were observed in crystalline Ge-Sb-Te compounds along the GeTe-Sb_2Te_3 pseudo-binary line (such as $Ge_2Sb_2Te_5$ and $GeSb_2Te_4$), which form the most important family of PCMs. Upon nanosecond crystallization induced by electrical/optical pulses or thermal annealing (at about 150-200 °C), Ge-Sb-Te alloys form an Anderson-insulating metastable rocksalt-like phase with a high concentration of randomly distributed atomic vacancies (~10%). Higher annealing temperatures induce a phase transition to a metallic rhombohedral phase. The two phases show similar band gap size and carrier concentration, but a large contrast in carrier mobility and opposite temperature-dependence of the resistivity. Subsequently, the microscopic origin of this transition was elucidated by our group. We found that, in the insulating phase, the electronic states at the Fermi energy E_F are strongly localized around vacancy clusters, and that the insulator-metal transition stems from the ordering of vacancies into two-dimensional vacancy planes.

In this project, we have investigated Anderson localization in the metastable rocksalt-like phase of binary Sb_2Te_3 [2], the parent compound of the Ge-Sb-Te alloys. We have shown that this compound also displays disorder-induced exponential localization of the electronic states near the Fermi level. The states are localized inside vacancy clusters, as evidenced by the calculation of the local density of states and the inverse participation ratio (see Figure 2A-B). Our computational findings are corroborated by transport experiments, which indicate an insulator-metal transition induced by annealing (see Figure 2C-E). Interestingly, a structural transition from a rocksalt-like phase to a hexagonal phase also occurs, nevertheless the two transitions are independent from each other. Our work has been recently published in Advanced Materials [2].

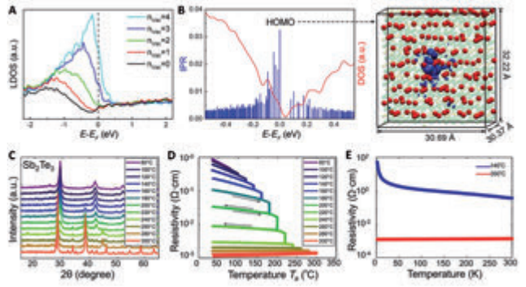

(A) The LDOS of Te atoms in rocksalt Sb_2Te_3.
(B) The inverse participation ratio (IPR), DOS and the HOMO state computed for rocksalt Sb_2Te_3.
C) XRD measurements of Sb_2Te_3 thin films annealed at different temperatures.
(D) Cycled resistivity measurement of the corresponding samples.
(E) Transport measurements of two Sb_2Te_3 samples annealed at 140 °C and 300 °C.
Figure adapted from Fig. 2 and 3 of Ref. [2].

References and Publications

[1] RONNEBERGER I, ZANOLLI Z, WUTTIG M, MAZZARELLO R. Changes of Structure and Bonding with Thickness in Chalcogenide Thin Films, Adv. Mater. 32, 2001033 (2020).

[2] XU Y, WANG X, ZHANG W, SCHÄFER L, REINDL J, VOM BRUCH F, ZHOU Y, EVANG V, WANG JJ, DERINGER VL, MA E, WUTTIG M, MAZZARELLO R. Materials screening for disorder-controlled chalcogenide crystals for phase-change memory applications, Adv. Mater. 33, 2006221 (2021)

Selected conference participations

- Atomistic simulations of phase-change materials, tutorial given at the 2020 Virtual Spring/Fall Meeting of the Materials Research Society, USA, November 27-December 4, 2020
- Materials screening for Anderson localization in disordered chalcogenides, invited virtual talk given at the 4th Forum on Materials Genome Engineering, Mianyang, China, October 21-23, 2020

National and international cooperations

- WEI ZHANG, Xi'an Jiaotong University, Xi'an, China
- ZEILA ZANOLLI, Debye Institute for Nanomaterials Science, Utrecht University, The Netherlands
- VOLKER L. DERINGER, University of Oxford, UK
- PETER ZALDEN, European XFEL, Schenefeld, Germany
- KLAUS SOKOLOWSKI-TINTEN, University of Duisburg-Essen, Germany

Natural Sciences

Condensed Matter Physics | DFG 307

Novel Materials by Design: The Treasure Map Approach

Project ID: rwth0508
MATTHIAS WUTTIG
CARL-FRIEDRICH SCHÖN
JEAN-FELIX DUSHIMINEZA
1. Institute of Physics,
RWTH Aachen University

MATHIAS SCHUMACHER
Institute for Theoretical Solid State Physics,
RWTH Aachen University

JEAN-YVES RATY,
Physique des solides,
interfaces et nanostructures,
Liège université, Belgium

Project Report

This project has had two major goals; the development of a predictive and quantitative material for solid materials and the classification of different bonding mechanisms to assist in the design of material properties. As this report shows, significant progress has been made regarding both goals, as also evidenced by publications and invited presentations at international conferences. Here, we briefly sketch the most relevant findings.

Figure 1 shows a map based on quantum-chemical calculations performed within this project. We can separate materials employing different bonding mechanisms based upon the determination of the sharing and transfer of electrons between adjacent atoms. Interestingly, this map also provides evidence for a novel fourth bonding mechanism, i.e. 'metavalent bonding'. The map can help to explain and predict property trends as shown on the following website: https://materials-map.rwth-aachen.de/

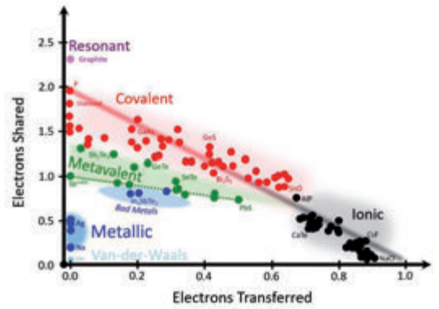

Figure 1: Map based on quantum-chemical calculations performed within this project. Upon determination of the sharing and transfer of electrons between adjacent atoms and the corresponding material properties we can distinguish three fundamental bonding mechanisms (metallic, covalent and ionic bonding) and can identify a novel fourth bonding mechanism, i.e. 'metavalent bonding'.

Subsequently, we have worked together with two colleagues from Computer Science (Prof. Martin Grohe and Leif Kobbelt) to classify the different materials according to their properties. Interestingly, the analysis confirms the existence of four different classes of materials, providing further confirmation of the class of metavalently bonded solids.

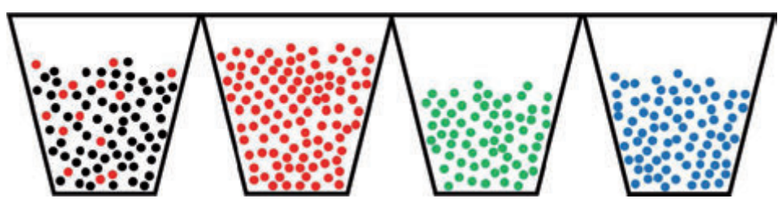

Figure 2: Illustration of the result. The four pots correspond to the clusters found by the algorithm purely numerically and without model knowledge. The color of the dots represents the clusters found on the basis of the model.

Metavalent bonded can be described as the competition zone between electron localization as in ionic and covalently bonded compounds and electron de-localization as in metallic compounds. It is striking that the competition zone between different bonding mechanisms is a well-defined bonding mechanism on its one, with a distinct property portfolio and bond rupture.

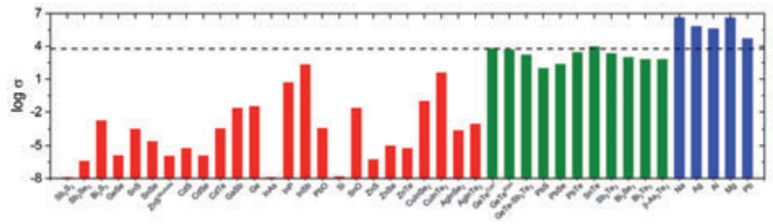

Figure 3: The electrical conductivity data of some representative covalently (red) and metallically bonded (blue) materials, compared with materials using MVB (green). To maximize the clarity of the viewgraph, we restrict the conductivity range between 10^7 S cm^{-1} (good metals such as Ag) and 10^8 S cm^{-1} (pure intrinsic semiconductors such as Si) at room temperature. Materials utilizing MVB all fall into a narrow range of conductivities close to the Mooij value of about 6 x10^3 S cm^{-1} (dashed line) for bad metals.

Selected conference participations

- Invited Talk, EPS Madrid,
  Designing metal – insulator transitions in heavy chalcogenides, August 2020

National and international cooperations

- RICCARDO MAZZARELLO, Department of Physics, Sapienza University of Rome, Italy
- JOHN ROBERTSON, Engineering Department, Camebridge University, UK
- CARLO GATTI, Istituto di Scienze e Tecnologie Molecolari,
  Università degli Studi di Milano, Italy
- JEAN-YVES RATY, Interfaces and Nanostructures, Université de Liège, Belgium
- CHRISTOPHE BICHARA, Centre Interdisciplinaire de Nanoscience de Marseille,
  CNRS and Aix-Marseille University, France

Publications

- WUTTIG M, SCHÖN CF, SCHUMACHER M, ROBERTSON J, GOLUB P, BOUSQUET E, RATY JY.
  Halide perovskites: third generation photovoltaic materials empowered by metavalent bonding, arXiv:2012.03794
- CHENG Y, WAHL S, WUTTIG M.
  Metavalent Bonding in Solids: Characteristic Representatives, Their Properties and Design Options, Physica Status Solidi: Rapid Research Letters 2000482 (2020)
- MAIER S, STEINBERG S, CHENG Y, SCHÖN CF, SCHUMACHER M, MAZZARELLO R, GOLUB P, NELSON R, COJOCARU-MIRÉDIN O, RATY JY, WUTTIG M.
  Discovering electron transfer driven changes in chemical bonding in lead chalcogenides (PbX, where X = Te, Se, S, O),
  Advanced Materials 32, 202005533 (2020)
- KOOI BJ, WUTTIG M.
  Chalcogenides by Design: Functionality Through Metavalent Bonding and Confinement, Advanced Materials 32, 1908302 (2020)

Natural Sciences

Condensed Matter Physics | DFG 307

Properties of magnetic materials calculated using a high throughput framework for ab-initio Korringa-Kohn-Rostoker Green function method

Project ID: jara0182

ROMAN KOVACIK
ROBIN HILGERS
Peter Grünberg Institute (PGI-1) and Institute for Advanced Simulation (IAS-1), Forschungszentrum Jülich, Germany

Project Report

Experimentally known crystalline materials without the inversion symmetry and containing magnetic elements were screened, based on the data available in the Inorganic Crystal Structure Database. Out of approximately 10000 unique materials as possible candidates, about 900 meet the additional criteria of being stoichiometric, having the concentration of the magnetic elements at least 20% and containing no f-elements. Such materials could be promising candidates to host non-trivial magnetic textures for data storage solutions and other spintronic applications. To identify the potential candidate compounds, the magnetic transition critical temperature has to be reasonably high and, e.g., the Dzyaloshinskii-Moriya interaction has to be present.

For the majority of them, the self-consistent potential, density of states and magnetic interaction parameters were computed using the Korringa-Kohn-Rostoker Green function (KKR-GF) method. In preparation to do so, several python codes were developed in order to utilize the high-throughput framework AiiDA (Automated Interactive Infrastructure and Database for Computational Science). Furthermore, python utility was developed to automatically find the best crystallographic coordinates for vacant positions, which is a particularly important part of the system setup in order to achieve a good angular momentum expansion convergence in the KKR-GF method.

In addition, for the selected materials exhibiting strong magnetic interactions, the magnetic transition critical temperature (e.g. the Curie temperature) and the magnetic anisotropy was calculated. The critical temperature was evaluated by applying the Monte Carlo method. Several techniques were developed in order to optimize the computational time usage while keeping the high quality of the collected data statistics. The magnetic anisotropy was calculated from the atom-resolved band energies.

The collected data are currently analyzed. Using this data, the spin dynamics simulations are planned in order to confirm the potential of various materials to stabilize non-trivial magnetic textures such as skyrmions or hopfions. Based on the sufficient volume of the output data, various machine learning techniques are in testing and preparation in order to gain a deeper insight in the relationship between the crystal structure, chemical composition and potential to form non-trivial magnetic textures.

Using the calculated Curie temperature as well as the determined magnetic and additional non-magnetic properties on the atomic level the possibilities to use machine-learning algorithms to predict the Curie temperature have been investigated. It was found that machine-learning models are easily capable to classify the Curie temperature based on the collected data. Given the scientific interest in magnetic materials with large Curie temperatures the models could be used to screen materials for this property without the necessity to compute the complete set of candidate materials. To improve the predictive power various models have been used and tuned in order to optimize the resulting accuracy of the predicted Curie temperatures. In the course of this optimization also regression models have been evaluated and applied.

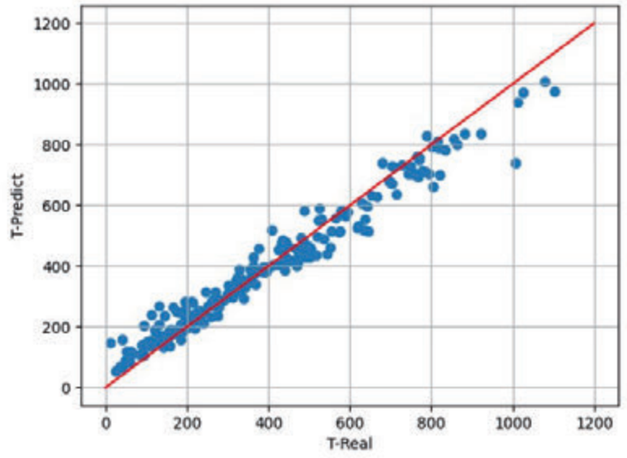

Figure: Predictions of the Curie temperature (in Kelvin) of the acquired data of magnetic Heusler alloys using a Random Forest Regression model compared to the real Curie temperatures. Matching predictions and simulated Curie temperatures would be located on the red line. Test Score on this model is ~0.8.

National and International Cooperations

- PHIVOS MAVROPOULOS, University Athens, Greece

Natural Sciences

Condensed Matter Physics | DFG 307

Impurity effects in next-generation topological materials

Project ID: jara0191

PHILIPP RÜSSMANN
STEFAN BLÜGEL
Peter Grünberg Institute (PGI-1) and Institute for Advanced Simulation (IAS-1), Forschungszentrum Jülich, Germany

PHIVOS MAVROPOULOS
Department of Physics, National and Kapodistrian University of Athens, Greece

Project Report

With our computing time project Impurity effects in next-generation topological materials we aim at using density functional theory calculations to understand and design physical properties in novel solid-state materials. A particular focus lies on the understanding the effect of, naturally occurring or intentionally deposited, defects and imperfections in topological matter. Topological materials are characterized by nontrivial twists in their electronic structure that can lead to protected edge or surface states, the quantum anomalous Hall insulator or even realization of Majorana zero modes. These exotic states of matter could lead to a plethora of technological advancements in the fields of low-energy electronics, spin-orbitronics or fault tolerant quantum computing.

Our investigations can be grouped into three topics: (i) combining magnetism with topological insulators, (ii) investigating the spin and orbital texture of the electronic structure in topological semimetals and (iii) extending our simulation software for the material-specific quantum mechanical description of heterostructures of superconductors and other (non-superconducting, magnetic, topological) materials.

Combining magnetism with topology can lead to the realization of the quantum anomalous Hall (QAH) insulator. We collaborated with colleagues from the University of Würzburg who perform experiments on magnetically doped topological insulators to investigate the exchange interactions in the V- and Cr-doped topological insulators $(Bi,Sb)_2Te_3$ [npj quantum materials 5, 87 (2020)] as well as in Eu-doped Bi_2Te_3. [Physical PRB 102, 184401 (2020)] In combination with photoemission and X-ray circular magnetic dichroism (XMCD) measurements we were able to understand the importance of microscopic control over the electronic structure for magnetism in V:$(Bi,Sb)_2Te_3$ and Cr:$(Bi,Sb)_2Te_3$. Our insights into the exchange coupling mechanism helps to understand and optimize the ferromagnetic magnetic state in these QAH systems. With the study of Eu:Bi_2Te_3 we ventured in the field of rare-earth doping which are often characterized by large magnetic moments. The combination of experiments and our calculations revealed that Eu dopants in Bi_2Te_3 exhibit weak antiferromagnetism due to the strongly localized nature and the half-filling of the f-electrons in the rare-earth's valence shell. We are now exploring the possibility to influence the magnetic coupling with co-doping with 3d or 4d elements where we hope to be able to stabilize a stable ferromagnetic state with, due to the presence of Eu, an increased average magnetic moment in the doped crystal.

In the field of topological semimetals, we explore the type-II Weyl semimetal candidates $MoTe_2$ and WTe_2 as well as the Dirac semimetal $NiTe_2$. In this research activity we collaborate with colleagues from the groups of C. Tusche and L. Pluczinski (both PGI-6, FZ Jülich) who perform angular resolved photoemission experiments in different setups. These experiments are able to resolve the spin polarization and circular dichroism in the electronic structure. Together with the experiments, our calculations of the spin and orbital texture in allow new insights into the electronic structure of topological semimetals. The investigated crystals belong to the class of layered crystals that are only weakly bound by van der Waals forces. Van der Waals materials are very interesting building blocks that offer unique possibilities of tailoring the (topological) properties of the electronic structure which we would like to continue to investigate in the future.

Finally, we have made significant progress on the development of a quantum mechanical simulation code that combines density functional theory with superconductivity on the basis of the Bogoliubov de Gennes (BdG) formalism. To this end we have extended our full potential relativistic Korringa-Kohn-Rostoker Green's function code (KKR) [https://jukkr.fz-juelich.de] by the BdG method that allows to treat inhomogeneous heterostructures of superconductors and non-superconductors.

In collaboration with colleagues from the Universities of Athens and Mainz we have been verifying the correctness of our implementation and started first productive calculations. We also began to extend our new KKR-BdG code with the possibilities to include defects and imperfections also in the superconducting state. This will allow us to investigate the interfaces of superconductors and, for example, topological insulators in more detail which may eventually help realizing stable Majorana edge modes.

The development and application of the KKR-BdG code is a core deliverable of our involvement in the cluster of excellence Matter and Light for Quantum Computing (ML4Q) [https://ml4q.de] where the backing with computing time granted on CLAIX is an invaluable support.

Selected Conference Participants

- PHILIPP RÜSSMANN, Calculating interfaces with superconductors based on DFT, ML4Q Conference 2020, Schleiden, Germany, February 2020.

National and international Cooperations

- KENTA HAGIWARA, Momentum microscopy group of C. Tusche, Peter Grünberg Institute (PGI-6), Forschungszentrum Jülich, Germany
- LUKASZ PLUCZINSKI, Peter Grünberg Institutee (PGI-6), Forschungszentrum Jülich, Germany
- THIAGO PEIXOTO, Experimental Physics VII, Würzburg University, Germany
- VLADIMIR HINKOV, Experimental Physics IV, Würzburg University, Germany
- TOM G. SAUNDERSON, Institute of Physics, Johannes Gutenberg-Universität Mainz, Germany

Publications

- KOSMA A, RÜSSMANNP, BLÜGEL S, MAVROPOULOS P.
  Strong spin-orbit torque effect on magnetic defects due to topological surface state electrons in Bi_2Te_3. Physical review. 2020; B 102: 144424.
- PEIXOTO TRF, ET AL.
  Non-local effect of impurity states on the exchange coupling mechanism in magnetic topological insulators. npj quantum materials. 2020; 5: 87.
- TCAKAEV A, ET AL.
  Incipient antiferromagnetism in the Eu-doped topological insulator Bi_2Te_3. Physical review. 2020; B 102: 184401.

Natural Sciences

Condensed Matter Physics | DFG 307

Transport mechanisms in nano-scaled amorphous phase-change materials

Project ID: jara0199

MARTIN SALINGA
Institute of Materials Physics,
WWU Münster, Germany

NILS HOLLE
Institute of Materials Physics,
WWU Münster, Germany

RICCARDO MAZZARELLO
Department of Physics,
Sapienza University of Rome, Italy

IDER RONNEBERGER
Institute for Theoretical Solid State Physics,
RWTH Aachen University

Project Report

In recent years, electronic memories based on phase-change materials (PCMs) have steadily matured reaching commercial availability as a storage class memory produced by Intel. The uniqueness of PCMs stems from their fast, reliable and durable, non-volatile memory capabilities. These materials, most of them found in the ternary phase diagram of Ge, Sb, and Te, exist in at least two structurally distinct solid phases, the amorphous and the crystalline phase,which differ in their optical and electrical properties enabling the storage of information. PCMs can be repeatedly switched between the two phases, where the amorphous phase is formed by melting and rapidly quenching the liquid phase of the material.

The future impact of phase-change devices in electronics and storage applications significantly depends on the ability to be continuously scaled to smaller sizes. Such scaling will not only increase data density and enable neuromorphic hardware capable of processing large amounts of information, but may also lead to increased device speeds, stability, endurance, and decreased power consumption per operation. This project aimed at gaining a deeper understanding of the transport mechanism in highly nano-scaled phase-change devices in the melt-quenched amorphous state. We focused onsingle-elemental amorphous antimony, which was recently introduced as a viable candidate for aggressively nano-scaled phase-change devices.

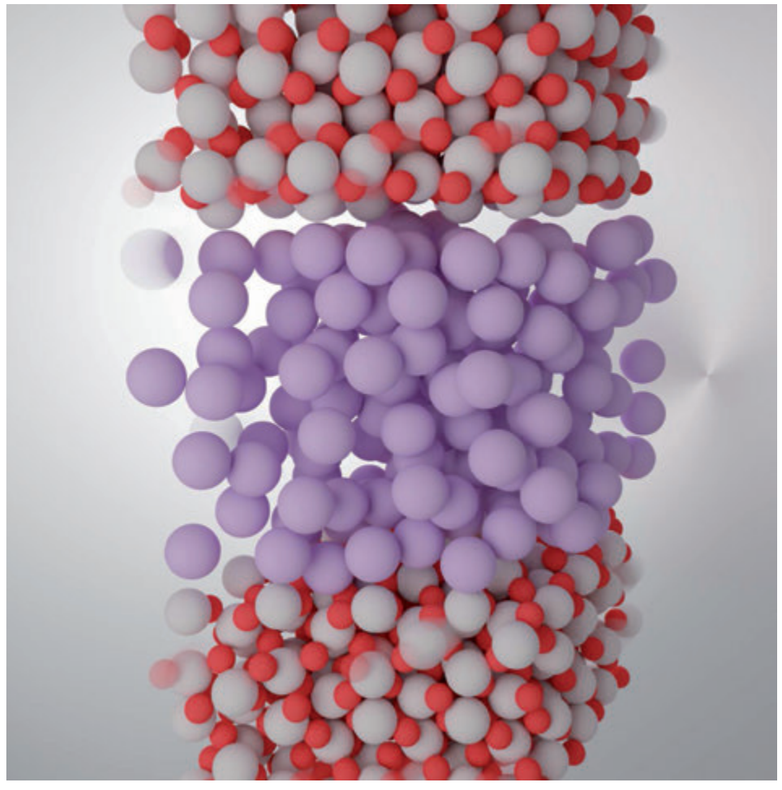

Figure 1: Model of an antimony thin film confined by a dielectric layer.

Existing transport models for the amorphous phase of phase-change materials are mainly based on a multiple-trapping picture within a Poole-Frenkel model, which is based on thermal emission from ionizable defect centers. Both due to the progressing nano-scaling of phase-change devices as well as the single-elemental character of recently proposed devices consisting of pure Sb, the applicability of these models in aggressively nano-scaled devices has by now become highly questionable.

In this project we therefore aimed at studying transport by means of ab-initio methods reflecting the nano-scaled dimensions of the devices of interest. Using Density Functional Theory (DFT) as implemented in the Quantum Espresso suite of programs, we studied the electronic structure of the pure PCM (antimony), mainly based on models that have already been generated in previous projects, as well as the electronic properties in interfacial models including a dielectric material, which represents the substrate material used in the fabrication of actual devices. A large set of interfacial models of amorphous antimony thin films and the dielectric material were obtained within this period using melt quenching in ab-initio molecular dynamics simulations with the CP2K DFT code.

We used most of the granted computing resources for this purpose. Subsequent extensive calculations of the local and projected density of states at different temperatures in combination with a statistical evaluation of the atomic structure gave us valuable insight into the temperature-dependent electronic structure of pure and confined antimony and the influence of confinement both on the electronic structure and on the dynamic properties.

Our final goal is an investigation of full device-like structures with the PCM confined in all three dimensions through both a dielectric and the electrodes. In an intermediate step, interfacial models including the PCM and an electrode material only will allow us to perform first direct calculations of the transmission in the amorphous phase.

Natural Sciences

Condensed Matter Physics | DFG 307

Quantum Monte Carlo Simulations of Magnetic Phase Transitions

Project ID: jara0205
STEFAN WESSEL
LUKAS WEBER
NILS CACI
FLORIAN KISCHEL
ALEXANDER SUSHCHYEV
Institute for Theoretical Solid State Physics, RWTH Aachen University

Project Report

Recent advances in the fabrication of two-dimensional electron systems, such as in twisted bilayer graphene, have exhibited the emergence of strongly correlated states, which are reminiscent of other material classes, e.g., the transition-metal oxides, where the interplay of competing electronic instabilities leads to rich phase diagrams [1,2]. In particular, these findings have renewed interest in the symmetry-broken phases of correlated Dirac fermions, due to the evidence of gap openings near charge neutrality.

Interacting Dirac fermion systems are also of fundamental interest from a general field-theoretical perspective, and are thus in focus of intensive recent research. Based on these developments, Dirac fermion systems were argued to host markedly intriguing phenomena, such as the emergence of enhanced symmetry lines or the stabilization of quantum criticality beyond the realms of the traditional Landau-Ginzburg-Wilson (LGW) theory of critical phenomena. For example, it was argued that Dirac fermions on graphene's honeycomb lattice support deconfined quantum critical points (DQCPs) via the condensation of topological defects or anticommuting mass terms [3,4].

Moreover, recent theoretical calculations suggest that emergent O(N) symmetries are a prevalent feature of deconfined quantum phase transitions and beyond. This recent progress raises two important, fundamental issues that are intimately related: (i) the stability of enhanced symmetry states in Dirac materials and (ii) their relation to the apparent emergence of unconventional criticality in such systems. In our Rapid Communication [5], we solved both of these issues by identifying the generic features of Dirac fermions interacting with the quantum fluctuations of competing symmetry-breaking order parameters using two complementary, non-perturbative approaches. For this purpose, we formulated a relativistic quantum field theory, which we analyzed using advanced renormalization group (RG) methods, and which describes both the Dirac fermions and the coupled symmetry-breaking order parameters.

Remarkably, we found for such systems, rather generically, a stable quantum multicritical fixed point, which moreover exhibits an emerging enhanced symmetry. Moreover, we identified an extended phase coexistence regime to expand from the high-symmetry fixed point, in which both order parameters take on finite values simultaneously. Furthermore, we confirmed this coexistence phase by direct unbiased and controlled quantum Monte Carlo (QMC) simulations.

For this purpose, we derived an effective quantum spin model that emerges in the strongly interacting regime of an interacting Dirac fermion model, and which can be simulated by more efficient, sign problem-free QMC methods using cluster updates and larger lattices than accessible to the QMC approach for the original fermionic model. Therefore, our combined approach sheds light on the nature of quantum critical fermions coupled to bosonic fields as in Ref. [4], and further challenges the scenario of deconfined quantum criticality in quantum spin-Hall insulators [3]. It appears promising to also experimentally probe the physics that we uncovered in Ref. [5] , given the very recent advances in the experimental studies of twisted bilayer graphene with Dirac points indeed located in proximity to several competing orders.

References

[1] Y. CAO, V. FATEMI, A. DEMIR, S. FANG, S. L. TOMARKEN, J. Y. LUO, J. D. SANCHEZ-YAMAGISHI, K. Watanabe, T. Taniguchi, E. Kaxiras et al., Correlated insulator behaviour at half-filling in magic-angle graphene superlattices, Nature (London) 556, 80 (2018).

[2] Y. CAO, V. FATEMI, S. FANG, K. WATANABE, T. TANIGUCHI, E. KAXIRAS, and P. JARILLO-HERRERO, Unconventional superconductivity in magic-angle graphene superlattices, Nature (London) 556, 43 (2018).

[3] Y. LIU, Z. WANG, T. SATO, M. HOHENADLER, C. WANG, W. GUO, and F. F. ASSAAD, Superconductivity from the condensation of topological defects in a quantum spin-Hall insulator, Nat. Commun. 10, 2658 (2019).

[4] T. SATO, M. HOHENADLER, and F. F. ASSAAD, Dirac Fermions with Competing Orders: Non-Landau Transition with Emergent Symmetry, Phys. Rev. Lett. 119, 197203 (2017).

[5] E. TORRES, L. WEBER, L. JANSSEN, S. WESSEL and M. M. SCHERER, Emergent symmetries and coexisting orders in Dirac fermion systems, Phys. Rev. Research 2, 022005 (2020).

National and international cooperations

- FREDERIC MILA, EPFL Lausanne, Lausanne, Switzerland
- THOMAS LANG, University of Innsbruck, Austria
- LUKAS JANSSEN, Technische Universität Dresden, Germany
- MICHAEL M SCHERER, Universität zu Köln, Germany

Publications

- D'EMIDIO J, WESSEL S, MILA F. Reduction of the sign problem near T=0 in quantum Monte Carlo simulations, Phys. Rev. B 102, 064420 (2020).
- HESSELMANN S, HONERKAMP C, WESSEL S, LANG TC. Quantifying the fragility of unprotected quadratic band crossing points, Phys. Rev. B 101, 075128 (2020).
- TORRES E, WEBER L, JANSSEN L, WESSEL S, SCHERER MM. Emergent symmetries and coexisting orders in Dirac fermion systems, Phys. Rev. Research 2, 022005 (2020).

Natural Sciences

Particles, Nuclei and Fields | DFG 309

Dark Simulations: Understanding the Dark Side of Particle Physics and Cosmology

Project ID: jara0184

JULIEN LESGOURGUES
FELIX KAHLHÖFER
CHRISTIAN FIDLER
JESÚS TORRADO
SILVIA MANCONI
NILS SCHÖNEBERG
PATRICK STÖCKER
KATHRIN NIPPEL
Institute of Theoretical Particle Physics and Cosmology (TTK), RWTH Aachen University

DEANNA HOOPER
Service de Physique Théorique, Université Libre de Bruxelles, Brussels, Belgium

JANINA RENK
OSKAR KLEIN
Centre for Cosmoparticle Physics, Stockholm University, Stockholm, Sweden

CHRISTIAN PARTMANN
Max Planck Institute for Astrophysics, Garching Germany (*)

NIKLAS BECKER
Institute for Theoretical Physics, Johann Wolfgang Goethe-Universität, Frankfurt, Germany

JONAS EL GAMMAL
Institute of Mathematics and Physics, University of Stavanger, Stavanger, Norway

Project Report

Sub-Project 1: N-body Simulations: We used the JARA cluster to run several high precision N-body simulations using both the gadget and Gevolution codes. In these runs we used a novel method that we have developed to efficiently include the impact of neutrinos and general relativity on structure formation. Exploiting these runs we were able to confirm the numerical stability and convergence of the new method and demonstrate that it produces results that are as accurate as competing methods while being numerically significantly more efficient. We further were able to confirm that our method works across the entire viable mass range for standard model neutrinos. Our results have been published in [1].

Sub-Project 2: Machine Learning in Astroparticle Physics and Cosmology: We have successfully developed, trained and validated a neural network able to substantially reduce the computation time needed for calculating Dark Matter (DM) signals expected in AMS-02 antiproton data for different models. An architecture based on recurrent neural networks has been found to outperform other tested deep neural networks. Computing resources have been fundamental to produce our training set, and to develop the neural network architecture. We have assessed the compatibility of the simulated signals with AMS-02 data by marginalizing over nuisance parameters, and developing a method based on importance sampling. We have finally applied our fast prediction setup to two specific DM models, finding constraints largely in agreement with previous works. Before releasing a public code and finalizing a publication we are currently updating the neural network to the new AMS-02 data released at the beginning of 2021. In a Gaussian Process related project, we utilised the cluster to test whether the dimensionality of the emulated posterior could be reduced by marginalising over fast-to-vary parameters. We showed this procedure to be reasonably successful when demonstrated with the Planck 2018 likelihood (20 marginalised fast parameters). For this sub-task, multiple publications are planned in 2021.

Sub-project 3: Testing non-standard Dark Matter Models: To ease a tension between the strength of clustering as measured through the shear of nearby galaxies and as inferred from the CMB anisotropies, many dark matter models have been proposed. The cannibal dark matter model remains close to relativistic due to a number-changing exothermal 3 to 2 self-interaction, which also allows it to avoid strong CMB constraints on similar models like warm or hot dark matter. By running several MCMC chains we observe that the cannibalistic dark matter model is able to ease the tension completely without strongly spoiling CMB observables, showing that the model is slightly preferred compared to the standard model [2]. Dark matter interacting with multiple particles and dark radiation has been investigated for its effects on the clustering and H0 tensions. With dedicated MCMC runs on the jara cluster, we show that the limits of one interaction are barely impacted by including another interaction, and that a combination of dark matter photon and dark matter dark radiation scatterings (as motivated from kinetic mixing) significantly eases both tensions [3]. Spectral distortions of the CMB allow to constrain energy release from DM decay and interactions, as well as the primordial power spectrum. Using the computing resources granted to us, we investigated the tight constraints that a future spectral distortion mission can place on various standard and non-standard DM and inflationary scenarios, updating and improving on previous analyses [4, 5, 6]. We have used current data from the CMB, from Lyman-alpha forests, etc. to publish new bounds on several further dark matter candidates for hot dark matter (including new bounds on neutrino masses, in [7, 8]) and warm dark matter [7].

Sub-project 4 : Global fits of axion-like particles: In order to study the effect of DM models on cosmological and astrophysical observables, as well as other observables of particle physics, by means of global fits, we have introduced the CosmoBit [9] module as an extension to the existing GAMBIT framework. Since DM models can affect cosmological observables at several stages in the cosmological history, such as inflation, Big Bang Nucleosynthesis, and recombination, as well as late-time observables, the initial release of CosmoBit includes many scans with dedicated sets of likelihoods in order to validate the results obtained with CosmoBit against existing results. We also showed how dark matter models can affect cosmological observables and provided a general structure in order to allow for studies of custom DM models. One of the testable consequences of these models is the modification of the radiation content, either by dark radiation or by a modified neutrino to photon temperature ratio. We performed high-resolution scans to show that allowing for both modifications as well as non-zero neutrino masses can loosen the cosmological bound on the neutrino masses up to the current sensitivity of laboratory measurements. Together with the release of CosmoBit [9], we published its first concrete showcase [10]. We combined the most robust data from cosmology and particle physics to constrain the mass of the lightest neutrino, leading to the tightest bound to date. We have performed many high-dimensional scans which differ by different assumptions on N_eff and the mass ordering of the neutrino sector [10].

Sub-project 5: Forecasts for the Euclid satellite mission
We have made progress on our project to build one possible analysis pipeline for the Euclid satellite collaboration. This will be published in 2021.

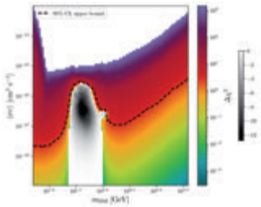

Publications and References

[1] PARTMANN C ET AL. Fast simulations of cosmic large-scale structure with massive neutrinos, 2020, JCAP09(2020)018, arXiv: 2003.07387
[2] HEIMERSHEIM S ET AL. Cannibalism hinders growth: Cannibal Dark Matter and the S8 tension, 2020, JCAP 12 (2020) 016, arXiv: 2008.08486
[3] BECKER N ET AL. Cosmological constraints on multi-interacting dark matter, 2021, JCAP 02 (2021) 019, arXiv: 2010.04074
[4] SCHÖNEBERG N ET AL. Constraining the inflationary potential with spectral distortions, 2021, JCAP 03 (2021) 036, arXiv: 2010.07814
[5] LUCCA M ET AL. The synergy between CMB spectral distortions and anisotropies, 2020, JCAP 02 (2020) 026, arXiv:1910.04619
[6] FU H ET AL. Unlocking the synergy between CMB spectral distortions and anisotropies, 2020, arXiv: 2006.12886
[7] PALANQUE-DELABROUILLE N ET AL. Hints, neutrino bounds and WDM constraints from SDSS DR14 Lyman-α and Planck full-survey data, 2020, JCAP 04 (2020) 038, arXiv:1911.09073
[8] BOLLIET B ET AL. Including massive neutrinos in thermal Sunyaev Zeldovich power spectrum and cluster counts analyses, 2020, Mon.Not.Roy.Astron.Soc. 497 (2020) 2, 1332-1347, arXiv: 1906.10359
[9] The GAMBIT Cosmology Workgroup CosmoBit: A GAMBIT module for computing cosmological observables and likelihoods, 2020, JCAP 02 (2021) 022, arXiv: 2009.03286
[10] The GAMBIT Cosmology Workgroup Strengthening the bound on the mass of the lightest neutrino with terrestrial and cosmological experiments, 2020, arXiv: 2009.03287

Selected conference participations

- CHRISTIAN FIDLER: "Efficient N-body simulations with massive Neutrinos", April 08, 2020, Harvard University, Cambridge, Massachusetts, USA
- JULIEN LESGOURGUES: "The sound Horizon from Big Bang Nucleosynthesis" - International cosmology conference "H0 2020", June 25, 2020, ESO, Munich, Germany
- PATRICK STÖCKER: "CosmoBit Tutorial", Tools for High Energy Physics and Cosmology Conference, Nov. 04, 2020, Institut de Physique des 2 Infinis de Lyon (IP2I), Lyon, France
- FELIX KAHLHÖFER: "CosmoBit and DarkBit: Building bridges between particle physics and cosmology" - Gordon Godfrey Workshop on Astroparticle Physics, December 03, 2020, University of New South Wales, Sydney, Australia

Selected national and international cooperations

- NATHALIE PALANQUE-DELABROUILLE, Institute for Research on the fundamental laws of the universe, Saclay, France
- JENS CHLUBA, Jodrell Bank Observatory, Manchester, UK
- SILVIA GALLI, Institut Astrophysique de Paris, France
- MICHAEL KORSMEIER, Oskar Klein Centre, Stockholm University, Sweden
- MATTEO LUCCA, Service de Physique Théorique, Université Libre de Bruxelles, Belgium

Natural Sciences

Particles, Nuclei and Fields | DFG 309

Nuclear Lattice Simulations

Project ID: jara0015

ULF-G. MEISSNER,
DILLON FRAME,
TIMO A. LÄHDE,
THOMAS LUU,
Institute for Advanced Simulation,
Institute for Nuclear Physics,
Theory of the strong
interactions (IKP-3/IAS-4),
Forschungszentrum Jülich, Germany;
Helmholtz-Institut für Strahlen- und Kernphysik (Theorie) and
Bethe Center for Theoretical Physics,
Universität Bonn, Germany

JOAQUIN DRUT,
Department of Physics & Astronomy,
University of North Carolina,
Chapel Hill, USA

SERDAR ELHATISARI,
Department of Engineering,
Karamanoglu Mehmetbey University, Turkey

EVGENY EPELBAUM,
HERMANN KREBS,
Ruhr University Bochum,
Fakultät für Physik und Astronomie,
Institut für Theoretische Physik II, Germany

DEAN LEE,
Facility for Rare Isotope Beams and
Department of Physics and Astronomy,
Michigan State University,
East Lansing, USA

NING LI,
Sun Yat-sen University, Guangzhou, China

BING-NAN LU,
Graduate School of the Chinese Academy
of Engineering Physics, Beijing, China

GAUTAM RUPAK,
Department of Physics & Astronomy,
Mississippi State University, USA

Project Report

During 2020, the Nuclear Lattice Effective Field Theory (NLEFT) collaboration has reached the milestone of including hyperons into NLEFT calculations for the first time. These ab initio calculations follow the pattern of chiral nuclear EFT, whereby interactions are included term by term in order of importance. We have also gained new insight into the connection between QCD in the limit of large number of colors and the (approximate) spin-isospin-exchange symmetry of the nuclear forces, known as Wigner's SU(4) symmetry.

In particular, we have investigated the impact of the QCD vacuum at non-zero vacuum angle theta on the properties of light nuclei, Big Bang nucleosynthesis, and stellar nucleosynthesis. The inclusion of lambda hyperons into the ab initio framework of NLEFT requires the use of specialized Monte Carlo (MC) methods to avoid large sign oscillations. We have made use of the fact that the number of hyperons (Y) is typically small compared to the number of nucleons (N) in realistic hypernuclei. This has allowed us to use the impurity lattice Monte Carlo (ILMC) method (developed by scientists within the NLEFT collaboration) where the minority species of fermions in the full nuclear Hamiltonian is treated as a worldline in Euclidean projection time. The nucleons are treated in ILMC as explicit degrees of freedom, with their mutual NN interactions described by auxiliary fields. This is the first application of ILMC to systems where the majority particles are interacting, and we have shown how ILMC can be applied to compute the binding energies of the light hypernuclei. In this exploratory work, we have used spin-independent NN and YN interactions to test the computational power of the ILMC method. We expect ILMC simulations of hypernuclei with up to one hundred or more nucleons to be possible.

We note that the particular set of interactions that we have used can also be directly applied to a bosonic impurity immersed in a superfluid Fermi gas. By modifying the included P-wave interactions of the impurity, we could describe alpha particles immersed in a gas of superfluid neutrons. Strong CP-violation is given in terms of the vacuum angle theta, which is a fundamental parameter of QCD. However, theta is constrained to be very small from the empirical bounds on the neutron eletric dipole moment, which constitutes the so-called strong CP-problem. In some versions of string theory, theta is expected to be of order one, with speculations that this could be realized in the early universe, thus altering nucleosynthesis considerably. We have investigated the impact of non-zero theta on the properties of light nuclei, Big Bang- and stellar nucleosynthesis. Our analysis starts with a calculation of the theta-dependence of the neutron-proton mass difference and neutron decay using chiral EFT. We then consider the theta-dependence of the NN interaction using a one-boson-exchange model and compute the properties of the two-nucleon system. The deuteron is more strongly bound than in nature, and the di-neutron and the di-proton become bound at theta = 0.2 and 0.7, respectively. Using the universal properties of four-component fermions at large scattering length, we deduce the binding energies of the 3N and 4N systems.

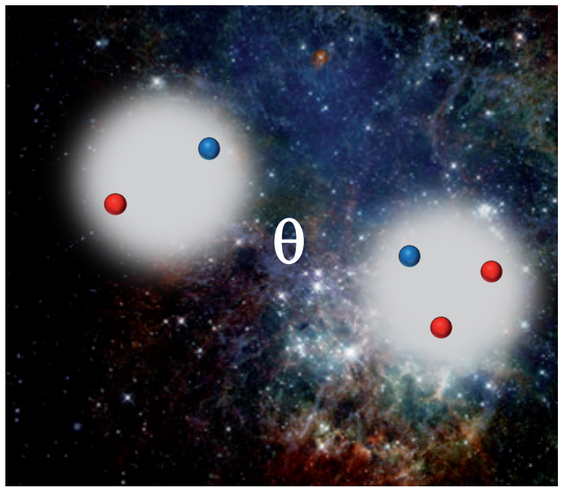

Based on these results, we discuss the primordial abundances of light nuclei, the production of nuclei in stellar environments, and implications for an anthropic view of the universe. Given the constraint that the world is as we observe it, we require theta < 0.1 to approximatively recover the nuclear reaction rates in the Big Bang- and stellar nucleosynthesis. In particular, the deviation of the neutron-proton mass difference to the real world should be < 1%.

Selected honors, prizes, and awards

- EVGENY EPELBAUM, ERC Advanced Grant, Ruhr University Bochum, Germany
- ULF-G. MEISSNER, John von Neumann Exzellenzprojekt 2020, Universität Bonn, Germany

Selected conference participations

- ULF-G. MEISSNER, invited talk, Nuclear lattice effective field theory: Status and perspectives, 10th NIC Symposium, Jülich Supercomputing Centre, Jülich, Germany, February 27-28, 2020

Selected national and international cooperations

- SCOTT BOGNER, B. ALEX BROWN, HEIKO HERGERT, MORTEN HJORTH-JENSEN, Facility for Rare Isotope Beams and Department of Physics and Astronomy, Michigan State University, East Lansing, USA, and Department of Physics and Center for Computing in Science Education, University of Oslo, Norway

Publications

- STELLIN G, MEISSNER UG.
  P-wave two-particle bound and scattering states in a finite volume including QED,
  Eur. Phys. J. A57, (2021) 1, 26.
- FRAME D, LÄHDE TA, LEE D, MEISSNER UG.
  Impurity Lattice Monte Carlo for hypernuclei,
  Eur. Phys. J. A56, (2020) 10, 248.
- MEISSNER UG.
  Precision predictions,
  Nucl. Phys. News 30, (2020) 2, 17-20.
- LU BN, LI N, ELHATISARI S, LEE D, DRUT JE, LÄHDE TA, EPELBAUM E, MEISSNER UG.
  Ab initio nuclear thermodynamics,
  Phys. Rev. Lett. 125 (2020) 19, 192502.
- LÄHDE TA, MEISSNER UG, EPELBAUM E.
  An update on fine-tunings in the triple-alpha process,
  Eur. Phys. J. A56 (2020) 3, 89.

Natural Sciences

Particles, Nuclei and Fields | DFG 309

Higher order QCD predictions for ttX, X = γ, Z, W, H, bb, tt, jj

Project ID: rwth0414
MALGORZATA WOREK
MICHAL CZAKON
HUAN-YU BI
JONATHAN HERMANN
MICHELE LUPATTELLI
JASMINA NASUFI
DANIEL STREMMER
TORSTEN WEBER
Institute for Theoretical Particle Physics and Cosmology, RWTH Aachen University

GIUSEPPE BEVILACQUA
MTA-DE, Debrecen, Hungary

HERIBERTUS BAYU HARTANTO
RENE PONCELET,
Cambridge University, UK

MANFRED KRAUS
Florida State University, USA

Project Report

In this project we have obtained state of the art theoretical predictions for processes that involve top quark pair production with an additional final state. Results for the LHC with NLO QCD higher order corrections to pp -> tt + X production, where X stands for X = γ and W have been provided in the form of the fully flexible Monte Carlo program, HELAC-NLO.

The latter can be used to generate any infrared safe observable with various phase-space cuts, parton distribution functions and the Standard Model input parameters. We calculated NLO QCD corrections to the multi-lepton channels with the top-quark off-shell effects included. Non-resonant and off-shell effects due to the finite W and Z boson width were also consistently taken into account.

In each case dedicated comparisons between the full off-shell theoretical results and the theoretical predictions in the full narrow-width-approximation (NWA) as well as in the NWA scheme but with leading order decays have been provided to check the quality of the approximation in various phase-space regions and to quantify the final size of the theoretical uncertainties due to scale dependence.

Results obtained in this project provide the state-of-the-art theoretical predictions for these processes, which are of high relevance for top quark physics at the LHC. They additionally impact current and future comparisons with experimental data, see e.g., Measurements of inclusive and differential cross-sections of combined ttγ and tWγ production in the eμ channel at 13 TeV with the ATLAS detector, ATLAS Collaboration, JHEP 09 (2020) 049.

Selected conference participations

MALGORZATA WOREK:

- A view on the top quark, QCD@LHC-X conference, Zoom, August 31-September 03, 2020
- Off-shell vs on-shell modelling of top quarks in photon associated production, 13th International Workshop on Top-Quark Physics – TOP 2020, Zoom, September 14-18, 2020
- Theory & MC for ttV, ATLAS HTop workshop, Zoom, October 05, 2020
- Precision top-quark physics at the LHC, Annual Meeting of the SFB TRR 257, Siegen, Germany, October 06-08, 2020
- Brief overview of theory results for on-shell ttW production, LHC Higgs WG1 - ttH/tH subgroup workshop, Zoom, October 23, 2020

GIUSEPPE BEVILACQUA:

- Effects of top-quark decay modeling in ttγ production at the LHC, XXVI Cracow EPIPHANY Conference - LHC Physics: Standard Model and Beyond, Cracow, Poland, January 07-10, 2020
- ttW at NLO accuracy in QCD with realistic final states, 13th International Workshop on Top-Quark Physics – TOP 2020, Zoom, September 14-18, 2020

National and international cooperations

- GIUSEPPE BEVILACQUA, Particle Physics Research Group, Hungarian Academy of Sciences, Debrecen, Hungary
- HERIBERTUS BAYU HARTANTO, Cavendish Laboratory, University of Cambridge, Cambridge, UK
- MANFRED KRAUS, Physics Department, Florida State University, USA

Publications

- BEVILACQUA G, HARTANTO HB, KRAUS M, WEBER T, WOREK M. Off-shell vs on-shell modelling of top quarks in photon associated production, JHEP 03 (2020) 154
- BEVILACQUA G, BI HY, HARTANTO HB, KRAUS M, WOREK M. The simplest of them all: ttW at NLO accuracy in QCD, JHEP 08 (2020) 043

Natural Sciences

Statistical Physics, Soft Matter, Biological Physics, Nonlinear Dynamics | DFG 310

Growth and Dynamics of Tissues

Project ID: rwth0475

JENS ELGETI
Institute of Biological Information Processing: Theoretical Physics of Living Matter (IBI-5/IAS-2), Forschungszentrum Jülich, Germany

TOBIAS BÜSCHER
Institute of Biological Information Processing: Theoretical Physics of Living Matter (IBI-5/IAS-2), Forschungszentrum Jülich, Germany

Project Report

During 2020 we studied competition of two different tissues on a substrate. As predicted we confirm that the stronger or more motile tissue invades the weaker one at constant velocity. Importantly we found two different mechanisms that lead to an instability of the interface between two competing tissues, one based on a difference in motility and the other based on a difference in homeostatic stress and viscosity of the two tissues. For a difference in collective motility, we found that small motility forces stabilize the interface, compared to the absence of motility, in which case the interface is unstable due to diffusion. However, above a critical motility strength, protrusions of the motile into the non-motile tissue form at a well defined wavelength. Interestingly, these protrusion still saturate at a finite width due to nonlinear effects and the overall pattern is remarkably stable.

It had been shown previously that a difference in homeostatic stress alone results in propagation of the interface with a stable front. We found that an additional viscosity contrast between the two tissues results in a fingering instability of the interface above a critical homeostatic stress difference, reminiscent of the Saffman-Taylor instability. In contrast to the motility case, the interface pattern is way more dynamic and the finger moves along the interface, detaches and reforms again.

Highlight result of 2020 was the “liquid-vacuum-coexistence” for self propelled cells. We found that our model of selfpropelled Brownian particles with extended interactions results in a fluid like cell colony, where however no cell escapes. Our simulations show many characteristica of observations made in in vitro experiments on MDCK colonies such as exactly this “liquid-vacuum coexistence” and an overall tension in the colony center. Furthermore, such colonies also display long-range correlations in the local velocity field, which we did not observe in our model initially. We thus proposed an additional velocity alignment interaction, which acts to align the current velocity with the propulsion direction. This results in enhanced coordinated motion of cells, with swirls forming in the center of the colony. The velocity alignment interaction furthermore results in the formation of fingers at the periphery of the colony with strong outward alignment of the cell velocities, reminiscent of growth of real MDCK-Cell colonies.

Selected conference participations

- JENS ELGETI, In-silico Tissue Growth - A Mechanical Model for Tissue Growth and Com petition, Lecture Series on Physics of Tissues (invited), College de France, Paris, France, February 10, 2020
- JENS ELGETI, Physics of Growth: Another form of active Matter, Frühjahrstagung der Deutschen Physikalischen Gesellschaft (invited), Online, March 17, 2020
- JENS ELGETI, Growth mechanics - coexistence and evolution, Physics of Cancer Conference (invited), Leipzig, Germany, September 23, 2020

Publications

- BÜSCHER T, DIEZ AL, GOMPPER G, ELGETI J.
  Instability and fingering of interfaces in growing tissue,
  New Journal of Physics, 22, no. 8, 2020.
- BÜSCHER T, GANAI N, GOMPPER G, ELGETI J.
  Tissue evolution: Mechanical interplay of adhesion, pressure, and heterogeneity,
  New Journal of Physics, 22, no. 3, 033048, 2020.

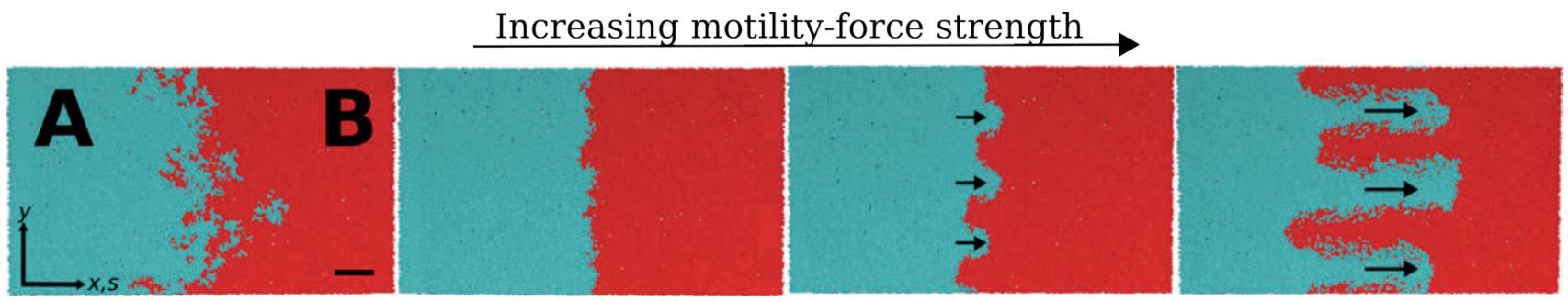

Astronomy and Astrophysics | DFG 311

Cosmic-Ray Physics with the AMS Experiment on the International Space Station

Project ID: jara0052

HENNING GAST
STEFAN SCHAEL
KLAUS LÜBELSMEYER
LEILA ALI CAVASONZA
SOFIA CHOURIDOU
CHAN HOON CHUNG
THOMAS KIRN
NIKOLAY NIKONOV
GEORG SCHWERING
THORSTEN SIEDENBURG
VALERY ZHUKOV
ANDREAS BACHLECHNER
MANBING LI
SICHEN LI
FABIAN MACHATE
ROBIN SONNABEND
Department of Physics, Institute I B, RWTH Aachen University

Project Report

AMS is a detector designed for precision spectroscopy of cosmic rays that was installed on the International Space Station in May 2011. With dimensions of 5x4x3 m³ and a weight of 7.5 tons, AMS is the largest cosmic-ray spectrometer ever built. Its construction began in 1995, and a successful prototype flight aboard the Space Shuttle Discovery proved the feasibility of the detector concept in 1998. Led by Nobel laureate Professor Samuel Ting from MIT, AMS has been constructed and is now operated by an international collaboration of more than 200 scientists and engineers, from Europe, America and Asia. The overall construction costs, including the flight of AMS to the Space Station aboard Space Shuttle Endeavour, have amounted to 1.5 billion US dollars. In Germany, RWTH Aachen has been strongly involved in the AMS project since its inception. One of the main components of AMS, the transition radiation detector (TRD), has been designed and constructed by the I. Physikalisches Institut B under the direction of Professor Stefan Schael. Today, the Aachen group, comprising 20 scientists and students, plays a major role in the analysis of the data gathered by AMS and in the operation and calibration of the instrument.

Since their discovery in 1912, cosmic rays have held many surprises in stock for us, from the discovery of new elementary particles to the most violent processes taking place in the Universe and accelerating cosmic rays to enormous energies. As a multi-purpose instrument for the precision spectroscopy of cosmic rays, AMS was conceived to answer fundamental questions about our Universe: What is the nature of Dark Matter? What happened to the antimatter that must have been produced in the Big Bang? Where are cosmic rays accelerated and how do they propagate through the Milky Way? Answers to these questions will have a profound impact on our understanding about the inner workings of our Universe and help advance fundamental science. In particular, the search for dark matter complements the endeavour to search for new elementary particles at the Large Hadron Collider (LHC) at CERN, Geneva.

AMS so far has recorded more than 170 billion individual particle crossings (so called “events“). The raw data volume collected is on the order of 40 TB per year. AMS employs redundant sub-detectors for particle identification and for energy or momentum measurements (the TRD, an electromagnetic calorimeter, a ring-imaging Cherenkov counter, a silicon tracker and a time-of-flight system). Before any physics analysis of the data can be performed, the information from all these subdetectors has to be pieced together and complicated reconstruction algorithms have to be run for each of them. The resulting high-level data serves as the input for physics analyses and occupies a volume of 160 TB per year of AMS flight on disk. Several processing runs of AMS data have already been conducted successfully on the JUROPA and JUAMS clusters at JSC as the result of the cooperation within JARA.

So far, eighteen publications from the AMS collaboration have appeared in the renowned Physical Review Letters. The findings have received considerable attention among astrophysicists and triggered an enormous amount of theoretical work.

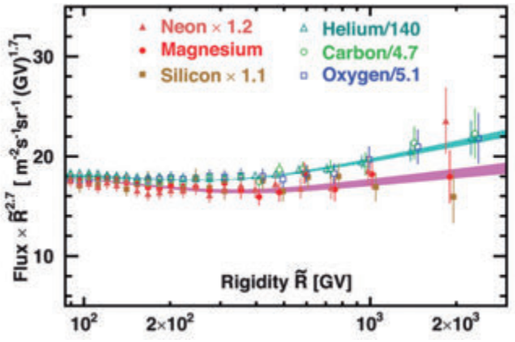

Figure 2: The rigidity dependence of the neon, magnesium, and silicon fluxes compared to the rigidity dependence of the helium, carbon, and oxygen fluxes above 86.5 GV. For display purposes only, the fluxes were rescaled as indicated.

The physics highlight of AMS in 2020 was the detailed study of the heavy ions neon, magnesium, and silicon in cosmic rays (Figure 2). Although these species are believed to be primaries, i.e. they are accelerated in astrophysical sources such as supernova remnants, their energy spectra are distinctly different than those of the lighter primaries, namely helium, carbon, and oxygen. This shows that there are two different classes of primary cosmic rays.

The PhD thesis by Bastian Beischer, completed in the context of this project in 2020, contains measurements of the diffuse gamma-ray emission from the Galactic plane, and energy spectra of the brightest sources of high-energy gamma rays in the sky. The results confirm the need for a correction of the energy scale of the Fermi-LAT detector as previously proposed by the Fermi-LAT team.

Selected conference participations

- STEFAN SCHAEL, “Searching for Antimatter Galaxies - the AMS Experiment on the International Space Station”, Deutsches SMART Meeting “Dubito Ergo Sum Rethinking Respiratory Intensive Care”, Frankfurt, Germany, January 2020.
- STEFAN SCHAEL, “AMS-100: The next generation magnetic spectrometer in Space”, DLR Oberpfaffenhofen, Germany, September 2020.

Selected national and international cooperations

- SAMUEL C. C. TING, Massachusetts Institute of Technology, USA
- BRUNA BERTUCCI, INFN and University of Perugia, Italy
- BERND HEBER, Christian-Albrechts-Universität zu Kiel, Germany

Publications

- AGUILAR M ET AL. (AMS Collaboration), Properties of Neon, Magnesium, and Silicon Primary Cosmic Rays Results from the Alpha Magnetic Spectrometer, Physical Review Letters, 2019; 124: 211102.
- AGUILAR M ET AL. (AMS Collaboration), The Alpha Magnetic Spectrometer (AMS) on the international space station: Part II – Results from the first seven years, Physics Reports, 2021; 894: 1-116.
- BEISCHER B. Measurement of High Energy Gamma Rays from 200 MeV to 1 TeV with the Alpha Magnetic Spectrometer on the International Space Station, PhD thesis, RWTH Aachen University, June 2020.

Natural Sciences

Geophysics and Geodesy | DFG 315

Dark Simulations: understanding the dark side of particle physics and cosmology

Project ID: rwth0316
SÖNKE REICHE
ARIEL T. THOMAS
Institute for Applied Geophysics and Geothermal Energy
RWTH Aachen University

Project Report

The existence of large reserves of fresh to brackish water in continental shelf sediments has been identified as a global phenomena (Post et al. 2013). Several studies have investigated the characteristics of these dynamic systems (Groen et al. 2000; Johnston 1983; Lofi et al. 2013; Micallef et al. 2020). The research has led to an increased understanding of the key driving factors in the emplacement and survival of offshore fresh groundwater. These include the influence of sea-level change both in lowstand periods (Meisler et al. 1984), as well as during marine transgressions (Kooi et al. 2000).

The impact of Pleistocene glaciation has also been examined in regional scale numerical studies on the North American Atlantic margin (Cohen et al. 2010; Siegel et al. 2014). These studies found that presence of ice-sheet cover contributed significantly to offshore fresh groundwater volumes via increased run-off of subglacial meltwater, and enhanced offshore hydraulic heads due to glacial loading.

The primary focus of the study was to test the hypothesis that fresh groundwater was emplaced in New Jersey shelf sediments during the period of extended low-stand associated with the Last Glacial Maximum. Transient numerical simulations of submarine groundwater discharge conducted on a geologically representative New Jersey shelf model, investigated the impact of 4 key factors that influence SGD: (1) Topography-driven flow, (2) Fluctuating sea-level, (3) Permeability anisotropy and (4) Enhanced terrestrial discharge.

The shelf model, originally presented in Thomas et al. (2019), combines sequence stratigraphic interpretation of depth migrated seismic lines (Riedel et al. 2018) with petrophysical properties derived from IODP Expedition 313 well data (Mountain et al. 2010). A simple stochastic analysis was performed to calibrate the facies distribution out of fifty equally likely geological model realizations. Variable-density groundwater discharge across the 2D shelf transect is simulated for a 60 000 year period of the Pleistocene when falling sea-level left much of the shelf sub-aerially exposed.

This study evaluates the relative contribution of each driving factor to the extent of emplaced fresh groundwater on the New Jersey shelf over the period. Finally, hydraulic conditions on the shelf during the subsequent marine transgression until present day were simulated to draw conclusions about the evolution of offshore fresh groundwater reservoirs observed in IODP Expedition 313. The analysis aims to expand the understanding of the freshwater emplacement mechanisms in this passive margin setting, as well as its implications for this global phenomena.

Summary of key scientific findings:

- We observe a correlation between topography and the depth of freshwater emplacement during sea-level lowstand on the New Jersey continental shelf. Our numerical simulations results point to topographic driven flow as the dominant factor driving freshwater emplacement in New Jersey shelf sediments during the low-stand period.
- The shape of the freshwater – seawater interface gives insight to the freshening process in the different regions of the shelf. It reveals the occurrence of convective mixing taking place during periods of recharge. The differential rate of freshening by lithology contributes to complex flow patterns across the model domain. This leads to very complex salinity distributions with an extensive mixing zone.
- Permeability distribution and anisotropy play a major role in the emplacement of fresh groundwater on the shelf. This subsurface property should be well constrained when attempting to characterize offshore freshened groundwater systems.
- The freshening trend exhibits a logarithmic regression with rapid freshening in the early stages of the exposed shelf and then slows to near linear trend as fresh water is driven deeper into sediments.

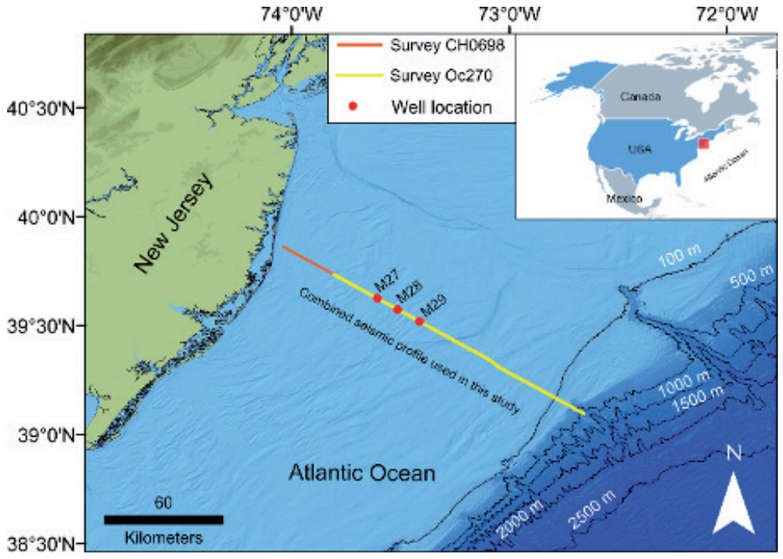

Figure 1: Study area map showing combined 2D seismic lines used to characterize subsurface model

Engineering Sciences

Picture: Pexels

Mechanics | DFG 402

Reconstruction of Damage Models for Thin Shells Based on Phase Field Methods

Project ID: rwth0433
ROGER SAUER
KARSTEN PAUL
Aachen Institute for Advanced Study in Computational Engineering Science,
RWTH Aachen University

Project Report

Phase field models for fracture have gained popularity as they do not require interface tracking techniques or the specification of ad-hoc criteria. In these models, the evolving discontinuity is smeared out and a high resolution of the underlying finite element mesh is required. Within this project, an isogeometric phase field framework to model brittle fracture of thin shell structures has been developed. LR (Locally Refinable) NURBS were used to adaptively locally refine the interface regions. Further, an adaptive time-stepping method was developed such that complicated crack patterns, including kinking, branching, merging and deflection, can be efficiently predicted (also see project rwth0401).

Further, the phase field fracture model was extended to model multi-patch surfaces. As a higher continuity is required for the thin shell and phase field framework, the required continuity has to be restored across patch interfaces. For this, patch constraints have been formulated in order to transmit bending moments across those interfaces and to make sure that the phase field gradient is continuous across the patch interfaces. The constraints are enforced by either a penalty or Lagrange multiplier formulation.

For the first, a problem-independent penalty parameter for the phase field framework is proposed. Qualitative and quantitative comparisons to single-patch and unstructured spline descriptions show excellent agreement with the novel multi-patch framework.

Selected conference participations

- KARSTEN PAUL, CHRISTOPHER ZIMMERMANN, THANG X. DUONG, ROGER A. SAUER, Isogeometric continuity constraints for coupled deformation and phase field models on deforming multi-patch surfaces, VIGA, virtual conference, August 11-12, 2020

Selected national and international cooperations

- THOMAS J.R. HUGHES, Oden Institute of Computational Engineering and Sciences, UT Austin, Texas, USA
- CHAD M. LANDIS, Department of Aerospace Engineering and Engineering Mechanics, UT Austin, Texas, USA
- KRANTHI K. MANDADAPU, Department of Chemical and Biomolecular Engineering, UC Berkeley, California, USA

Publications

- PAUL K, ZIMMERMANN C, MANDADAPU KK, HUGHES TJR, LANDIS CM, SAUER RA, An adaptive space-time phase field formulation for dynamic fracture of brittle shells based on LR NURBS, Computational Mechanics, 2020, Vol. 65, 1039-1062
- PAUL K, ZIMMERMANN C, DUONG TX, SAUER RA, Isogeometric continuity constraints for multi-patch shells governed by fourth-order deformation and phase field models, Computer Methods in Applied Mechanics and Engineering, Vol.370, 113219, 2020

Engineering Sciences

Chemical and Thermal Process Engineering | DFG 403

Speeding up Quantum Chemistry with Machine Learning

Project ID: rwth0396
STEFAN PALKOVITS
NINA SACKERS
Institute of Technical and Macromolecular Chemistry,
RWTH Aachen University

Project Report

The original proposal was tested in a student's research internship and did not work out as expected. Right now it is not clear if the original aim is target-oriented. The computing time was used by a Ph.D. student in the frame of the Cluster of Excellence "The Fuel Science Center". The computations done had the following scope:

Within this project, various covalent triazine frameworks (CTFs) were modeled using the VASP software. 2D periodic calculations were carried out by adding a vacuum layer to the third spatial direction. In order to model different CTFs, the triazine rings were connected by different linkers, i.e. p-dicyanobenzene (pDCB), dicyanopyridine (DCP) and dicyanobipyridine (DCBP) (Fig. 1).

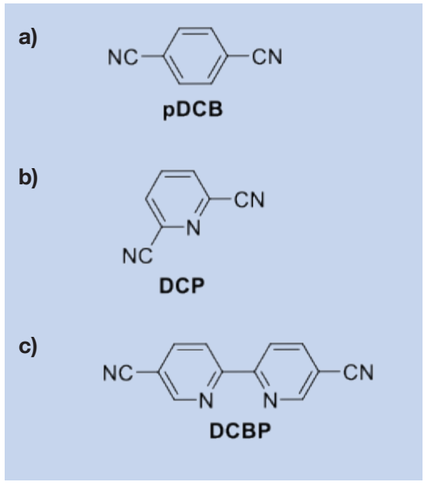

Figure 1: Different monomers used as linkers in CTFs.

After optimization of the lattice parameter of the CTF material, the coordination of single platinum atoms was investigated on the different nitrogen moieties. This includes the triazine ring as well as potential nitrogen atoms in the linker. Different coordination environments of the Pt were considered. Pt atoms surrounded by Cl atoms were modeled to represent the structure after impregnation of the CTF. A sole metal atom connected to the CTF was used to describe the material after reduction. In addition, interactions of Pt atoms with carbon atoms of the nearby aromatic rings were taken into account.

Finally, the stability of the adsorption of the substrates O2, NO, NO2 and N2O was tested on the Pt/CTF materials. These results will serve as a basis for a comparison to experimentally conducted adsorption studies.

Engineering Sciences

Heat Energy Technology, Thermal Machines, Fluid Mechanics | DFG 404

Numerical investigations of soot formation in a model aircraft combustor

Project ID: bund0009
CHRISTIAN HASSE
FEDERICA FERRARO
JEREMY KARPOWSKI
ÖMER ÇOKUSLU
Simulation of reactive Thermo-Fluid Systems, TU Darmstadt, Germany

Project Report

The use of advanced numerical simulations has enabled important achievements in increasing the cycle efficiency of thermal machines, reduction of pollutant emissions, and the use of alternative fuels in practical applications. Numerical tools are employed routinely to design and optimize combustion systems for aircraft, automotive, or gas turbine manufacturers. The modeling of realistic aero-engine combustors is extremely challenging because complex multiscale and multiphysics phenomena need to be accounted for. Current jet engines operate at pressures up to 50 bar, while temperatures easily exceed 2000 K. Due to these elevated operating conditions, pollutant emission and thermo-acoustic instabilities become major issues for the new generation of jet engines. Therefore, the development process of low emission aero-engine combustors requires insights regarding combustor design and reliable, accurate soot models. However, soot is a challenging modeling problem due to the interactions between turbulence, chemical reactions, and particulate evolution, happening over a large range of time scales.

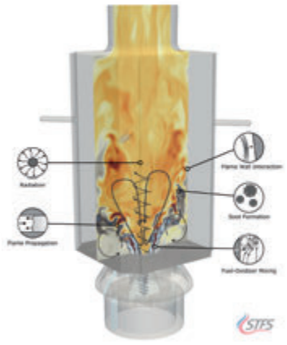

The main goal of this project is to study the turbulent sooting flows in aero-engine conditions, by using advanced turbulence combustion models and soot formation models. Two configurations are investigated with LES: (i) the Delft Adelaide flame III, a benchmark methane/air piloted jet flame of the International Sooting Flame (ISF) workshop; (ii) the dual swirl model combustor (Geigle et al. 2013; Geigle et al. 2015), a pressurized ethylene/air burner experimentally investigated with and without secondary air injection, which presents similar characteristics of a Rich-Burn/Quick-Quench/Lean-Burn (RQL) aero-engine combustor.

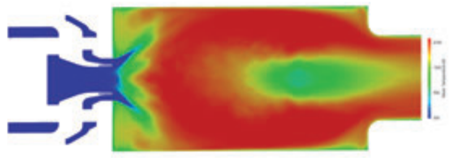

Soot is commonly studied by solving the population balance equation (PBE) that evolves the particle number density function (NDF). The direct solution of the PBE is numerically expensive and therefore unfeasible in most cases. The computational most efficient approach for solving the PBE is given by the method of moments (MOM). Here the PBE is not solved directly, but only a few lower-order moments of the distribution are tracked. The recently proposed Extended Quadrature Method Of Moment (EQMOM) allows reconstructing the full NDF from the set of transported moments. The method was successfully applied to predict soot (Salenbauch et al. 2015) and soot oxidation (Salenbauch et al.2019, Wick et al. 2017) in laminar flames, demonstrating that it yields results almost as accurate as high-fidelity reference simulations. EQMOM solves the long-standing issue of moment methods to describe particle oxidation accurately while keeping the computational efficiency of MOM. A robust cell-centered finite-volume (FV) framework in the open-source toolbox OpenFOAM, developed for turbulent reacting flows, is employed here. A detailed and accurate C++ library for the evaluation of soot formation using the quadrature-based method of moments approach has been integrated into the CFD solver. The coupled numerical framework provides wide runtime-selectable flexibility: different turbulence models, e.g. RANS and LES, with several turbulent closures; different combustion models, based on tabulated chemistry and different moment closure strategies to account for the soot particle size distribution, as standard QMOM, Extended QMOM and split-based extended QMOM approach.

Numerical results of the Delft Adelaide Flame III, used to validate the numerical framework, show a good quantitative agreement for the gas-phase flow variable like temperature and velocity as well as for the soot volume fraction. Moreover, they demonstrate that the split-based EQMOM soot model is able to reconstruct instantaneous and continuous particle size distributions (PSD), which are not directly available in the classical method of moments. The results are not discussed here for brevity.

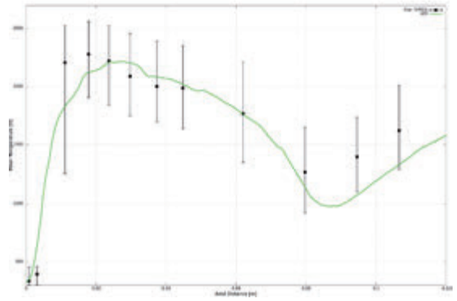

Using the previously validated simulation framework, LES of the model combustor at 3 bar and with secondary air injection is carried out including heat losses at the burner walls. The results indicate a good agreement of the flow-field with the experimental data. The flow characteristics, such as the position and dimension of the inner and outer recirculation zones, compare well with the experiments. As shown in the figure, the time-averaged temperature evolution on the centerline is correctly captured by the simulation. More specifically, the temperature increases to its maximum value close to the injection plane at axial position x = 0.025 m, where stoichiometric conditions are reached, and decreases downstream due to the secondary air injection. It can be observed that the simulation captures the trend of measured temperature values but slightly underpredicts the dip in temperature near the secondary air interaction region. The time-averaged temperature contour shows several characteristics of the combustion with secondary air injection. A V-shape flame structure can be observed near the nozzle, while a low-temperature zone is formed due to secondary air injection in the center of the combustor due to the mixing of the secondary air with hot combustion products. This leads to persisting temperature gradients along with the axial distance of the combustor. Moreover, the mixing of the secondary air injection in the inner recirculation zone has an important effect on the flame soot oxidation in the upstream regions, as it decreases the local equivalence ratio and enhances soot particle oxidation. As a result, low-temperature regions are formed along the axial length of the combustor, whereas higher temperatures are present near the walls and the sheer layers, enhancing the convective heat transfer in near-wall regions. The discussed LES results of the model combustor simulations require a numerical grid of approximately 15 million cells and are parallelized with a total number of 480 cores per simulation. The required total core hours were 1,000,000.

Selected national and international cooperations

- WOLFGANG MEIER, German Aerospace Center, Stuttgart, Germany
- CHRISTOPH ARNDT, German Aerospace Center, Stuttgart, Germany
- HENNING BOCKHORN, Karlsruhe Institute of Technology, Karlsruhe, Germany
- CHRISTIAN KRAUS, Karlsruhe Institute of Technology, Karlsruhe, Germany

Publications

- KARPOWSKI TJP, FERRARO F, ARNDT CM, KRAUS C, BOCKHORN H, MEIER W, HASSE C. Numerical investigations of the thermo-acoustic cycle in a dual swirl gas turbine model combustor (Under review)

Engineering Sciences

Heat Energy Technology, Thermal Machines, Fluid Mechanics | DFG 404

Flexible Simulation of Fuel cells with OpenFOAM / FlexSim

Project ID: jara0070

WERNER LEHNERT
IEK-14, Forschungszentrum Jülich, Germany

DIETER FRONING
IEK-14, Forschungszentrum Jülich, Germany

STEVEN B. BEALE
IEK-14, Forschungszentrum Jülich, Germany

SHIDONG ZHANG
IEK-14, Forschungszentrum Jülich, Germany

UWE REIMER
IEK-14, Forschungszentrum Jülich, Germany

TIANGLIANG CHENG
IEK-14, Forschungszentrum Jülich, Germany

STEFFEN HESS
IEK-14, Forschungszentrum Jülich, Germany

Project Report

1. Polymer electrolyte fuel cell

A new PEFC model was developed and implemented into the open source package, OpenFOAM. This model enables simulations concerning two-phase (liquid-gas) flow, heat and mass transfer with phase change, charge transfer, and electrochemical reactions in a PEFC. Among these processes, two-phase flow is the step that consumes most of the computational resources. The model was verified with analytical results and validated by comparing with the experimental data. The comparison can be found in the PhD thesis of Dr. S. Zhang. Additional applications were conducted on an in-house designed PEFC prototype. It consists of three serpentine flow paths, with a nominal active area of 16 cm².

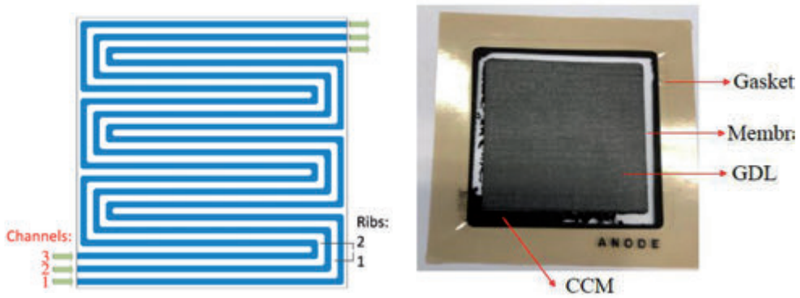

Figure 1: (a) Flow path design; (b) MEA failure.

Figure 1 shows the flow path design and the membrane-electrode-assembly (MEA) used in one of the experimental tests. It can be seen that the gas diffusion layers GDLs do not cover all catalyst-coated-membrane. Simulations were conducted to investigate the possible reasons that led to the membrane electrode assembly (MEA) failure. JARA-HPC was used to perform parallel calculations. The OpenFOAM model is going to be extended for water electrolyzers in 2021.

2. Volume of Fluid studies in Complex Geometries

Volume-of-fluid (VOF) studies were investigated in porous transport layers (PTLs) and gas channels of fuel cells (conjugate problem) using OpenFOAM. Obtaining numerical convergence required substantial tuning of the code, the problem being not so much the size of the mesh, which was a relatively coarse 7.8×10^6 computational cells, but rather the time stepping, with $\Delta t = O(10^{-7})$ sec and total time $t = O(10^{-3}\text{-}10^{-2})$, weeks (and in some cases months) of computer time were consumed. The relatively coarse meshes were employed following a suggestion by a reviewer of last year's proposal. Finer meshes are to be employed in 2021. The rate-limiting factor here is the Courant number, which cannot exceed unity (1) as well as the related Capillary Courant number.

The geometry considered is in the form of a 'T-shape' with the porous transport layer (PTL) in the form of a thin rectangular prism of size $0.5\times0.5\times0.1$ mm³ located at the base of the 'T', and the gas flowing across the top in the channel, as shown in Figure 2. The PTL is reproduced by digital reconstruction of nano-computer tomography images of a Freudenberg H2315 PTL in the form of an STL file. From this, the domain was tessellated with an unstructured castellated/octree mesh. Subsequently a volume-of-fluid method was employed to obtain solutions on the constructed mesh.

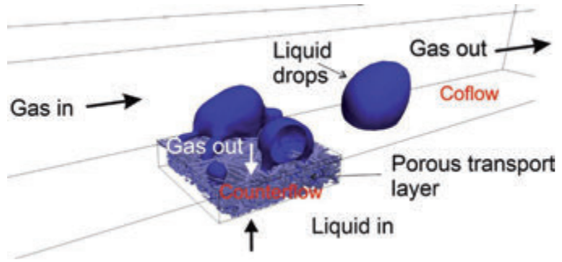

Figure 2. Volume-of-fluid studies in gas channels/ porous transport layers

Selected conference participants

- SHIDONG ZHANG, STEVEN BEALE, YAN SHI, HOLGER JANSSEN, UWE REIMER, WERNER LEHNERT.
  Development of an open-source Solver for Polymer Electrolyte Fuel cells,
  The Electrochemical Society 2020 – PRiME, Honolulu, Hawaii,
  September 20-October 4, 2020.
- STEVEN BEALE, MARTIN ANDERSSON, NORBERT WEBER, HOLGER MARSCHALL, WERNER LEHNERT.
  Combined Two-phase Co-flow and Counter-flow in a Gas Channel and Porous transport Layer Assembly, The Electrochemical Society 2020 – PRiME, Honolulu, Hawaii,
  September 20-October 4, 2020.
- ABOUZAR GHAZEMI, PAUL GIBBON, STEVEN BEALE.
  Performance Evaluation of OpenFOAM on Juelich Supercomputing Facilities (JURECA, JUWELS and JUSUF). 8th ESI OpenFOAM conference (online),
  October 13-15, 2020.

Selected national and international cooperations

- HRVOJE JASAK, Cambridge University, United Kingdom
- JON PHAROAH, Queen's University, Canada
- NORBERT WEBER, Institut für Fluiddynamik, Helmholtz-Zentrum Dresden-Rossendorf e.V. Germany
- HOLGER MARSCHALL, TU Darmstadt, Germany
- BENOÎT MATHIEU, CEA, France

Publications

- ZHANG S, BEALE SB, REIMER U, ANDERSSON M, LEHNERT W.
  Polymer Electrolyte Fuel Cell Modeling – A Comparison of Two Models with Different Levels of Complexity
  Int. J. Hydrogen Energy 45; 19761-19777, 2020.
  https://doi.org/10.1016/j.ijhydene.2020.05.060
- ZHANG S, BEALE SB, SHI Y, JANSSEN H, REIMER U, LEHNERT W.
  Development of an Open-source Solver for Polymer Electrolyte Fuel Cells, ECS Trans. 98(9): 317-329, 2020. https://doi.org/10.1149/09809.0317ecst
- BEALE SB, ANDERSSON M, WEBER N, MARSCHALL H, LEHNERT W.
  Combined Two-phase Co-flow and Counter-flow in a Gas Channel/Porus Transport Layer Assembly, ECS Trans. 98(9): 305-315, 2020.
  https://doi.org/10.1149/09809.0305ecst

Engineering Sciences

Heat Energy Technology, Thermal Machines, Fluid Mechanics | DFG 404

Parallel Stabilized Finite Element Methods for Aero-, Hemo-, and Hydrodynamics

Project ID: jara0185

MAREK BEHR
STEFANIE ELGETI
NORBERT HOSTERS
LINDA GESENHUES
FLORIAN ZWICKE
PATRICK ANTONY
MAX VON DANWITZ
SEBASTIAN EUSTERHOLZ
FELIPE GONZALEZ
JAN HELMIG
DANIEL HILGER
VIOLETA KARYOFYLLI
FABIAN KEY
KONSTANTIN KEY
MICHEL MAKE
ANNA RANNO
JAYGHOSH RAO
EUGEN SALZMANN
MAXIMILIAN SCHUSTER
THOMAS SPENKE
STEFAN WITTSCHIEBER
DANIEL WOLFF
Chair for Computational Analysis of Technical Systems (CATS), RWTH Aachen, Germany

Project Report

Among the various advances in parallel stabilized finite element methods for flow simulation, we highlight a computational model of blood flow inside an arterial stent.
Cardiovascular diseases are the most common cause of death worldwide. In particular, 30% of global mortality is due to coronary artery diseases. The treatment of such diseases largely involves the implantation of coronary stents, which can give rise to in-stent restenosis or thrombosis. The critical areas where such side effects occur highly depend on the micro-dynamics inside the artery. For this reason, the analysis of blood flow in stented arteries is of great interest. In-stent restenosis is due to the vessel inflammatory reaction after the implantation of the stent, which can lead to long-term lesions (40% occurrence rate). Thrombus formation can be predicted by identifying the areas of rapid platelet aggregation.
Numerical modeling and simulation is an increasingly important tool used during the development of blood-handling medical devices. Computational fluid dynamics (CFD) helps reduce the number of expensive and time-consuming experiments during prototype development, and helps with surgery planning. In the frame of a DFG project BE 3689/15, performed in a cooperation with the Institute of Applied Mechanics IFAM (Prof. Stefanie Reese), and with Cardiology Clinic at the Aachen University Hospital (Dr. Felix Vogt), a computational model of stent-related biophysical processes is being developed, with the goal of linking the detailed blood flow prediction, the fluid-structure interaction, and cell growth and mediation within the arterial wall.
To help the healing process and reduce the risk of restenosis, coated stents have a layer of drug that is slowly released into the blood stream. The elution and deposition of the drug on the vessel wall can be analyzed by means of an advection-diffusion equation and tailored boundary conditions. The convective field is obtained by the Navier-Stokes equations used to model the blood flow (Fig. 1). To resolve the fine areas of stent struts protruding from the vessel wall into the lumen (where blood flow occurs) exceptionally fine computational meshes are required. Pulsatility of the coronary flow means that the time dependent simulations need to be performed. This motivates strongly the use HPC resources provided by the CLAIX cluster.
The analysis of streamlines show that recirculation areas and vortices are often located near the stent struts. These critical areas strongly influence also the deposition of the drug on the vessel wall. However, coupling the blood flow, whose characteristic time scale is in the order of seconds, and the drug elution process, which can last up to three months, is computationally very expensive. Progress is being made towards reduced-order alternative models that reduce the spatial and temporal resolution requirements. This involves collaboration with Politecnico di Milano, Prof. Simona Perotto and Prof. Paolo Zunino, within an IDEA League research grant awarded to the co-worker on the project, Anna Maria Ranno.

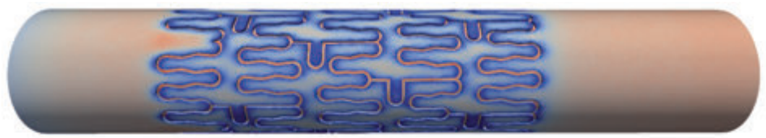

Figure 1: Wall shear stress (high in red, low in blue) around the struts of the implanted Xience V stent in a simulated coronary artery. The variability of the flow-induced stress leads to variation of the healing and growth processes on the artery surface and within the arterial wall, affecting local restenosis.

Selected honors, prizes and awards

Elected (Behr) as President of German Association for Computational Mechanics
Selected (Behr) for semi-plenary at the 14th World Congress on Computational Mechanics 2020 (held in 2021).

Selected conference participations

Short courses CISM Advanced Webinar, Udine, Italy, December 03-09, 2020

National and international cooperations

- LESZEK DEMKOWICZ, University of Texas at Austin, Austin, TX, USA
- NIKOS CHRISOCHOIDES, Old Dominion University, Norfolk, VA, USA
- KAZUO KASHIYAMA, Chuo University, Tokyo, Japan
- LUCA BIFERALE, University of Rome Tor Vergata, Italy
- WOLFGANG WALL, Technical University of Munich, Germany

Publications

- HELMIG J, KEY F, BEHR M, ELGETI S. Combining boundary-conforming finite element meshes on moving domains using a sliding mesh approach, International journal for numerical methods in fluids 93(4), 1053-1073, 2020.
- REIMER L. Simulation environment for CFD-based aeroelastic analysis of aircraft, PhD thesis, 2020.
- FRINGS M, HOSTERS N, MÜLLER C, SPAHN M, et al. SplineLib: A modern multi-purpose C++ spline library, Advances in engineering software 146, 102826, 2020.
- ZWICKE F. Inverse shape design in injection molding based on the finite element method, PhD thesis, 2020.
- HASSLER S, RANNO A, BEHR M. Finite-element formulation for advection–reaction equations with change of variable and discontinuity capturing, Computer methods in applied mechanics and engineering 369, 113171, 2020.
- GUGLIETTA F, BEHR M, BIFERALE L, FALCUCCI G. On the effects of membrane viscosity on transient red blood cell dynamics, Soft matter 16(26), Seiten/Artikel-Nr.:6191-6205
- GESENHUES L. Advanced methods for finite element simulation of rheology models for geophysical flows, PhD thesis, 2020.
- SPENKE T, HOSTERS N, BEHR M. A multi-vector interface quasi-Newton method with linear complexity for partitioned fluid-structure interaction, Computer methods in applied mechanics and engineering 361, 112810, 2020
- HINZ J, HELMIG J, MÖLLER M, ELGETI S. Boundary-conforming finite element methods for twin-screw extruders using spline-based parameterization techniques, Computer methods in applied mechanics and engineering 361, 112740, 2020.
- MAKE M, HOSTERS N, BEHR M, ELGETI S. Space-Time NURBS-Enhanced Finite Elements for Solving the Compressible Navier-Stokes Equations, in Numerical Methods for Flows: FEF

2017 Selected Contributions
HARALD VAN BRUMMELEN, ALESSANDRO CORSINI, SIMONA PEROTTO, GIANLUIGI ROZZA, Editors, Springer, 97-107, 2020.

Engineering Sciences

Heat Energy Technology, Thermal Machines, Fluid Mechanics | DFG 404

Penny Cavity Flow in an Annular Cascade Wind Tunnel

Project ID: jara0193

PETER JESCHKE
JOHANNES JANSSEN
Institute of Jet Propulsion and Turbomachinery, RWTH Aachen University

Project Report

A part of the world's electrical energy will continue to be generated by fossil fuels in the coming decades. The gas turbine as a particularly flexible and low-emission energy conversion machine plays a special role against the background of the increasing share of volatile renewable energy sources. For this reason, the increase in efficiency of gas turbines continues to be an important component of current research.

The gas turbine compressor plays a central role here. In addition to the high impact of the compressor efficiency on the overall efficiency, the operating flexibility of the gas turbine is particularly determined by the compressor, since the aerodynamic stability limit of the compressor is the working range limitation of the whole machine. For stable and efficient operation of the gas turbine in various operating points adjustable stators are used in the front stages of multi-stage axial compressors. As a result, even in partial load operation, incidence flow and a thereby induced stall on the blade profile can be prevented, so that the efficiency and the aerodynamic stability of the compressor are increased.

In shrouded stators, the blades are mounted in the hub via a turntable, the so-called penny. Due to the necessary twistability because of thermal and mechanical loads, the formation of an annular cavity is unavoidable. Since a pressure difference between the pressure and suction side is applied to the blade profile during operation, there is a flow through the penny cavity, whereby additional losses are generated.

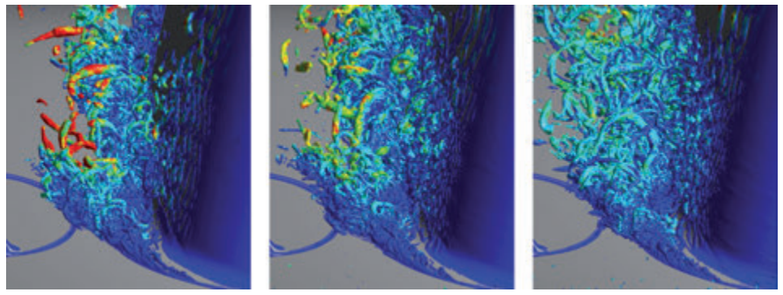

Figure 1 Vortex system formed by leakage from the penny cavity in compressor variable stator vane rows, results of turbulence resolving simulations, comparison of three meshes from coarse (left) to fine (right)

Only in recent years various work has been carried out to minimize these losses. For example, in order to avoid the penny cavity, non-circular blade platforms have been investigated, [1] which, however, in turn led to higher flow losses. The positioning of the blade pin relative to the blade has also been the subject of several experimental and numerical investigations [2] - [4]. It has been found that the positioning has a great influence on the loss origin in the blade passage and that a pin located under the front part of the blade is optimal with respect to the induced flow losses.

First insights into the physical understanding of the influence that the penny cavity has on the flow through the compressor are provided [5]. It could be shown that the reentry of the leak through the penny cavity produces vortices that cause an additional loss. In [6], the flow through the cavity was examined for the first time in more detail by means of scale-resolving simulations, whereby a counter-rotating vortex pair as well as unsteady shear layer vortices has been identified in the resulting vortex structures. Based on this, adaptations for the modeling of penny cavities in multistage high-pressure compressors were derived in [7] and influences of the profile design on the cavity flow were investigated. For the first time, the penny cavity flow has recently been evaluated based on scale-resolving simulations [8]. It has been shown that only this type of simulation in contrast to state-of-the-art RANS simulations is able to predict the flow features correctly. In order to evaluate the impact of different penny geometries, more scale-resolving simulations need to be conducted.

References

[1] GOTTSCHALL M, VOGELER K.
Vortex development induced by part gap geometry and endwall configurations for variable stator vanes in a compressor cascade. Journal of Power and Energy 227, pp. 692–702. Special Issue Article, 2013.

[2] GOTTSCHALL M, VOGELER K, MAILACH R.
The Effect of four Part Gap Geometry Configurations for Variable Stator Vanes in a Compressor Cascade. Proceedings of ASME Turbo Expo 2012, 2012.

[3] GOTTSCHALL M, MAILACH R, VOGELER K.
Penny Gap Effect on Performance and Secondary Flowfield in a Compressor Cascade. Journal of Propulsion and Power 28, No. 5, pp. 927–935, 2012.

[4] GOTTSCHALL M, VOGELER K, MAILACH R.
The Effect of two different Endwall-Penny Concepts for Variable Stator Vanes in a Compressor Cascade. Proceedings of ASME Turbo Expo 2012, 2012.

[5] WOLF H, FRANKE M, HALCOUSSIS A, KLEINCLAUS C, GAUTIER S.
Investigation of Penny Leakage Flows of Variable Guide Vanes in High Pressure Compressors. Proceedings of ASME Turbo Expo 2016, 2016.

[6] STUMMANN S, POHL D, JESCHKE P, WOLF H, HALCOUSSIS A, FRANKE M.
Secondary Flow in Variable Stator Vanes with Penny-Cavities. Proceedings of ASME Turbo Expo 2017, 2017.

[7] WOLF H.
Aerodynamische Bewertung von Pennykavitäten bei Verstellstatoren in Hochdruckverdichtern. PhD Thesis, Ruhr-Universität Bochum, 2017.

[8] STUMMANN S, Sekundärströmung und Verluste aufgrund von Penny-Kavitäten in Verstellleitschaufeln. PhD Thesis, RWTH Aachen University, 2018.

Selected national and international cooperations

- MTU Aero Engines AG, Munich, Germany

Publications

- POHL D, JANSSEN J, JESCHKE P, HALCOUSSIS A, WOLF H.
Variable Stator Vane Penny Gap Aerodynamic Measurements and Numerical Analysis in an Annular Cascade Wind Tunnel. International Journal of Gas Turbine, Propulsion and Power Systems, Vol. 11 No. 2, 44-55, 2020.

Engineering Sciences

Heat Energy Technology, Thermal Machines, Fluid Mechanics | DFG 404

Unsteadiness of Görtler Vortices in Hypersonic Compression Ramp Flow

Project ID: rwth0491
IGOR KLIOUTCHNIKOV
SHIBIN CAO
Shock Wave Laboratory,
RWTH Aachen University

Project Report

In the present project, a hypersonic compression ramp flow with a free stream Mach number of 7.7 and a free stream Reynolds number of 4.2×10^5 based on the flat plate length has been numerically investigated. The DNS results agree well with experimental data in terms of the time-averaged wall pressure and surface heat flux distributions as well as the wavelength of the observed heat flux streaks. Grid-convergence has been achieved for a mesh resolution of 124 million grid points regarding the flow phenomenon of interest.

It was shown that in the absence of external disturbances, streamwise heat flux streaks form on the ramp surface downstream of reattachment. The DNS results indicate that the considered compression ramp flow initially undergoes an exponential growth stage and subsequently a stage of nonlinear saturation until the quasi-steady state is achieved. The saturated flow was shown to be unsteady. Downstream of reattachment, the surface heat flux exhibits a strong fluctuation associated with a broadband spectrum. The dominating frequencies are concentrated on the low-frequency region. Moreover, the fluctuation of the heat flux and therewith the unsteadiness of the heat flux streaks is coupled with a pulsation of the reattachment position. The downstream flow unsteadiness was shown to originate from the separation bubble flow.

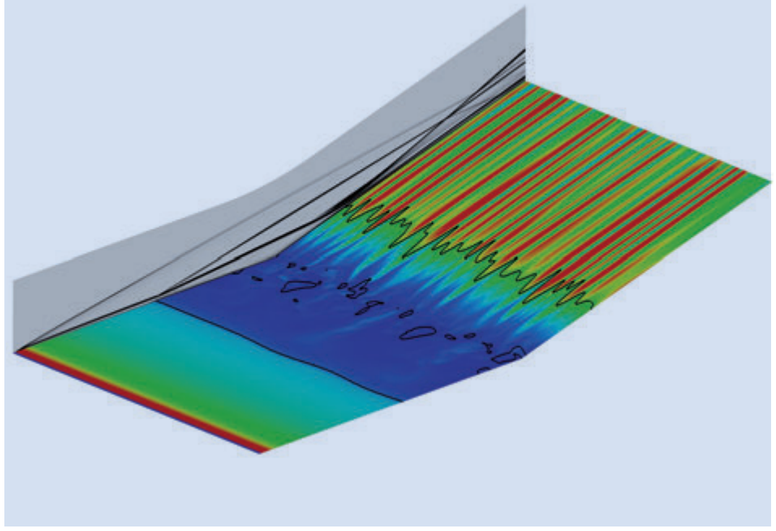

Dynamic mode decomposition (standard DMD and SPDMD) was then employed to analyse the dominant oscillatory modes in the saturated separation bubble flow. The identified modes having strongest influence on the given snapshot sequence are also characterised by low frequencies similar to those found by the PSD analysis. These oscillatory modes exhibit streamwise periodicity in the separation bubble. This flow structure is linked to the downstream reattached flow by the shear layer above the separation bubble. The oscillatory modes extracted by DMD share similar flow structures with the oscillatory modes found by the present GSA as well as the low-frequency oscillatory mode found for a separated double wedge flow. Therefore, it can be concluded that the unsteadiness of the considered hypersonic compression ramp flow has its origin in the intrinsic instabilities of the fluid dynamic system.

National and international cooperations

- JIAAO HAO, Department of Aeronautical and Aviation Engineering, The Hong Kong Polytechnic University, Hong Kong

Publications

[1] CAO S, KLIOUTCHNIKOV I, OLIVIER H. Görtler number evaluation for laminar separated hypersonic compression ramp flow, AIAA Journal, Vol. 58, No. 8, 2020, pp.3706-3710.
[2] CAO S, HAO J, KLIOUTCHNIKOV I, OLIVIER H, WEN CY. Unsteady effects in a hypersonic compression ramp flow with laminar separation, Journal of Fluid Mechanics, Vol. 912, A3, 2021.
[3] CAO S. Streamwise vortices in hypersonic flow on a compression ramp, PhD Thesis, RWTH Aachen University, Aachen, 2021.

Engineering Sciences

Heat Energy Technology, Thermal Machines, Fluid Mechanics | DFG 404

Analysis of Respiratory and Cerebrospinal Flows by a Coupled Lattice-Boltzmann Method

Project ID: jara0203

ANDREAS LINTERMANN
SEONG-RYONG KOH
JENIA JITSEC
Jülich Supercomputing Center (JSC),
Forschungszentrum Jülich, Germany

MARIO RÜTTGERS
Aerodynamic Institute and Chair of Fluid Mechanics, RWTH Aachen University,
Jülich Supercomputing Center (JSC),
Forschungszentrum Jülich, Germany

MORITZ WALDMANN
Aerodynamic Institute and Chair of Fluid Mechanics, RWTH Aachen University

Project Report

Methods to diagnose pathologies in the human respiratory system have evolved recently from mainly focusing on medical imaging data to the consideration of computational fluid dynamics (CFD) and machine learning (ML) techniques. CFD methods allow to numerically qualify the nasal cavity by analyzing the fluid mechanical properties of the respiratory flow, such as the pressure loss, the temperature distribution, and the mass flux distribution. However, the preparation for a numerical analysis requires time-intensive manual interactions. Furthermore, the highly resolved simulations required for such analyses are still very time-consuming, even when running on current high-performance computing (HPC) systems. ML techniques help to automatize and accelerate such flow simulations. Furthermore, if trained with medical diagnostic and image data, as well as simulative data, they can be used to detect and classify pathologies automatically. In the reporting period, the two projects (i.) Data-Driven Analysis of Medical and Simulation Data for Improved Patient Treatment in Rhinology (AM-SIT) and (ii.) Rhinodiagnost were processed.

(i.) The main goal of the JARA-CSD project AM-SIT is to create an automated simulation pipeline that makes the previously described features available in clinical environments. It is a joint project of the SDL FSE, the Institute of Aerodynamics and Chair of Fluid Mechanics (AIA), RWTH Aachen University, and medical partners sharing data and expertise.

(ii.) The project Rhinodiagnost, which was successfully completed in 2020, aimed at supporting medical staff in the diagnosis of pathologies, in decision making for their treatment, and for possible surgical interventions. By analyzing the respiration of the patient from a fluid mechanical point of view, additional physics-based information is integrated into the decision making process.

In these projects, the lattice Boltzmann method implemented in the Zonal Flow Solver (ZFS) [1], developed at the AIA, is used to simulate quasi-incompressible flows in realistic CT-data based geometries of the nasal cavity. In the past, this method has been used to analyze various aspects of respiratory flows [2]. To support physicians in finding the correct diagnoses and the best possible treatment for a rhinological disease, a simulation pipeline that conducts numerical simulations on HPC systems automatically was developed in Rhinodiagnost [3]. That is, subsequent to the generation of a three-dimensional watertight surface geometry using ML algorithms, the grid generation and the numerical simulation using a thermal LB (TLB) method are executed automatically. Thus, a physician without basic knowledge of CFD methods and HPC systems is enabled to conduct highly resolved simulations of respiratory flows. This approach was further developed to enable virtual surgeries inside the nasal cavity. Therefore, the surgeon modifies the segmented dataset of the nasal cavity generated from the CT volume data of the patient. These segmentations have a similar appearance as the original CT image such that the surgeon can modify the shape of the cavity in a known environment. The segmentation of the pre- and post-surgical cavities are written to an STL file, which is subsequently used to initialize a level-set (LS) field. A TLB approach coupled with the LS solver is employed to simulate respiratory flows in the pre-operative nasal cavity. When the quasi-steady state is reached, the LS solver is used to temporally interpolate between the LS field of the pre- and the post-surgical case to assure a smooth transition. All states between the initial and the final state of the geometry can be investigated to find the optimal shape.

In AM-SIT, a two-dimensional ANN for segmenting nasal cavities from CT datasets has been developed. It is capable of identifying the airway and has learned enough features to identify the nostril areas. A three-dimensional ANN focuses on the nostril regions and improves the segmentation at the inflow areas. A third ANN predicts the location and main flow directions at the inlets for the prescription of the boundary conditions. The location of the outlet region and the corresponding main flow direction are identified with an averaged centerline. It is computed from two centerlines starting in the left and right nostrils. All ANNs are embedded into a data pipeline, which generates a surface from the segmentation and prepares it for the simulation. Based on the identified inlet regions in the segmentation, the surface is automatically subdivided into the corresponding inlet areas at each nostril, the outlet area at the pharynx, and the remaining main nasal cavity. The results of the flow through a pipeline-generated surface have been compared to those through a surface generated by a medical professional. The mean deviation of the area-averaged pressure loss between cross-sections along the left and right centerlines and the inflow areas is less than 1% of the pressure loss between the outlet and the inlets. These developments enable to conduct a huge amount of nasal cavity flow simulations.

References:

[1] LINTERMANN A, MEINKE M, SCHRÖDER W.
Zonal Flow Solver (ZFS): a highly efficient multi-physics simulation frame work,
International Journal of Computational Fluid Dynamics, 2020, pp. 1 - 28, doi: 10.1080/10618562.2020.1742328

[2] LINTERMANN A, SCHRÖDER W.
A Hierarchical Numerical Journey Through the Nasal Cavity: from Nose-Like Models to Real Anatomies, Flow, Turbulence and Combustion, 102 (1), 2019, pp. 89-116, doi: 10.1007/s10494-017-9876-0

[3] GROSCH A, WALDMANN M, GÖBBERT JH, LINTERMANN A.
A Web-Based Service Portal to Steer Numerical Simulations on High-Performance Computers, in:
Jarm, T. and Cvetkoska, A. and Mahnic-Kalamiza, S. and Miklavcic, D. (Eds.) 8th European Medical and Biological Engineering Conference (EMBEC 2020), IFMBE Proceedings, 80th Edition, Springer Cham, 2020, pp. 57-65, doi: 10.1007/978-3-030-64610-3

Conference Participations

- MARIO RÜTTGERS, Prediction of Acoustic Fields using a Lattice-Boltzmann Method and Deep Learning, International Supercomputing Conference (ISC), Frankfurt, Germany, June 10-14, 2020

National and international cooperations

- MORITZ WALDMANN,
  Angewandte Informationstechnik Forschungsgesellschaft mbH, Graz, Austria
- HUSSEIN ALJAWAD,
  Chonnam National University Dental Hospital, Gwangju, South Korea
- JUSTUS ILLGNER,
  Klinik für Hals-, Nasen-, Ohrenheilkunde und Plastische Kopf- und Halschirurgie, Universitätsklinikum Aachen

Publications

- WALDMANN M, GROSCH A, WITZLER C, LEHNER M, BENDA O, KOCH W, VOGT K, KOHN C, SCHRÖDER W, GÖBBERT JH, LINTERMANN A. An effective simulation- and measurement-based workflow or enhanced diagnostics in rhinology, Medical & Biological Engineering & Computing, submitted in 2020, (under revision)
- RÜTTGERS M, KOH SR, JITSEV J, SCHRÖDER W, LINTERMANN A. Prediction of Acoustic Fields using a Lattice-Boltzmann Method and Deep Learning, High Performance Computing, Springer International Publishing, p.81-101, 2020
- ALJAWAD H, RÜTTGERS M, SCHRÖDER W, LINTERMANN A, KYUNGMIN CL. Effects of the Nasal Cavity Complexity on the Pharyngeal Airway Fluid Mechanics: A Computational Study, Journal of Medical Imaging, submitted in 2020, (under revision)

Engineering Sciences

Heat Energy Technology, Thermal Machines, Fluid Mechanics | DFG 404

Mixing Processes in Internal Combustion Engines and Noise Reduction by Porous Material

Project ID: jara0202

MATTHIAS MEINKE
TIM WEGMANN
SVEN BERGER
Institute of Aerodynamics Aachen,
RWTH Aachen University

WOLFGANG SCHRÖDER
Institute of Aerodynamics Aachen,
RWTH Aachen University and JARA
Center for Simulation and Data Science

Project Report

A CO_2 neutral transportation with future use of internal combustion (IC) engines requires biofuels as energy carriers. However, their different thermo-physical properties such as viscosity and heat capacity pose new challenges for an efficient combustion process. Thus, engine geometry and process parameters of IC engines need to be optimized for the specific biofuel to simultaneously obtain high efficiencies and low emissions. Such engine optimizations require numerical models, which are able to accurately predicting the fuel distribution prior to combustion for different geometries and changes to valve, and injection parameters. Large-eddy simulations (LES) involving high mesh resolution are necessary to accurately predict relevant turbulent and large-scale vortical flow structures which are responsible for the fuelair mixing process and thus are major influencing factors for the subsequent combustion. In this study the fuel distribution of Ethanol and 2-Butanone from a direct injection in a gasoline engine is analyzed. The differences in mixing formation of the two biofuels will be discussed at the time of ignition by assessing the concentration and fuel distribution functions. The multiphysics solver m-AIA developed at the Institute of Aerodynamics RWTH Aachen University, offers different partial-differential equation (PDE) solvers based on a joint hierarchical grid. Due to different grid spacing requirements, each solver uses an individual subset of the joint unstructured Cartesian mesh. This implementation allows for automatic mesh generation and efficient implementation of independent solution adaptive refinement. Dynamic load balancing is achieved by using a space-filling curve on the base level of the hierarchical octree mesh for the domain decompositioning [4]. In this application a semi-Lagrange multiple level-set (LS) solver is used to track the interface of the different embedded moving boundaries e.g., piston and valves, based on forced motion functions.

The combined levelset can be further modified to allow for a gap-closing algorithm in narrow regions at the valve-seat. Additionally a cell-centered finite volume (FV) method is used to solve the compressible Navier-Stokes equations and the advection-diffusion equation of the fuel-concentration. The moving boundaries are represented by a conservative sharp multiple-cut-cell and split-cell boundary formulation with a multipleghost cell approach. A Lagrangian Particle Tracking (LPT) with an implicit Euler method is used to solver the equation of motion the liquid fuel spray, where multiple droplets are combined to a single parcel. Additionally the PDEs for the parcel temperature and evaporation mass are included. A two-way coupling between the FV- and the LPT solver with a drag formulation is used. In the validation step, the predicted in-cylinder flow-field for an optical testengine was compared with PIV measurements from [2]. A good qualitative agreement of the cycle averaged velocity field in the tumble plane was observed.

Additionally the spray formation was validated in pressure chamber setups with experimental results of the spray penetration in [1]. As seen in Figure 1 a significant difference in the fuel concentration of Ethanol and 2-Butanone can be seen at the start of ignition at 340°. In agreement with previous experimental studies [3], a higher evaporation rate of 2-Butanone compared to Ethanol caused by the higher fuel-air ratio and a lower specific heat of vaporization for 2-Butanone are observed. The difference in the fuel-air mixing caused by the varying fuel properties is correctly predicted by the simulation method in the IC engine. Pressure chamber setups however show no significant distinctions in the spray behavior and are thus not sufficient for injection optimization. Additionally, the otherwise symmetrical cone shaped concentration deteriorates under engine conditions and large differences between the intake- and exhaust side can be seen in Figure 1.

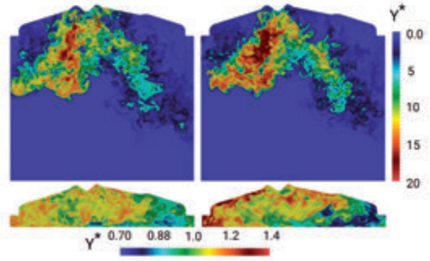

Fig. 1: Evaporated Ethanol (left) and 2-Butanone (right) fuel concentration in the tumble plane at 105° CA (top) and 340° CA (bottom). The fuel concentration is non-dimensionalized by the volume-averaged concentration at corresponding CA.

The fuel distribution function at ignition crank angle (see Fig./refpdf) is more favorable for a clean combustion for Ethanol compared to 2-Butanone, when using the same engine parameters. The Ethanol concentration distribution function shows less rich fuel regions compared to 2-Butanone. This difference is caused by a larger axial penetration of Ethanol due to its slower evaporation rate. Consequently, a better distribution of the fuel in the in-cylinder volume prevails during the intake and compression stroke. In the next step, a cost function based on the concentration distribution function will be defined, which will enable quantitative comparison of the mixing quality for subsequent optimization studies, i.e., with modified injection angles, positions and timings.

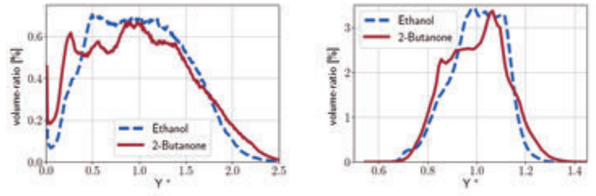

Fig. 2: Dimensionless fuel concentration distribution functions in the engine volume for 2-Butanone and Ethanol at 180° CA (left) and 340° CA (right).

References

1. BERGER S, WEGMANN T, MEINKE M, SCHRÖDER W. Large-eddy simulation study of biofuel injection in an optical direct injection engine. SAE Technical Paper 01-2121, 2020.
2. BRAUN M, KLAAS M, SCHRÖDER W. Influence of Miller cycles on engine air flow. SAE Int. J. Engines 11, 161–178, 2018.
3. BRAUN M, PALMER J, OVERBRUEGGEN TV, KLAAS M, KNEER R, SCHRÖDER W. Influence of in-cylinder air flow on spray propagation. SAE Int. J. Engines, 2017.
4. NIEMÖLLER A, SCHLOTTKE-LAKEMPER M, MEINKE M, SCHRÖDER W. Dynamic load balancing for direct-coupled multiphysics simulations. Computers a. Fluids 199 (104437), 2020.

Selected conference participants

- SVEN BERGER, TIM WEGMANN, MATTHIAS MEINKE, WOLGANG SCHRÖDER, Large-Eddy Simulation Study of Biofuel Injection in an Optical Direct Injection Engine, 8th International Conference “Fuel Science: From Production to Propulsion”, (Online) Aachen, Germany, June 23-25, 2020
- SVEN BERGER, TIM WEGMANN, MATTHIAS MEINKE, WOLFGANG SCHRÖDER, Large-Eddy Simulation Study of Biofuel Injection in an Optical Direct Injection Engine, SAE Powertrains, Fuels & Lubricants Meeting, (Online) Krakow, Poland, September 22-24, 2020

Selected national and international cooperations

- Cluster of Excellence „The Fuel Science Center“, RWTH Aachen University

Publications

- BERGER S, WEGMANN T, MEINKE M, SCHRÖDER W. Large-Eddy Simulation Study of Biofuel Injection in an Optical Direct Injection Engine. SAE Technical Paper 2020-01-2121, 2020, doi:10.4271/2020-01-2121.

Engineering Sciences

Heat Energy Technology, Thermal Machines, Fluid Mechanics | DFG 404

CFD Simulations Ecurie Aix

Project ID: rwth0213
UWE NAUMANN
Software and Tools for Computational Engineering, RWTH Aachen University

ENES ÖKSÜZ
ALEXANDER MÜLLER
MIGUEL CIPRIANO GARCES
SIMON KINKEL
JOHANNES LOSACKER
JAVI MANCHENO
GERRIT WEBER
BERCAN KILIC

Project Report

Introduction

Every year we, the Formula Student Team of RWTH Aachen University, develop a completely new electric race car and adapt a previous car to be able to drive autonomously. For our aerodynamics team, the electric vehicle is the focus. We try to find the best geometries for our car within the regulatory constraints while keeping performance compromises with other design areas in mind. To help us design and improve our aerodynamic package, we carry out extensive CFD simulations, using Siemens Star-CCM+.

Project Details

Over the years, our simulations have been developed further and further to improve accuracy, resulting in several simulation approaches being used currently, depending on the desired information about the different aerodynamic phenomena and influences on the racetrack. These include a straight-line half car simulation using a symmetry plane which consists of around 50 million cells, a full car simulation with a yawed car and turned front tires as weil as a cornering simulation, the latter two both using around 90 million cells. In our development process, we mainly use the straight-line and yaw-angle simulations as they provide much quicker turnaround times and yield enough information.

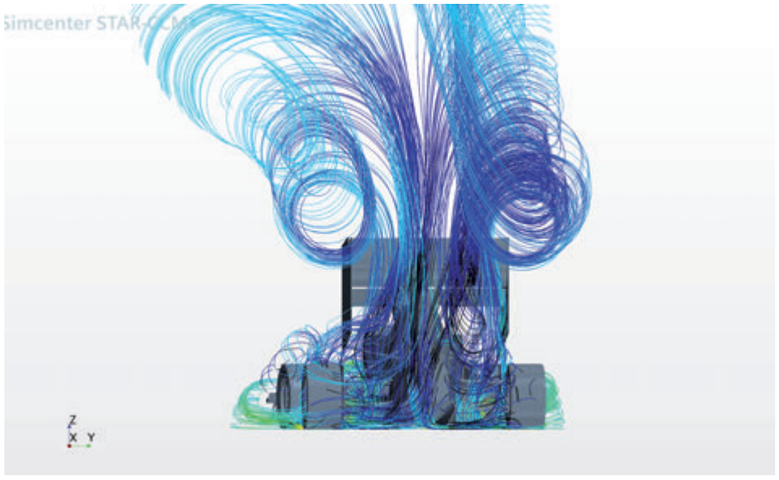

The yawed car is used to include the influence of various driving states on our aerodynamic performance. This is especially important because the purpose of our high-downforce vehicle concept is to increase performance in grip-limited driving conditions, which means those are also the situations in which the car state differs most from the neutral state. That is also the reason for the development of the cornering simulation. Here, the car can be fully transformed to represent real driving situations in corners, including a curved wind tunnel which makes sure that the air flow relative to the vehicle matches the real air flow during cornering. For these simulations we switched from the k-epsilon turbulence model to the k-omega SST model. K-omega models vortices in a more realistic way than the k-epsilon, which we used in previous years. This is important for the accuracy of our CFD simulation since the flow around our car is dominated by strong vortices. Apart from the external aerodynamics, we also use CFD simulations for the design of our cooling systems. These include a water cooling circuit for our four electric motors and the corresponding inverters as well as an air-cooled battery. Apart from system simulation in MATLAB Simulink and Siemens Amesim, we use thermal CFD simulations to analyze their behavior.

Achievements

Over the course of 2020, we put a lot of effort in developing a completely new aerodynamic package including the development of a new front wing, undertray and a new cooling package. The next seasons car will be able to compete in both autonomous and electric disciplines. With the merge of our driverless car into the electric car and other major geometry changes like a new monocoque and a new wheel package we saw the need of developing a new aerodynamic package as well.

Our aerodynamic package is currently in a state where it is competitive with our previous one despite still having a lot of areas to improve in our current development state. We are aiming to increase our downforce in comparison to our previous car by 20% until the end of this season.

In terms of our cooling package we were able to increase the heat flux in our cooling sleeves for our electric motors by 100 % while maintaining the same pressure drop. We are currently developing our own microtube radiators. This type of radiator enables a much higher heat dissipation, taking advantage of the principle of Carman's vortex street. Dur first estimations done in a MATLAB model show a potentially 25 % higher heat dissipation with a 60 % reduction in weight and size. To prove these estimations, we are currently developing a transient simulation to characterize these microtube radiators.

Publications

· MÜLLER V, WULF R.
Konzeptstudie zur Entwicklung einer aerodynamisch verbesserten Radaufhängung

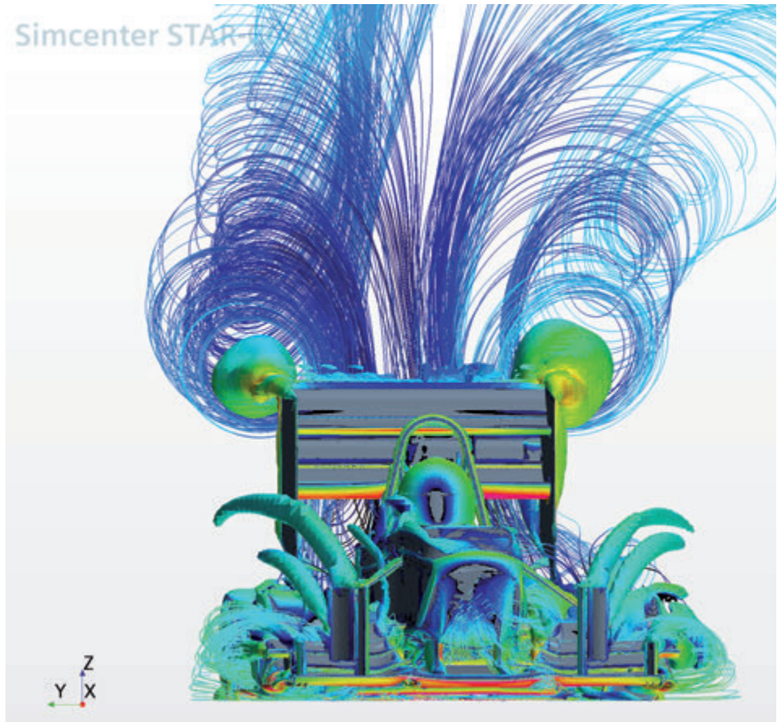

Engineering Sciences

Heat Energy Technology, Thermal Machines, Fluid Mechanics | DFG 404

Direct numerical simulation of turbulent Poiseuille flow

Project ID: bund0008

MARTIN OBERLACK,
Department of Mechanical Engineering,
TU Darmstadt, Germany

SERGIO HOYAS,
Universitat Politècnica de València,
València, Spain

STEPHANIE KRAHEBERGER,
Department of Mechanical Engineering,
TU Darmstadt, Germany

FRANCISCO ALCÁNTARA-ÁVILA,
Universitat Politècnica de València,
València, Spain

Project Report

Wall turbulence is probably one of the open problems in physics with most applications in daily life. Even if the equations ruling out these flows, the Navier-Stokes equations have been known for 150 years, we still lack a complete theory. Research on turbulent flows has been dominated by experimental techniques until the eighties of the last century, where supercomputers started to be powerful enough to solve turbulent flows. However, due to the highly non-linear behavior of wall-turbulent flows, Direct Numerical Simulation (DNS) of these flows are restricted to simplified geometries. The most successful of these idealized flows are Poiseuille turbulent channels, where the fluid is confined between two parallel plates and the flow is driven by a pressure-gradient. Since the seminal paper of Kim, Moin, and Moser, the friction Reynolds number Re_τ has grown steadily. In this project, we have been able to run a simulation reaching the Re_τ=10k frontier. This simulation allows us to study high Reynolds numbers effects. This Re_τ is still less than the largest realization of the flow obtained by experimental means. Still, the main advantage is that the DNS allows one to compute any imaginable quantity in the whole domain.

Unfortunately, the computational cost of a DNS is very high, such that the DNS of a commercial jet-airliner is several decades away, even for the biggest to date supercomputers.

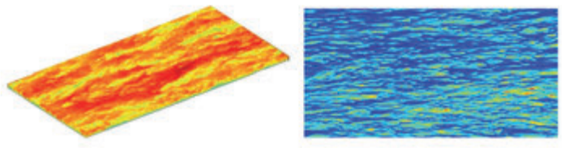

Figure 1: Left, Instantaneous visualization of the streamwise velocity at the logarithmic layer. Right, details of the streaks of the flow at the viscous layer.

For most applications, instantaneous flow details are unnecessary to know and statistical quantities such as the mean velocity are sufficient. However, considering turbulence as a statistical process in fact leads to an infinite dimensional hierarchy of moment-equations, which are extremely difficult to solve. Hence, for most applications a truncated system is considered at the expense of introducing semi-empirical closure models (i.e. RANS methods).
An approach developed by the PI and his co-workers follows a very distinctive route as it considers the entire infinite dimensional hierarchy of moment equations using Lie symmetry methods. Since the work of the mathematician Lie, symmetries have experienced a striking evolution at the heart of physics. Einstein in his 1905 seminal work on special relativity contemplated the symmetry principle as the key feature of physics. Today, Lie symmetry group methods act as the foremost guiding principle to understand and mathematically model new physical laws. This project is the first simulation ever that allow us to test the application of the symmetry-based theory in the field of turbulence.

Results and Methods: The program code, LISO, performs a turbulence simulation only using the Navier-Stokes equations for an incompressible fluid in a plane channel between two parallel plates. The computation is carried out in a sufficiently large doubly periodic domain $2\pi h \times 2h \times \pi h$ in the two wall-parallel directions x (streamwise) and z (spanwise), to avoid spurious statistics due to the finite length of the box and h is the channel half-thicknesses.

Numerical methods: The code uses a low-storage third-order semi-implicit Runge-Kutta (R-K) time-stepper. This R-K scheme allows a longer time step than purely explicit methods while at the same time, the memory requirements are as low as those of a Euler method.
A Fourier discretization in x- and z-directions and a sixth-order Compact Finite Differences (CFD) discretization in the wall-normal y direction are used. This allows a greater flexibility in the choice of the mesh, which consists of 6144x2101x6144 points in space.

LISO is written in Fortran90 and for CLAIX, it is built with the Intel ifort compiler. It has been carefully checked and optimized for CLAIX using a test account and in a SuperMUC extreme scaling workshop. The implementation uses FFTW routines for the Fourier transforms (MKL library) and MPI + OpenMP for the parallelization. I/O routines use the CLAIX parallel HDF5. It took less than 15sec to save the whole field of 280 GB, distributed in as many as 2048 cores. This is done each 7 hours, so the time needed for the I/O routines is negligible.

Due to limitations on the code, the maximum number of processors is 2048 cores. As we had to run the code more than two years, to get enough turbulence statistics, we ran three independent cases at the same time on several supercomputers, one of them CLAIX. In total LISO has been running for about 50M CPU-HOURS, 4M of them in CLAIX.

MPI	RAM	MEM/Task	Restart file	Tape
2048	1.8 TB	886MB	262GB	100TB
4096		443MB		

Table 1: Memory requirements in a computational box of (6144, 2101, 6144)~8e10 points

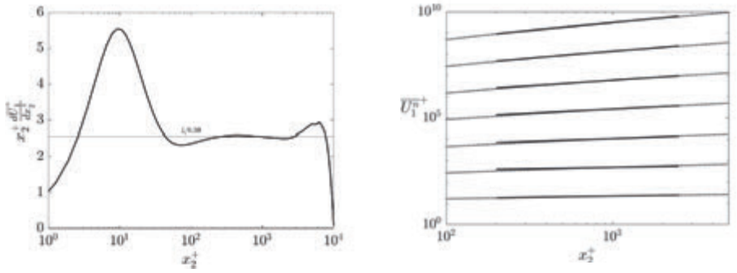

Figure 2: A) Log-indicator function. The flat region between 200 and 2500 indicates the existence of a very long logarithmic layer. The value of 0.39 for the Karman constant can be taken as almost definitive. B) From bottom to top, scaling of moments of the streamwise velocity from 1 to 7. Dotted line, data coming from DNS. Continuous line, data from theory

This simulation is the first one where a clear separation of scales can be observed. One of the most important features it that it has allowed us to check the symmetry-theory, where new scaling laws are obtained directly from theory, without any further simplification or modelling. As one example, we can cite the indicator function of figure 2A. It indicates that the flow follows a logarithmic profile in this region. This layer is the most difficult to model as it is the region of the flow where the largest eddies of the flow, interact with the smaller, and short live eddies that grow from the walls. The symmetry-based theory not only predicts this logarithmic behavior but also forecasts scaling laws for all the moments of the streamwise velocity, and thus characterizing completely the flow. Figure 2B shows the scaling of the moments up to order 7, with an excellent agreement between theory and data. Our final objective is to provide a better knowledge of turbulence and improve the modelling of this thrilling phenomena.

References and Links

Statistics from these and other simulations can be downloaded from our webpage.

[1] https://www.fdy.tu-darmstadt.de/fdyresearch/dns/direkte_numerische_simulation.en.jsp

Selected conference participants

- MARTIN OBERLACK, SERGIO HOYAS, STEPHANIE KRAHEBERGER, FRANCISCO AL CÁNTARA-ÁVILA, Australasian Fluid Mechanics Seminar Series, October 15, 2020

National and international cooperations

SERGIO HOYAS, Universitat Politècnica de València, València, Spain

Engineering Sciences

Materials in Sintering Processes and Generative Manufacturing Processes | DFG 405

Mechanical properties and behavior of glass fiber-reinforced silica aerogel nanocomposites: Insights from all-atom simulations

Project ID: jara0201

BERND MARKERT
Chair and Institute of General Mechanics, RWTH Aachen University

MIKHAI ITSKOV
Continuum Mechanics, RWTH Aachen University

Project Report

Silica aerogels are amorphous nanoporous materials that exhibit a combination of unique properties such as low thermal conductivity and high surface area. This has made them attractive for a broad spectrum of applications such as insulation, energy, Knudsen pumps, aerospace applications, shock-absorbing material, and many more. However, the properties making these aerogels so fascinating also make them brittle. Hence, in many practical applications where the product is required to carry loads or even maintain structural integrity, silica aerogels become unsuitable.

Therefore, several approaches have been proposed in the literature to improve the mechanical properties of silica aerogel. A prominent approach to enhance the mechanical properties of silica aerogel by reinforcement. Many researchers have focussed on silica aerogel composites by the addition of particles, polymers, or fibers. Recently, carbon nanomaterials such as carbon nanofibers, carbon nanotubes (CNTs), carbon aerogels and graphene, are being used as reinforcement materials in silica aerogels. Therefore, the idea of this proposal is to study the mechanical properties of silica aerogel nanocomposites. Nanocomposites reinforced with CNTs, graphene sheets, and glass fibers. On the one hand, experimentally fabricating these nanocomposites of silica aerogels is still challenging, with only a few successful examples.

On the other hand, surprisingly, a composite material has never been investigated before in a computational study to the best of our knowledge. Computer simulations act as a bridge between the theory and the experiment and provide a powerful insight into the systems. Therefore we propose a systematic study of the mechanical properties of silica aerogels nanocomposites material using molecular dynamics (MD) simulations. The testing, manipulating, and design of viable mixtures of reinforcements and polymers present challenges from an experimental perspective. For this reason, numerical modeling at the atomistic scale of CNT reinforced polymers is crucial for the design of future CNT reinforced systems.

National and international cooperations

- AMEYA REGE
  Department of Aerogels and Aerogel Composites Institute of Materials Research, German Aerospace Center, Cologne, Germany
- HYUNG-HO PARK
  Department of Materials Science and Engineering, Yonsei University, South Korea

Publications

1. PATIL SP.
   Enhanced mechanical properties of double-walled carbon nanotubes reinforced silica aerogels: An all-atom simulation study,
   Scripta Materialia, 2021:196,113757
2. PATIL SP, PARALE VG, PARK HH, MARKERT B.
   Mechanical modeling and simulation of aerogels: A review, Ceramics International,
   2021:47 (3), 2981-2998
3. PATIL SP, KULKARNI A, MARKERT B.
   Shockwave response of graphene aerogels: An all-atom simulation study,
   Computational Materials Science, 2021: 189, 110252
4. HERMAN J, GOVEDNIK M, PATIL SP, MARKERT B.
   Molecular Dynamics Simulation Study of the Mechanical Properties of Nanocrystalline Body-Centered Cubic Iron,
   Surfaces, 2020:3 (3), 381-391
5. PATIL SP, SHENDYE P, MARKERT B.
   Molecular Investigation of Mechanical Properties and Fracture Behavior of Graphene Aerogel,
   The Journal of Physical Chemistry B, 2020:124 (28), 6132-6139
6. REGE A, PATIL SP.
   On the Molecular to Continuum Modeling of Fiber Reinforced Composites,
   Advanced Theory and Simulations, 2020: 1900211.
7. PATIL SP, SHENDYE P, MARKERT B.
   Mechanical properties and behavior of glass fiberreinforced silica aerogel nanocomposites: Insights from all-atom simulations,
   Scripta Materialia, 2020:177, 65-68.

Engineering Sciences

Materials Science | DFG 406

Atomistic modeling of energy materials

Project ID: jara0037

PIOTR KOWALSKI,
Institute of Energy and Climate Research, Nuclear Waste Management and Reactor Safety (IEK-6), Forschungszentrum Jülich

Computational team:

REBEKKA TESCH,
OSKAR CHEONG,
ZHENGDA HE,
BINNY ALANGADAN DAVIS,
MICHAEL EIKERLING,
Institute of Energy and Climate Research, Theory and Computation of Energy Materials (IEK-13), Forschungszentrum Jülich, Germany

MENGLI SUN,
Lanzhou University, China and Institute of Energy and Climate Research, Theory and Computation of Energy Materials (IEK-13), Forschungszentrum Jülich, Germany

BART VERLINDEN, SEC CEN, Belgium

SAMUEL EDWARDS, Trinity College, Ireland

EUGENIA KUO, ANSTO, Australia

MILAN PSENICKA, CHARLES U., Prague, Czechia

TIMOTHY CONNOR, UC Irvine, USA

Project Report

Understanding the behavior of energy materials, such as those needed in batteries, fuel or electrolysis cells as well as nuclear fuel or waste is a challenge for science and engineering. For instance, nowadays societies need efficient materials for energy storage, conversion or electrocatalysis processes. In addition, spent nuclear fuel rods contain radioactive fission products, which will remain radioactive for thousands of years.

This requires in-depth understanding of materials for safe nuclear waste disposal. The limited understanding of processes associated with the interaction of electrochemically active species or radionuclides with different materials limits the availability of efficient materials for energy storage and conversion, or safe disposal of nuclear waste.

The aim of the research is to investigate the ability of different materials (electrolytes, catalysts, electrodes, waste forms) to catalyse organic compounds (e.g. CO_2 reduction), incorporate charge carriers or radionuclides, perform characterization of the organic ligands used in the liquid-liquid extraction and to investigate further the parameters of materials constituting different electrochemical devices and nuclear waste forms, including layered materials (e.g. NiOOH or layered double hydroxide (LDH)), metals, ceramics and glasses, some of which have been successfully investigated in the scope of the previous proposals (2012-2020). Cations ordering is an important process that determines the properties of solid materials. In that respect we performed a detailed investigation of disordering tendencies in various materials and the role of mixed materials in enhancing electrocatalytic performance.

The research involved calculations of the structural and energetic parameters of incorporation of elements into different solid phases, including derivation of the thermodynamic data for cation exchange reactions between solid phases and aqueous solutions, characterization of the behavior at the interfaces and characterization of metal-organics-solvent interactions and thermodynamics. The systematic simulations of various materials properties performed up to date, together with the relevant experimental effort of our collaborators, have helped to set up the consistent models that accurately describe materials properties of interest and that could be used for better characterization of energy devices and nuclear waste, including their long-term stability. The long-term goal of simulation-based research at IEK-13 is to support the computer-aided development of new, advanced materials and technologies for energy storage and conversion.

Selected honors, prizes and awards

- GABRIEL MURPHY received the Australia Institute of Nuclear Science and Engineering (AINSE) Gold Medal for research excellence as a result of the research out comes of his PhD work that was highly supported by the JARA-HPC project (https://www.fz-juelich.de/iek/iek-6/EN/ News/Announcements/Documents/2020-05-20-AINSE.html).

Selected Conference participations

- TESCH, R., EIKERLING, M. H., & KOWALSKI, P. M.
  Deriving Hubbard U Parameters for d-Metals from First Principles,
  Poster at NIC-Symposium, Jülich, 2020
- CHEONG, O., PHAM, T. , KOWALSKI, P. M., EIKERLING, M., DESKINS, A.,
  Determining the CO_2 Photoreduction Mechanismover TiO_2 Surfaces using Density Functional Theory,
  10th NIC Symposium by the John von Neumann Institute for Computing (NIC), Jülich, Germany, February 27-28, 2020
- SUN, M., STACKHOUSE, J., VINOGRAD, V., ALEKSEEV, E., KEGLER, P., MURPHY, G., WANG, T., KENEDY, B., ZHANG, Z., KVASHNINA, K., BOSBACH, D., JAHN, S., EIKERLING, M., KOWALSKI, P. M.
  Nuclear Materials from Experiments and Atomistic Simulations,
  10th NIC Symposium by the John von Neumann Institute for Computing (NIC), Jülich, Germany, February 27-28, 2020
- VERLINDEN, B., KOWALSKI, P. M., VAN HECKE, K., WILDEN, A., VERWERFT, M., MODOLO, G., BINNEMANS, K. & CARDINAELS, T.
  Radiolytic degradation of a new modified diglycolamide for Grouped Actinide Extraction,
  10th NIC Symposium by the John von Neumann Institute for Computing (NIC), Jülich, Germany, February 27-28, 2020

Selected National and international cooperations

- BRENDAN KENNEDY, GABRIEL MURPHY, ZHAOMING ZHANG, EUGENIA KUO & GREG LUMPKIN, ANSTO/U. of Sydney Australia
- MENGLI SUN AND TIESHAN WANG, Lanzhou U., China
- MILAN PSENICKA AND MIRESLAV POSPISIL, CHARLES U, Prague, Czechia
- BART VERLINDEN, SEC CEN, Belgium
- TIMOTHY CONNOR AND SARAH FINKELDEI, UC Irvine, USA

Publications

- KOWALSKI PM.
  Formation enthalpy of $Ln_2B_2O_7$-type (B=Ti,Sn,Hf,Zr) compounds,
  Scripta Materialia, 189, 7-10 (2020)
- SUN M, STACKHOUSE J, KOWALSKI PM.
  Oxidation state of Cr incorporated into the UO_2 matrix,
  Communications Materials 1, 13 (2020)
- BOSBACH D, BRANDT F, BUKAEMSKIY A, DEISSMANN G, KEGLER P, KLINKENBERG M, KOWALSKI PM, MODOLO G, NIEMEYER I, NEUMEIER S, VINOGRAD V.
  Research for the safe management of nuclear waste at Forschungszentrum Jülich: Materials chemistry and solid solution aspects,
  Advanced Engineering Materials 22, 1901417 (2020).
- KOWALSKI PM, LANGE S, DEISSMANN G, SUN M, KVASHNINA KO, BAKER R, KEGLER P, MURPHY G, BOSBACH D.
  Modeling of Nuclear Waste Forms: State-of-the-Art and Perspectives,
  MRS Advances 5, 213-222 (2020)
- FINKELDEI S, STENNETT M, KOWALSKI PM, JI Y, DE VISSER-TÝNOVÁ E, HYATT N, BOSBACH D, BRANDT F.
  Insights into the fabrication and structure of plutonium pyrochlores,
  Journal of Materials Chemistry A 8, 2387-2403 (2020)

Collaborating (experimental partners):

EVGENY ALEKSEEV,
Institute of Energy and Climate Research, Fundamental Electrochemistry (IEK-9), Forschungszentrum Jülich, Germany

BRENDAN KENNEDY,
U. of Sydney, Australia

GABRIEL MURPHY,
FELIX BRANDT,
Institute of Energy and Climate Research, Nuclear Waste Management and Reactor Safety (IEK-6), Forschungszentrum Jülich, Germany

ROBERT BAKER,
Trinity College Dublin, Ireland

ZHAOMING ZHANG, ANSTO, Australia

AXEL GROSS,
Universität Ulm, Germany

ANDREAS FRIEDRICH,
Institute of Engineering Thermodynamics, German Aerospace Center (DLR), Germany

ELENA R. SAVINOVA,
Université de Strasbourg, Strasbourg, France

MIROSLAV POSPISIL,
Charles University, Prague, Czechia

DANIEL GUAY,
Institut National de la Recherche Scientifique INRS, Quebec City, Canada

SARAH FINKELDEI,
UC Irvine, USA

Engineering Sciences

Materials Science | DFG 406

Quantum mechanically guided design of wear-protective coatings for polymer forming tools

Project ID: jara0151
JOCHEN M. SCHNEIDER
DENIS MUSIC
MARCUS HANS
PAVEL ONDRAČKA
HOLGER RUESS
LENA PATTERER
Materials Chemistry,
RWTH Aachen University

Project Report

Novel hard coatings, namely transition metal nitrides, and their interaction with polycarbonate were explored in this JARA project within the framework of the DFG-funded Collaborative Research Center SFB-TR 87. During the current project period, we have investigated the interaction between polycarbonate and $M_{0.5}Al_{0.5}N$ (M = Ti, V, and Cr) (001) surfaces as well as spinodal decomposition in cubic $V_{1-x}Al_xN$ thin films.

Poly(bisphenol A carbonate), or polycarbonate (PC), is a technologically important thermoplastic polymer, frequently used in the construction, medical, automotive, aerospace, food, and electronic industries. Conventional forming routes for PC include extrusion and injection molding, where molten PC has been observed to interact with and, in some cases, degrade at the tool surfaces. Depositing metastable cubic nitride thin films on steel tool surfaces is a promising way to reduce the interaction with PC.

We employed molecular dynamics (MD) simulations based on density functional theory (DFT) to classify the interaction strength of all functional groups of PC (carbonic acid, benzene, phenol, and propane) with the cubic $Ti_{0.5}Al_{0.5}N(001)$ surface at 300 K. Benzene, phenol, and propane molecules exhibit no dissociation and C atoms in these functional groups mostly prefer the hollow surface sites on $Ti_{0.5}Al_{0.5}N(0\,0\,1)$. The carbonic acid dissociates at the surface with the favoured reaction product being $CO_3^{2-} + 2H^+$. The reaction has two extremes, the weak interaction ($CO_3^{2-} + 2H^+$) and the strong interaction ($CO^{2+} + 2OH^-$). Both CO_3^{2-} and OH^- adsorb onto the metal surface atoms via O, while H^+ and CO^{2+} favor the N sites, where the C/H atom is bonded to the surface.

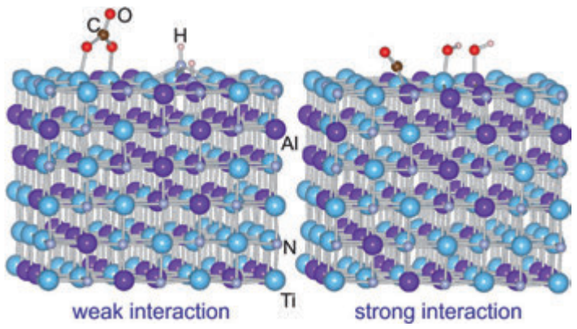

Figure 1: Reaction products for a carbonic acid molecule interacting with $Ti_{0.5}Al_{0.5}N$ (001) [1]

Based on these quantum-mechanical MD data, the adsorption energy was calculated for carbonic acid, benzene, phenol, and propane, clearly assigning the strongest surface interaction to carbonic acid, thus identifying it as the performance-limiting functional group in minimizing the interaction with the cubic nitride surfaces relevant for PC forming. The carbonic acid molecules were further considered in a systematic exploration of the influence of valence electron concentration of the transition metal M. Here, the affinity of carbonic acid to $M_{0.5}Al_{0.5}N$ (001) decreases as the valence electron concentration is increased from M=Ti to M=Cr [1].

Another topic of investigation was the mechanism of the decomposition of metastable cubic $(V_{0.64}Al_{0.36})_{0.49}N_{0.51}$ by combination of density functional theory calculations with structural and compositional characterization at the nanometer scale. The decomposition process is important for materials properties and can be utilized to enhance the hardness of protective transition metal nitride coatings.

By using DFT calculations to obtain the mixing enthalpy, we predicted that spinodal decomposition is expected for cubic $V_{1-x}Al_xN$ for $x \geq 0.35$. In agreement with our ab initio predictions, we have demonstrated the concurrent spinodal decomposition as well as nucleation and growth of hexagonal AlN in cubic $(V_{0.64}Al_{0.36})_{0.49}N_{0.51}$ after annealing at 900 °C. Local chemical modulations were quantified by atom probe tomography with maximum variations of x in $V_{1-x}Al_xN$ in the range of 0.36 to 0.50. Based on DFT data, the local variation in x from 0.30 to 0.61 would cause a lattice parameter change of just 0.012 Å. This variation corresponds to a (200) peak shift of just 0.1° and is significantly smaller than what can be measured by laboratory XRD. Spinodal decomposition in $V_{1-x}Al_xN$ cannot therefore be unraveled purely by diffraction data. However, consistent with DFT predictions, spinodal decomposition in cubic $(V_{0.64}Al_{0.36})_{0.49}N_{0.51}$ was revealed by chemical composition characterization at the nanometer scale [2].

References and Publications

[1] MUSIC D, RUESS H, SCHNEIDER JM. Quantum-mechanical study of interaction between polycarbonate and $M_{0.5}Al_{0.5}N(0\,0\,1)$ surfaces (M = Ti, V, Cr) Appl. Surf. Sci. 520, 146306 (2020).

[2] HANS M, RUESS H, CZIGÁNY Z, KRAUSE J, ONDRAČKA P, MUSIC D, EVERTZ S, HOLZAPFEL DM, PRIMETZHOFER D, SCHNEIDER JM. Spinodal decomposition of reactively sputtered $(V_{0.64}Al_{0.36})_{0.49}N_{0.51}$ thin films, Surf. Coatings Technol. 389, 125641 (2020).

[3] RUESS H, MUSIC D, BAHR A, SCHNEIDER JM. Effect of chemical composition, defect structure, and stress state on the elastic properties of $(V_{1-x}Al_x)_{1-y}N_y$ J. Phys. Condens. Matter 32, 025901 (2020).

Selected honors, prizes and awards

- JOCHEN M. SCHNEIDER, Bill Sproul Award and Honorary ICMCTF Lecture Recipient, The Bill Sproul Award and Honorary ICMCTF lectureship is to recognize the achievements of a mid-career researcher who has made outstanding scientific and/or technological contributions in areas of interest to the Advanced Surface Engineering Division (ASED) of the AVS, with emphasis in the fields of surface engineering, thin films, and related topics.
- The Editors of Surface and Coatings Technology recently published an Editor's Choice selection of key papers that highlight some of the best current research published in the journal until June 2020. The article "Spinodal decomposition of reactively sputtered $(V_{0.64}Al_{0.36})_{0.49}N_{0.51}$ thin films" is among this Editor's Choice selection.

Selected conference participations

- JOCHEN M. SCHNEIDER, Are Protective Coatings Predictable? A Mid-Career Assessment, virtual ICMCTF 2020: Bill Sproul Award and Honorary ICMCTF lecture, April 29, 2020

Selected national and international cooperations

- PETER AWAKOWICZ, Department of Electrical Engineering and Information Technology, Ruhr-Universität Bochum, Germany
- GUIDO GRUNDMEIER, Technical Chemistry, Paderborn University, Germany
- DAVID HOLEC, Department of Physical Metallurgy and Metallic Materials, University of Leoben, Leoben, Austria

Engineering Sciences

Materials Science | DFG 406

Quantum mechanically guided materials design

Project ID: jara0131
JOCHEN M. SCHNEIDER
DENIS MUSIC
SIMON EVERTZ
APARNA SAKSENA
DIMITRI BOGDANOVSKI
SIDA LIU
PHILIPP KEUTER
PAVEL ONDRAČKA
Materials Chemistry,
RWTH Aachen University

Project Report

With the help of quantum-mechanical simulations we aim to gain the necessary understanding to allow the design and synthesis of specifically tailored structural and functional materials. These simulations allow insight into phase stability, electrical and magnetic behaviors as well as the mechanical properties of materials. They complement the experimental analysis tools available, including atom probe tomography, scanning tunneling electron microscopy, X-ray diffraction, energy-dispersive X-ray spectroscopy and X-ray photospectroscopy. The combination of experiments and simulations allow for a full-spectrum characterization of experimentally synthesized materials, resulting in our core approach of quantum-mechanically guided materials design. Many novel materials classes, such as high entropy alloys, transition metal nitrides, negative thermal expansion oxides and metallic glasses were explored in this JARA project within the framework of several DFG research grants. The results have been communicated in peer-reviewed, international scientific journals. A selection of two of these projects is presented in the following.

The combination of high strength and toughness makes metallic glasses promising candidates for structural applications. In a combined ab initio and experimental study, the influence of the B content in Co-Ta-B glasses on their electronic structure was investigated as it plays a critical role in the material behavior. In the simulation part of the study, the cells with varying B content were heated with the help of ab initio molecular dynamics and then quenched to 0 K to create amorphous structures. Bonding analysis revealed that there is a shift in the Fermi level towards lower energies with increasing of B content. This increase also leads to the formation of an icosahedral B network due to the dominance of covalent B-B bonds, for B contents above approx. 39 at. %. Below that, the structures behave like metallic glasses. Above a concentration of approx. 69 at. %, the B structure changes further, with the network now enclosing the metal atoms and thus, the material can be described as a covalent glass. The simulation results are supported by experimental methods such as X-ray scattering analysis and X-ray photospectroscopy (XPS) of reference samples with comparable compositions (with a lower B variation range) synthesized via magnetron sputtering. Further studies will lead to the possibility to selectively tune material properties via the B content in the range 39 to 69 at.%.

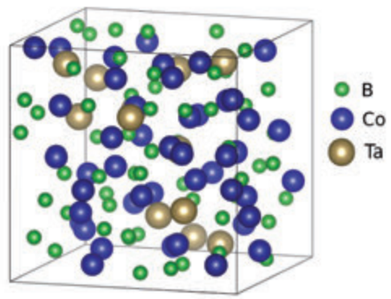

Figure 1: $Co_{46}Ta_{12}B_{57}$ metallic glass atomic structure model

In another, purely theoretical, study the influence of the free volume in metallic $Cu_{70}Zr_{30}$ glasses was investigated. In amorphous structural models, free volume regions of different size were created and their influence on the bonds was analyzed. The results reveal that crystal orbital Hamilton populations change only marginally, while the populated electronic states and bond energy contributions increase (by 0.1 eV) with larger free volumes. The average coordination number, on the other hand, decreases from 14.3 to 13.5 with free volumes of 0 and 4.6% of the total cell volume, respectively. The larger free volume weakens the bonding locally due to a rise in anti-bonding states. Under shear and hydrostatic deformation those sites show a further decrease in strong short-ranged bonding. The described electronic structure is proposed by us as the reason why glasses with higher free volume exhibit enhanced elastic behavior.

Besides metallic glasses, further important theoretical results obtained in the framework of this projects include elastic properties of the HfV_2O_7 high-temperature phase with negative thermal expansion, thermal conductivity of amorphous niobium monoxide, modeling of metastable phase formation for sputtered $Ti_{1-x}Al_xN$ and $V_{1-x}Al_xN$ thin films and prediction of energy barriers for surface diffusion in PtIrCuAuX (X = Ag, Pd) compositionally complex thin films.

It is not possible to list all the important results obtained in the framework of this project due to length constraints; however, we stress again, that, as highlighted in the introduction, quantum-mechanical calculations are crucial for both the design and understanding of novel coatings and materials, and would not be possible without HPC resources.

Selected honors, prizes and awards

- JOCHEN M. SCHNEIDER, Bill Sproul Award and Honorary ICMCTF Lecture Recipient, The Bill Sproul Award and Honorary ICMCTF lectureship recognizes the achievements of a mid-career researcher who has made outstanding scientific and/or technological contributions in areas of interest to the Advanced Surface Engineering Division (ASED) of the AVS, with emphasis in the fields of surface engineering, thin films, and related topics.
- SIMON EVERTZ, Bronze ICMCTF Graduate Student Award, Award established by the ASED of the AVS in 2006 to honor and encourage outstanding graduate students carrying out research in areas of interest to ASED, with emphasis on the fields of surface engineering, thin films, and related topics.

Selected conference participations

- JOCHEN M. SCHNEIDER, Modeling of the metastable phase formation for sputtered $Ti_{1-x}Al_xN$ and $V_{1-x}Al_xN$ thin films, Invited talk at the TMS 2020 Annual Meeting & Exhibition, San Diego, California, USA, February 23 - 27, 2020
- JOCHEN M. SCHNEIDER, Are Protective Coatings Predictable? A Mid-Career Assessment, virtual ICMCTF 2020: Bill Sproul Award and Honorary ICMCTF lecture, April 29, 2020
- SIMON EVERTZ, Electronic Structure based Design of Thin Film Metallic Glasses with Superior Fracture Toughness, virtual Award Ceremony for the ICMCTF 2020 Graduate Student Awards, December 14, 2020

Selected national and international cooperations

- DIERK RAABE, Max-Planck-Institut für Eisenforschung, Düsseldorf, Germany
- DANIEL PRIMETZHOFER, Department of Physics & Astronomy, Uppsala University, Sweden

Publications

- KEUTER P, et al. A Proposal for a Composite with Temperature-Independent Thermophysical Properties: HfV_2–HfV_2O_7. Materials 13, 5021 (2020).
- EVERTZ S, SCHNEIDER JM. Effect of the free volume on the electronic structure of $Cu_{70}Zr_{30}$ metallic glasses. Materials 13, 1–10 (2020).
- SAKSENA A, BOGDANOVSKI D, SAHASRABUDDHE H, MUSIC D, SCHNEIDER JM. Kinetically limited phase formation of Pt-Ir based compositionally complex thin films. Materials 13, 1–11 (2020).
- RAVENSBURG AL, KEUTER P, MUSIC D, MILJANOVIC DJ, SCHNEIDER JM. Experimental and Theoretical Investigation of the Elastic Properties of HfV_2O_7. Crystals 10, 172 (2020).
- EVERTZ S, ET AL. Boron concentration induced Co-Ta-B composite formation observed in the transition from metallic to covalent glasses. Condens. Matter 5, 18 (2020).
- EVERTZ S, ET AL. Electronic structure based design of thin film metallic glasses with superior fracture toughness. Mater. Des. 186, 108327 (2020).
- MUSIC D, PRÜNTE S, KEUTER P, SAKSENA A. On thermal conductivity of amorphous niobium monoxide. J. Phys. D. Appl. Phys. 53, (2020).
- LIU S, ET AL. Stress-dependent prediction of metastable phase formation for magnetron-sputtered $V_{1-x}Al_xN$ and $Ti_{1-x}Al_xN$ thin films. Acta Mater. 196 (2020).

Engineering Sciences

Materials Science | DFG 406

Quantum mechanically guided design of semicrystalline and amorphous Zn phosphate adsorption and reaction layers for tribofilm models

Project ID: jara0206
JOCHEN M. SCHNEIDER
DIMITRI BOGDANOVSKI
Materials Chemistry,
RWTH Aachen University

RAJIB SAHU
Materials Chemistry,
RWTH Aachen University and
Max-Planck-Institut für Eisenforschung,
Düsseldorf, Germany

THORBEN BÖGER
RWTH Aachen University

Project Report

The original intent of this project was to employ the quantum-mechanical expertise of MCh within the framework of a proposed Collaborative Research Center (CRC) “Reaction layers in Machine Elements”, focusing on the computational modeling of semicrystalline and amorphous Zn phosphate layers as model tribofilms for wear mitigation and the determination of their electronic structure, bonding characteristics, elastic and thermodynamic properties. However, despite excellent evaluation of the two subprojects pertaining to MCh, the CRC as a whole was not chosen for funding; thus, the majority of the granted computational resources were adapted towards other projects methodically linked with the proposed approach, establishing a long-term perspective of continuing the research in another format.

The thermal conductivity **κ**, which is an indicator for, e.g., the performance of thermal barrier coatings and other insulating materials, is an important parameter in multiscale modeling and can be predicted from ab initio data. To validate the methodological approach, two methods to calculate the thermal conductivities of Al_2O_3 and ZrO_2, in both crystalline and amorphous configurations, were employed: (i) ab initio molecular dynamics (AIMD) simulations using density functional theory (DFT), in which the system is simulated at a certain temperature, followed by DFT calculations of the elastic tensor and the application of the Voigt-Reuss-Hill (VRH) approximation, finally arriving at **κ** via the acoustic phonon propagation speeds; and (ii) anharmonic lattice dynamics simulations, in which individual atoms in supercells are displaced and force constants up to the third order are obtained, and the relaxation time approximation (RTA) is used to calculate **κ**. While differing in computational demand and precision, both methods yield the temperature-dependent thermal conductivity, allowing comparison against each other. The material systems were chosen for their structural simplicity, thus being well-suited as test cases.

Both approaches yield qualitatively correct results, with the thermal conductivity decreasing at higher temperatures for Al_2O_3 and both modifications of ZrO_2 (monoclinic and tetragonal); however, their quantitative accuracy is insufficient. For the AIMD-VRH approach, there is excellent agreement with literature data from other simulations (1.45 vs. 1.47 $Wm^{-1} K^{-1}$, a deviation of <2% for ZrO_2) for both materials in the ground state, but at higher temperatures, **κ** is consistently lower by ca. 50% in comparison to the experimental values for Al_2O_3 (for ZrO_2, experimental values usually refer to yttrium-stabilized zirconia, rendering a comparison meaningless) - a disappointing result; however, the trend is reflected very well. Using the RTA method, the discrepancy between the obtained values and theoretical data from literature is about 10% for ZrO_2 (e.g., 1.9 vs 2.1 W $m^{-1} K^{-1}$ at 1400 K), and around 33% in the case of comparisons to experimental data for Al_2O_3 (e.g., 4 W $m^{-1} K^{-1}$ vs. the experimental 6 W $m^{-1} K^{-1}$ at 1500 K). Particularly in the latter case, this is a marked improvement vs. the AIMD-VRH approach, but still falls short of being quantitatively accurate; in addition, this higher precision (and the capacity of calculating anisotropic contributions to **κ**) comes at a higher computational cost. Thus, both approaches show qualitative agreement with prior data and yield physically meaningful results, but exhibit low quantitative accuracy, and thus seem to only be usable as rough predictive tools unless refined further.

In another project, the coexistence of several defect phases in the so-called MAB phase MoAlB, as well as the presence of the corresponding two-dimensional MB phase, MoB, all experimentally observed using electron microscopy (STEM) techniques in a sample synthesized via physical vapor deposition (PVD), was studied via DFT phase stability calculations and ab initio bonding analysis tools. Such MAB phases are promising candidates for applications in chemically harsh environments, with good corrosion and wear resistance, but also useful catalysts, and the 2D MBene phases have even further enhanced properties, thus turning them into promising functional materials.

Starting from a known literature structure for MoAlB, the morphology of the phases observed in STEM was closely replicated by manual adjustment of the structural models; their formation energies at the ground state were calculated after structural optimization. The differences between the phases, in terms of energy per atom, are small to negligible, exhibiting an energy difference between < 10 meV/atom and 0.18 eV/atom: even the latter value is easily overcome by the high energy of incident ions in the PVD scenario (often used in metastable phase formation), thus theoretically explaining the simultaneous coexistence of the MAB phase, the MBene and the defect phases.

The bonding analysis results clarify that, when comparing MoAlB and MoB, on an individual bond basis, the B–B interaction is the strongest, but weaker in MoB than in MoAlB, while the strength of the Mo–Mo- and Mo–B interactions increases, due to electronic orbital rearrangement upon removal of Al. In the overall picture, the Mo–B interaction, due to the much higher number of contacts than in the B–B case, dominates. Such comparisons of the bonding situation, if coupled with structure-property relationships, allow for selectively guided materials design.

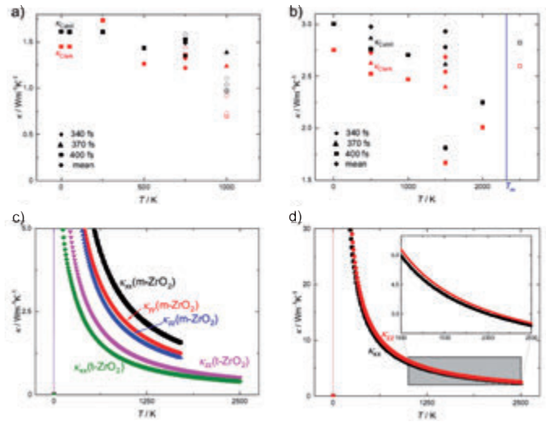

Figure: Calculated thermal conductivities using the AIMD-VRH and RTA approaches for ZrO_2 (AIMD-VRH: a, RTA: c) and Al_2O_3 (AIMD-VRH: b, RTA: d); for the AIMD-VRH approach, two different models of approximating **κ** from sound velocities and different MD runtimes were used.

National and international cooperations

- CHRISTINA SCHEU, Max-Planck-Institut für Eisenforschung, Düsseldorf, Germany
- RICHARD DRONSKOWSKI, Institute of Inorganic Chemistry, RWTH Aachen University
- DAVID HOLEC, Department of Physical Metallurgy and Metallic Materials, Leoben University, Leoben, Austria

Engineering Sciences

Materials Science | DFG 406

Atomistic Mechanisms of the Plasticity in Magnesium Alloys

Project ID: rwth0407
JULIEN GUÉNOLÉ
ZHUOCHENG XIE
Institute for Physical Metallurgy and Materials Physics (IMM), RWTH Aachen University

Project Report

The project is focused on the simulation of the fundamental deformation mechanisms in magnesium alloys in general, and in particular in the magnesium based Laves phase. In Mg-Al-Ca alloy systems, the formation of Laves phases is commonly observed. However, these phases are usually showing brittle behavior during deformation, thus limiting the formability and the employability the Mg alloy.

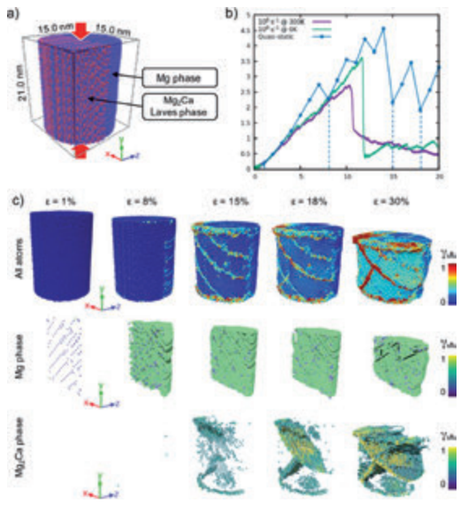

Figure 1: Indirect slip transfer at the Mg-Mg_2Ca interface during nanomechanical compression tests. a) setup of the compression test simulation. Red arrows indicate the compression direction. Atoms in blue (red) are Mg (Ca). b) stress-strain curves of the compression tests. The green and purple solid lines correspond to dynamic deformation at ≈50K and 300K. The dots of the blue line correspond to the relaxed states of the quasi-static deformation. Vertical dashed lines are guide for the eyes at strains 1%, 8%, 15% and 18% that correspond to the snapshots shown in c. c) snapshots of the quasi-static deformation test. First row: all atoms are shown. Second (third) row: only atoms of the Mg (Mg_2Ca) phase with an atomic shear strain greater than 0.3 are shown. Atoms are colored according to the atomic shear strain.

Generally, the mechanical behavior of Mg-Al-Ca alloys can be largely improved by the formation of an intermetallic Laves phase skeleton, in particular the creep strength. Recent nanomechanical studies revealed plasticity by dislocation glide in the $(Mg,Al)_2Ca$ Laves phase, even at room temperature. As strengthening skeleton, this phase remains, however, brittle at low temperature. In this project, we investigated slip transfer from the Mg matrix to the Mg_2Ca skeleton at room temperature and explore associated mechanisms by means of atomistic simulations. Thanks to the availability of an accurate interaction model based on the modified embedded atom model (MEAM), we are capable of performing small to large scale molecular static and molecular dynamic simulations. We designed numerical nano-mechanical tests of Mg/Mg_2Ca composites and ran simulation at different strain rate and temperature to explore the plastic response of the system. An example of a nanomechanical test is shown in Figure 1: the compression of a dual-phase nano-pillar. The simulation gives access the stress-strain curve, similarly to experiments. In addition, it provides a unique access to the deformation mechanisms with a very high accuracy, both spatially and temporally. As an example, Figure 1c is showing the deformation of the pillar at different strain level, from 1% to 30%. It evidences the initiation of plasticity (permanent deformation) and the transfer of the deformation from the Mg phase to the Mg_2Ca phase.

Overall, we identify two possible mechanisms for transferring Mg basal slip into Laves phases depending on the crystallographic orientation: a direct and an indirect slip transfer triggered by full and partial dislocations, respectively. Our numerical observations also highlight the importance of interfacial sliding that can prevent the transfer of the plasticity from one phase to the other. This work has been published in peer reviewed international journal [Guénolé et al., Materials & Design 202 (2021) 109572].

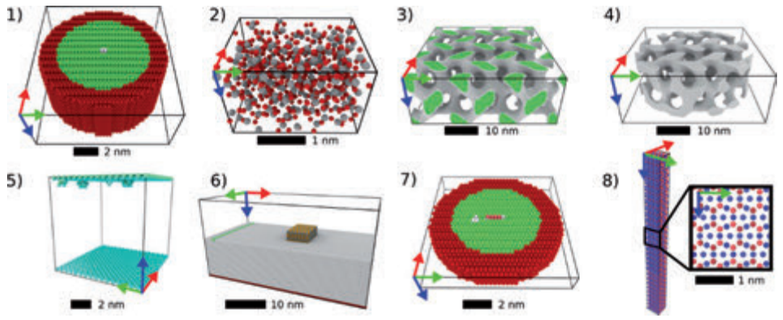

Figure 2: Snapshots of the atomistic samples used for the assessing FIRE. Color coding in (1, 3, 4, 7) is based on the common neighbor analysis (CNA): green, fcc; light red, stacking fault; white, others; Color coding in (2, 8) based on chemical species: grey, Si; dark-red, O; blue, Ca; light-red, Mg. Color coding in (5) based on diamond structure analyses: turquoise, non-diamond atoms; atoms in diamond configuration are removed for clarity. Color coding in (6): light-grey, Mg hcp matrix atoms; green, fcc dislocation atoms. Within the cuboidale precipitate, orange and blue atoms are Mg and Al, respectively. Half of the Mg matrix atoms have been removed for clarity. In (1, 7) dark-red colored atoms are frozen. The simulation box axes x, y, z are represented by red, green, blue arrows, respectively. The scale bars indicate the dimension of each sample in nm.

In parallel to the investigation of the deformation properties of Mg alloys and Mg_2Ca Laves phase, we have worked on the development of the optimization of a widely used numerical method. In fact, optimization methods are of prime importance for molecular statics simulation. In atomistic simulations, pseudo-dynamics relaxation schemes often exhibit better performance and accuracy in finding local minima than line-search-based descent algorithms like steepest descent or conjugate gradient. In this project, we worked on an improved version of the fast inertial relaxation engine (FIRE) and its implementation within the open-source atomistic simulation code LAMMPS. We took a special care in the assessment of the novel implementation of the algorithm by considering a large variety of materials science problems. Figure 2 illustrates the different simulations setup that have been required to assess FIRE. Beside the method itself that is now freely and widely available, we evidenced that the correct choice of time integration scheme and minimization parameters is crucial for the performance of fire. This work has been published in peer reviewed international journal [Guénolé et al., Computational Materials Science 175 (2020) 109584].

Publications

· GUÉNOLÉ J, ZUBAIR M, ROY S, XIE Z, LIPIŃSKA-CHWAŁEK M, SANDLÖBES-HAUT S, KORTE-KERZEL S. Exploring the transfer of plasticity across Laves phase interfaces in a dual phase magnesium alloy, Materials & Design 202 (2021) 109572.
· GUÉNOLÉ J, NÖHRING WG, VAID A, HOULLÉ F, XIE Z, PRAKASH A, BITZEK E. Assessment and optimization of the fast inertial relaxation engine (FIRE) for energy minimization in atomistic simulations and its implementation in LAMMPS, Computational Materials Science 175 (2020) 109584.

Engineering Sciences

Materials Science | DFG 406

Atomistic insight into metallurgical slags: high temperature properties investigation and new model development

Project ID: rwth0355

GUIXUAN WU
MICHAEL MÜLLER
Institute of Energy and Climate Research, Microstructure and Properties of Materials (IEK-2), Forschungszentrum Jülich GmbH, Germany

MENGYI ZHU
Department of Materials Science and Engineering, Norwegian University of Science and Technology (NTNU), Norway

Project Report

Slags play a crucial role in a wide variety of high temperature metallurgical processes. In the past decades, considerable attention has been paid to metallurgical slag falling within compositional dependence of physical and chemical properties. However, ongoing challenges still remain for the direct structure observation of slag melt due to the high temperature (usually around 1500°C) in the metallurgical process. The present project aims at performing comprehensive classical molecular dynamics (MD) simulations of multi-component molten slags to improve the understanding of the complex slag composition-structure-property relationship.

In our previous work, a structure-based viscosity model has been developed for SiO_2-Al_2O_3-CaO-MgO-Na_2O-K_2O-FeO-Fe_2O_3 multi-component slag melts. Comprehensive molecular dynamics simulations have also been performed to decode the “genome” of slags, especially for the Al_2O_3 and Fe_2O_3 bearing charge compensation systems. The proposed slag genome was demonstrated and decoded as novel oxygen-based “gene units” obtained from MD simulation, which are further classified and linked to different functional groups.

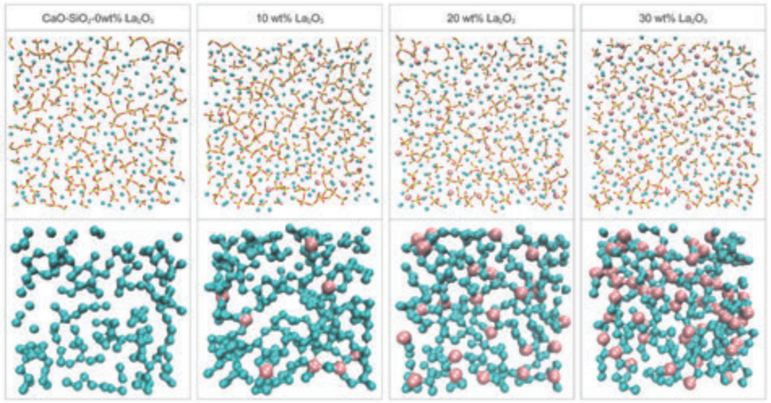

Figure 1: Silica network depolymerizes with increasing La_2O_3 addition shown as sectional view of a slice with 6 Å thickness and with the visualized expanding network modifier migration channels of Ca (cyan) and La (pink)

The variation of physical properties such as density, diffusivity, and structural properties was linked to the slag genome profiles. The viscosity maximum of important slag systems, e.g., fayalite slags and aluminosilicate slags was well interpreted by the distribution of the novel slag structural gene units obtained from MD simulation.

Recently, to shed light on the mixed network modifiers effect on slag melts, a series of MD simulations were performed as represented by the rare earth element containing CaO-La_2O_3-SiO_2 slag system. The different behaviour of calcium and lanthanum cations were characterized through the oxygen-based slag genomes. As presented in Fig. 1, the depolymerization process of silica network with increasing La_2O_3 addition is visualized from the snapshots of simulated slags where the long [SiO_4] chains in the initial CaO-SiO_2 slag finally depolymerized to the chains in short-range and even in monomers after 30 mass pct La_2O_3 addition. Moreover, nano-segregation of Ca^{2+} can be also observed from the visualized volumetric space of modifiers.

Figure 2: Distribution percentage of different oxygen species obtained from MD simulation in the investigated CaO-La_2O_3-SiO_2 slags. The presented oxygen species are with the percentage > 0.05 pct in at least one of the simulated slags where the left side shows the Ca-based oxygen species and the right side shows the La-based oxygen species

As the potential diffusion pathways of modifiers, it can be clearly seen that the volumetric space developed from small pockets to a more channel-connected network, which indicates the significant mobility enhancement of the modifiers. The detailed distribution of oxygen species population is presented in Fig. 2 for all studied slags. A clear trend can be observed that the dominant oxygen species shift from Ca-based oxygen to La-based oxygen, with increasing La_2O_3 addition, which also indicates the increasing reactivity of the slag system.

Although not all the obtained important results can be shown in the framework of the present project report, it has been verified and highlighted that computational simulation with HPC resources has provided novel insights and understanding into the complicated behaviour of molten slags and high temperature metallurgical process.

Selected Conference participations

- MENGYI ZHU, JAFAR SAFARIAN, GUIXUAN WU,
  Effects of La_2O_3 addition to CaO-SiO_2 slag on boron and phosphorus removal from Sn-doped silicon for solar grade silicon production,
  The 11th International Conference on Molten Slags, Fluxes and Salts, Virtual, Korea, February 21-25, 2021

Selected National and International Cooperations

- MORITZ TO BABEN
  GTT-Technologies, Herzogenrath, Germany
- KLAUS HACK
  GTT-Technologies, Herzogenrath, Germany
- JAFAR SAFARIAN
  Norwegian University of Science and Technology, Trondheim, Norway

Engineering Sciences

Computer Science | DFG 409

Privacy-Preserving Machine Learning for Intrusion Detection

Project ID: rwth0438
ARTHUR DRICHEL
MALTE BREUER
VINCENT DRURY
SEBASTIAN SCHÄFER
BENEDIKT HOLMES
Research Group IT-Security,
RWTH Aachen University

Project Report

The security of complex systems and networks often depends on data aggregated from several sources such as end-user devices, or industry control systems. These devices can create a vast amount of alerts, that make it hard for analysts to discern attacks from benign behavior. There exist several approaches for Intrusion Detection Systems (IDS) and Intrusion Prevention Systems (IPS) to handle these alerts, including machine learning approaches, to filter relevant output. However, such approaches raise questions on privacy, as they often include interactions with end-user systems and can be used to create user profiles or monitor user activity. Furthermore, the question arises how threats can be addressed preemptively, e.g. by leveraging alerts or public information to identify and secure vulnerable systems. The goal of this project is to research privacy-preserving machine learning approaches to several known problem domains.

Detection of Domain Generation Algorithms: Botnets can have severe effects on the availability and confidentiality of systems. Botnet creators often use Domain Generation Algorithms (DGAs) to communicate with the infected systems to make it harder to block their commands. Machine learning classifiers can be used to monitor the DNS traffic of a network enabling network operators to find and clean infected systems. In this project, we engineered two novel classifiers which are based on residual neural networks (ResNets), one for DGA binary and one for DGA multiclass classification. While the binary classifier is able to separate benign from malicious domain names, the multiclass classifier is able to attribute domain names to the DGAs which generated them, enabling the execution of malware specific countermeasures. In two binary classification scenarios (detection of known DGAs and detection of unknown DGAs), we demonstrated that our proposed binary classifier is able to achieve state-of-the-art classification performance while yielding the lowest false positive rate. In the context of DGA multiclass classification, we showed that our proposed multiclass classifier outperforms the state of the art by over 5% in macro F1-score and is thus able to correctly classify samples of several DGAs, which the other state-of-the-art classifiers are not able to attribute correctly. We provide the confusion matrix of the multiclass classifier in Fig.1 to visualize ist performance. A perfect classifier would yield an identity matrix of black cells.

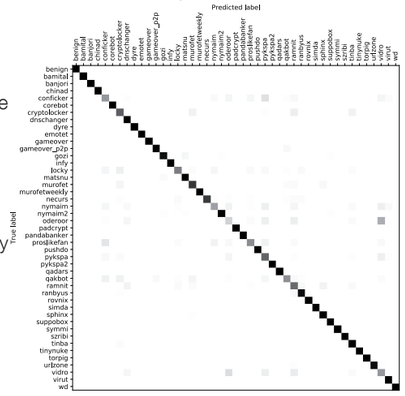

Figure 1: Confusion matrix of proposed DGA multiclass classifier.

Passive Detection of Outdated Software To preemptively detect systems vulnerable to Malware, Domain Name System (DNS) queries can be analyzed and classified. This can help operators to create an overview of their network, including the usage of outdated and vulnerable software. If outdated, misconfigured, or unauthorized software can be detected in a network, it is possible to update, block, or at least notify the responsible administrators, in order to prevent possible attacks in the future. In this project, we developed different approaches for this task based on rules or statistical models, machine learning, and process mining. We solely rely on DNS traffic For the identification of applications. For the rulebase approach, we simply create rules that match to either single DNS queries or sequences. If a rule matches, a label is added to the corresponding host indicating a specific application or version. Complex rules have to be generated either manually or using our process mining approach. Process mining is a technique to analyze event logs in order to extract the underlying processes. We use it to analyze DNS events to find patterns that are specific for a given application. The output of process mining consists of petri nets, which can either be used to model and detect the behavior of an application, or to extract detection rules from.

Automated Detection of Phishing Websites: Phishing is a severe threat to end-users, and as a result to whole organizations. It can be used to deliver Malware, or steal confidential information from users by directing them to malicious websites. This sub-project aims to research different types of phishing detection, preemptive as well as reactive, to improve the security of end-users, and organizations. Defenses against phishing attacks are already integrated into different software solutions, e.g. in the form of blocklists in popular browsers. However, these reactive blocklists leave a short period of time, a “window of opportunity”, in which an attack cannot yet be detected. This leaves potential victims of phishing attacks unprotected. Certificate Transparency (CT) logs offer a possibility to detect these attacks earlier, as the acquisition of a certificate is likely to happen before the attack is mounted. As such, one goal of this sub-project is to create a pipeline that can be utilized to work with the massive scale of data that is included in these logs. The pipeline offers functionality to train classifiers on certificate data, test the classifiers on certificates obtained from real CT logs, and finally use the trained classifiers to detect the certificates of phishing websites as soon as they are added to the logs.

Simulation of Privacy-Preserving Applications: In this part of the project we develop a distributed system that supports the finding and selecting of exchange structures between donors and recipients in the context of kidney donor exchanges in an automated, privacy-preserving, and fair fashion. As a first step, we have developed and implemented a Secure Multi-Party Computation (SMPC) protocol that enables static kidney donor exchange in a privacy-preserving fashion. We have simulated and evaluated the protocol’s performance for different numbers of recipient- donor pairs and observed that the protocol exhibits feasible runtimes for small numbers of recipient-donor pairs.

Selected conference participations

- ARTHUR DRICHEL, International Workshop on Next Generation Security Operations Centers / NG-SOC 2020, Virtual Event, Ireland, August 25, 2020
- TOMAS JIRSIK, SEBASTIAN SCHÄFER, International Workshop on Next Generation Security Operations Centers / NG-SOC 2020, Virtual Event, Ireland, August 25, 2020

National and international cooperations

- SUSANNE WETZEL, Stevens Institute of Technology, New Jersey, USA
- EU project SAPPAN: Fraunhofer FIT, Sankt Augustin, Germany, University of Stuttgart, Germany, CESNET, Prague, Czech Republic, Dreamlab Technologies, Bern, Switzerland, Hewlett Packard Enterprise, Galway, Ireland, F-Secure, Helsinki, Finland
- DOMINIK TEUBERT, Siemens CERT, Munich, Germany

Publications

- DRICHEL A, MEYER U, SCHÜPPEN S, TEUBERT D. 2020. Analyzing the Real-World Applicability of DGA Classifiers. In International Conference on Availability, Reliability & Security. ACM.
- DRICHEL A, MEYER U, SCHÜPPEN S, TEUBERT D. 2020. Making Use of NXt to Nothing: Effect of Class Imbalances on DGA Detection Classifiers. In International Conference on Availability, Reliability and Security. ACM.
- BECKER F, DRICHEL A, MÜLLER C, Ertl T. 2020. Interpretable Visualizations of Deep Neural Networks for Domain Generation Algorithm Detection. In Symposium on Visualization for Cyber Security. IEEE.
- BREUER M, MEYER U, WETZEL S, MÜHLFELD A. 2020. A Privacy-Preserving Protocol for the Kidney Exchange Problem. In Proceedings of the 19th Workshop on Privacy in the Electronic Society. ACM.

Thinking the Future
Zukunft denken